# EXPERIMENTAL WHIPLASH ANALYSIS WITH HYBRID III 50 PERCENTILE TEST DUMMY

A THESIS SUBMITTED TO
THE GRADUATE SCHOOL OF NATURAL AND APPLIED SCIENCES
OF
MIDDLE EAST TECHNICAL UNIVERSITY

BY

ULAŞ GÖÇMEN

IN PARTIAL FULFILLMENT OF THE REQUIREMENTS
FOR
THE DEGREE OF MASTER OF SCIENCE
IN
MECHANICAL ENGINEERING

SEPTEMBER 2009

Approval of the thesis:

**EXPERIMENTAL WHIPLASH ANALYSIS WITH HYBRID III 50 PERCENTILE TEST DUMMY**

submitted by **ULAŞ GÖÇMEN** in partial fulfillment of the requirements for the degree of **Master of Science in Mechanical Engineering, Middle East Technical University** by,

Prof. Dr. Canan Özgen
Dean, Graduate School of **Natural and Applied Sciences** _____

Prof. Dr. Süha Oral
Head of the Department, **Mechanical Engineering** _____

Prof. Dr. Mustafa İlhan Gökler
Supervisor, **Mechanical Engineering Dept., METU** _____

**Examining Committee Members:**

Prof. Dr. Y. Samim Ünlüsoy
Mechanical Engineering Dept., METU _____

Prof. Dr. Mustafa İlhan Gökler
Mechanical Engineering Dept., METU _____

Prof. Dr. Kemal İder
Mechanical Engineering Dept., METU _____

Prof. Dr. Haluk Darendeliler
Mechanical Engineering Dept., METU _____

Dr. Mustafa Erdener
Ford Otosan _____

**Date:** September 10th, 2009

**I hereby declare that all information in this document has been obtained and presented in accordance with academic rules and ethical conduct. I also declare that, as required by these rules and conduct, I have fully cited and referenced all material and results that are not original to this work.**

Name, Last name: Ulaş Göçmen

Signature:

## ABSTRACT

EXPERIMENTAL WHIPLASH ANALYSIS WITH HYBRID III 50 PERCENTILE TEST DUMMY

Göçmen, Ulaş

M.Sc., Department of Mechanical Engineering
Supervisor: Prof. Dr. Mustafa İlhan Gökler

September 2009, 129 pages

Whiplash injuries as a result of rear impact are among the most common injuries in traffic accidents. This is why whiplash injuries have reached a high priority in the research area. In this study, the effects of head restraint position and impact pulse to the whiplash injury have been analyzed by performing whiplash tests using the sled test facility of METU-BILTIR Center Vehicle Safety Unit. Although there are many whiplash test protocols, the test sample has been prepared according to the most recent one, Euro NCAP Whiplash Test Protocol. Three different head restraint positions and three different impact pulses with different severities, totally nine tests have been performed. The tests are performed with a three point generic seat belt and an instrumented Hybrid III 50th percentile male adult crash test dummy is used as the occupant in driver seat of a light commercial vehicle. High speed cameras, sensors on the crash test dummy and a data acquisition system are used to take the test data. This test data has been analyzed and presented according to the defined whiplash assessment criteria and the performance scores of the particular seat for each test have been determined using the whiplash assessment criteria values according to the Euro NCAP Test Protocols.



**Keywords:** Whiplash, Rear Crash, Euro NCAP, Hybrid III, Sled Test, Test Dummy.

# ÖZ

HİBRİD III %50LİK TEST MANKENİ İLE BOYUN YUMUŞAK DOKU İNCİNMESİNİN DENEYSEL ANALİZİ

Göçmen, Ulaş

Yüksek Lisans, Makina Mühendisliği Bölümü
Tez Yöneticisi: Prof. Dr. Mustafa İlhan Gökler

Eylül 2009, 129 sayfa

Arkadan gelen darbeler sonucu oluşan whiplash incinmeleri trafik kazalarında en yaygın olarak ortaya çıkan incinmelerden biridir. Bu durum whiplash üzerine yapılan araştırmaların öncelik kazanmasına sebep olmuştur. Bu çalışmada koltuk kafalık pozisyonunun ve çarpışma darbe sinyalinin whiplash incinmesine olan etkileri ODTÜ-BİLTİR Merkezi Araç Güvenlik Birimi'ndeki hasarsız çarpışma benzetim sisteminde yapılan whiplash testleri ile analiz edilmiştir. Birçok whiplash test protokolü olmasına rağmen, kullanılan test düzeneği en yeni whiplash test protokolü olan Euro NCAP Whiplash Test Protokolüne göre hazırlanmıştır. Üç değişik kafalık pozisyonu ve üç değişik şiddeteki darbe sinyali ile toplam dokuz test yapılmıştır. Testler üç noktalı emniyet kemeri ve bir hafif ticari araç sürücü koltuğuna yolcu olarak oturtulan Hibrid III serisi %50lik yetişkin erkek çarpışma test mankeni ile yapılmıştır. Gerekli test bilgileri kullanılan hızlı kameralar, test mankeni üzerindeki sensörler ve veri toplama sistemi ile toplanmıştır. Bu bilgiler Euro NCAP Test Protokollerinde yer alan whiplash değerlendirme kriterlerine göre analiz edilmiş, sunulmuş ve kullanılan koltuğun her test için performans değerleri belirlenmiştir.

**Anahtar Kelimeler:** Whiplash, Arkadan Çarpma, Euro NCAP, Hibrid III, Hasarsız Çarpışma Benzetim Testi, Test Mankeni.

***To My Wife,***

## ACKNOWLEDGEMENTS

I would like to express my deepest gratitude to my supervisor Prof. Dr. Mustafa İlhan Gökler for his guidance, advice, criticism, encouragement and insight throughout the study.

The author was supported by The Scientific and Technological Research Council of Turkey (TÜBİTAK) with National Scholarship Program for MSc Students (Program no: 2210).

I would like to thank to METU-BILTIR Research and Application Center Vehicle Safety Unit Sled Test Facility, for the facilities provided for my study.

I also would like to thank Dr. Mustafa Erdener and Dr. Polat Şendur from FORD OTOSAN Company. The technical assistance of them is gratefully acknowledged.

I wish to thank to my senior colleagues İlker Durukan, Kazım Arda Çelik, Mehmet Maşat and Sevgi Saraç for their valuable support and assistance.

Special thanks go to my colleagues, Arda Özgen, Özgür Cavbozar, Hüseyin Öztürk, Cihat Özcan, Ali Murat Kayıran, Gökhan Biçer and Sinem Demirkaya for their supports and encouragement.

Further, thanks go to Osman Mumcu, Halit Şahin, Ali Demir, Hüseyin Ali Atmaca, Tarık Öden, Filiz Güngör Sütekin, Arzu Öztürk, Tuğba Karakurum, Halime Küçük and Mehmet Ali Sarıhan for their endless efforts and aids.

I am deeply indebt to my wife Zeynep Özge Göçmen and my parents, Yeter and İbrahim Göçmen, my brother Ünal Göçmen for their encouragement and faith in me.

## TABLE OF CONTENTS

## LIST OF TABLES

TABLES

## LIST OF FIGURES

FIGURES

## LIST OF SYMBOLS

SYMBOLS

b : Backset

h : Distance from top of the head

α : Cushion angle

OC : Occipital Condyles

$M_y^{OC}$ : Upper neck moment about the OC

$M_y^{upper}$ : Upper neck moment about y-axis

$F_x^{upper}$ : Upper neck shear force

$N_{ep}$ : Neck extension posterior

$N_{ea}$ : Neck extension anterior

$N_{fp}$ : Neck flexion posterior

$N_{fa}$ : Neck flexion anterior

# CHAPTER 1

# INTRODUCTION

## 1.1 Whiplash Injury During Low Speed Rear End Crash

Neck injury in vehicle collisions, often referred to as "whiplash injury", is one of the most common traffic related safety problems, resulting in serious implications for the society [1]. Although these injuries are typically considered minor, their high incidence rate and often long-term consequences lead to significant costs. Many accident studies and claims statistics coming from the insurance industry [2-4] clearly indicate that low severity rear crash may lead to injuries causing long-term disablement and discomfort. The costs of such injuries are very high both medically and economically.

Although the whiplash was firstly defined in 1928 by Crowe as neck injury caused by acceleration forces, the precise definition of whiplash injury still remains controversial [5-8]. A widely accepted definition that is formulated by the Quebec Task Force (QTF), a task force sponsored by the Société de l'assurance automobile du Québec, the public auto insurer in Quebec, Canada, in 1995 based on an extensive literature review is stated below [8]:

"Whiplash is an acceleration-deceleration mechanism of energy transfer to the neck. It may result from rear end or other motor vehicle collisions, but can also occur during diving or other mishaps. The impact may result in bony or soft tissue (whiplash) injuries, which may lead to a variety of clinical manifestations which is Whiplash-Associated Disorders (WADs)".

As seen from this general definition, WADs may result from rear end or other motor vehicle collisions, or during diving or other mishaps, however, the whiplash injuries very predominantly occur in the rear end crashes of the vehicles [9]. In addition, crash analyses performed on whiplash studies reveal that these injuries usually occur at the velocity differences of 10 to 20 km/h. So it can be understood that majority of whiplash injuries occur at low speed and low acceleration rear end crashes. In this thesis, whiplash-associated disorders (WADs) resulting from low speed rear end crashes of the vehicles will be considered.

### 1.2 Medical Aspects of Whiplash Injury

WADs basically result from the excess relative motion between the head and torso and are difficult to diagnose. Often no clear sign of structural injuries of the tissues within the neck is found with medical imaging, neurological, or orthopedic investigations [10]. A clinical classification of WAD published by the Quebec Task Force is presented in Table 1.1 [8]. In addition to the ones described in Table 1.1, symptoms and disorders may also include deafness, dizziness, ringing in the ears, headache, memory loss, difficulty in swallowing, and joint pain in jaws. Although there are different grades of whiplash, this thesis study does not specific to any grades. The tests performed during the study may result in any of these grades, however, this can only be understood by medical investigation in corresponding real life cases.

45.9 % of the symptoms described in Table 1.1 occur within 1 hour after the accident, 28.6 % of those occur later but within 24 hours, while 25.5 % of the symptoms occur after 24 hours [11]. However, the public health problems concerning WADs are those leading to long term disability.

Related to the whiplash injury classification given in Table 1.1, one-year cumulative recovery curves of WADs for the grades 1, 2 and 3 are presented in Figure 1.1 [12].

**Table 1.1 The Quebec Classification of WADs [8]**

| GRADE | CLINICAL PRESENTATION OF WHIPLASH INJURIES |
|---|---|
| Grade 0 or WAD 0 | - Client does not complaint of neck pain and no physical signs are observed by examining health care practitioner.<br>- These clients are uncommon and will not usually seek assistance, thus going undocumented. |
| Grade 1 or WAD 1 | - Client complains of pain to health practitioner.<br>- No physical signs are found i.e. normal range of motion, normal strength, normal swelling.<br>- Usually these clients suffer from muscle lesions that are not significant enough to cause muscle spasm. |
| Grade 2 or WAD 2 | - Client complains of pain to health practitioner.<br>- Signs are found that could include:<br>Limited range of motion<br>Spasm or Swelling<br>Point tenderness in neck or shoulders<br>- Usually these clients have dislocated ligaments in their neck and the muscle tears have caused bleeding and swelling. |
| Grade 3 or WAD 3 | - Client complains of pain to health practitioner.<br>- Neurological signs are found that could include:<br>Decreased or absent reflexes<br>Decreased or limited skin sensation (Dermatomes)<br>Muscular weakness (Myotomes)<br>- Usually these clients suffer from injuries to the neurological system because of pressure on nerves or irritation secondary to sustained stretch of neural tissue.<br>- These clients will almost have limited range of motion and other musculoskeletal signs as well. |
| Grade 4 or WAD 4 | - Client complains of pain to health practitioner.<br>- X-rays reveal fracture or dislocation. |

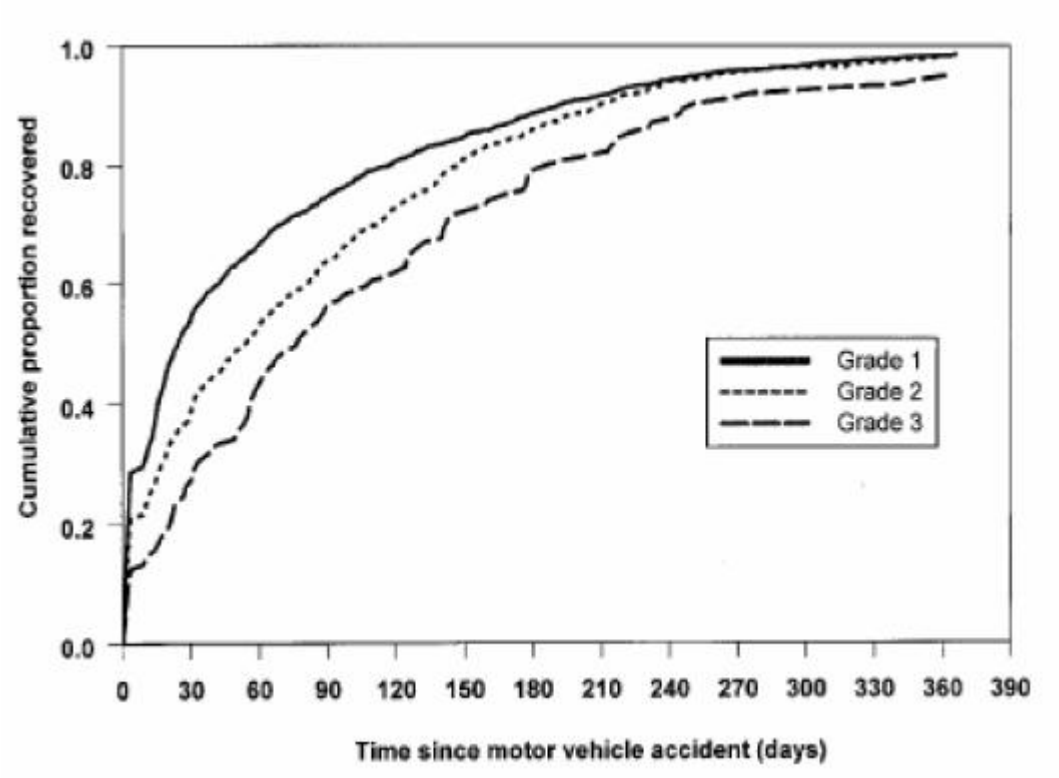


**Figure 1.1 One-year Cumulative Recovery Curve by the Grades 1,2 and 3 of the Quebec Classification of WADs [12]**

A Canadian study showed that 2.9 % of people with WADs were still absent from their usual activities or work, one year after the collision [8]. In 1994, Barnsley et al. [10] published a clinical review on WADs concerning the related studies in all over the world. This review indicates that around 40 % of patients with whiplash injuries develop chronic neck pain and approximately 10 % will have constant, severe pain indefinitely [10].

### 1.3 Human Anatomy Related to Whiplash Injury

Whiplash injury is directly related with the relative movements of the parts in the human neck region. In order to understand what happens during whiplash injury, it is required to have some information about the biomechanics of the human neck. So,

the human spine anatomy is summarized in this section and more detailed information is given in Appendix A.

Human neck is a part of the spine and the spine consists of three main sections; cervical spine, thoracic spine and lumbar spine as shown in Figure 1.2. Each of these spine sections are formed by small bony elements which are called "vertebrae". Cervical, thoracic and lumbar spines have 7, 12 and 5 vertebrae respectively.

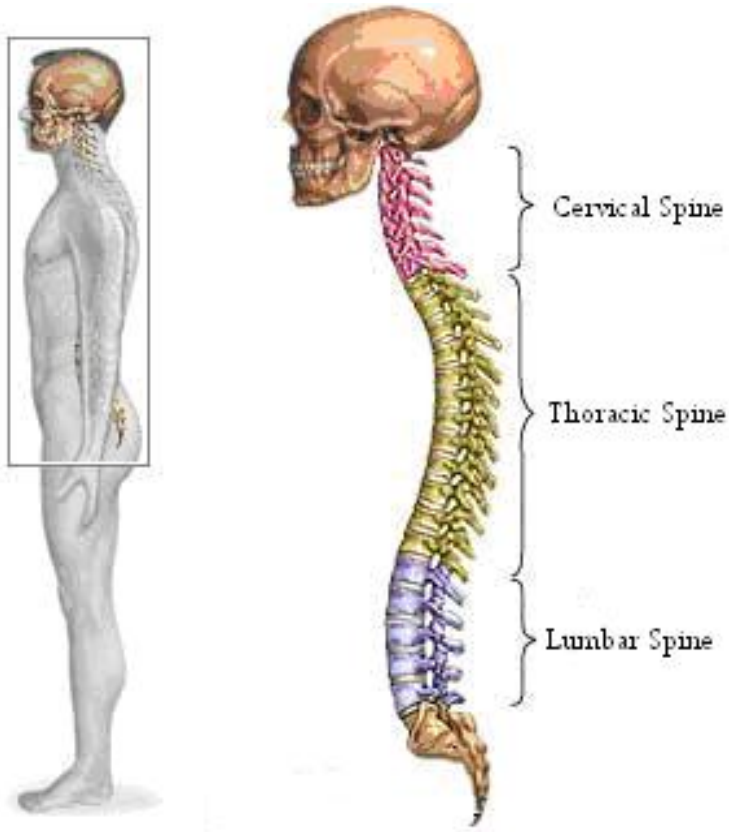


**Figure 1.2 Human Spine [13]**

Cervical spine is the uppermost portion of the human spine and it constitutes the human neck as shown in Figure 1.2. It is the connection between head and the

thoracic spine. It supports the head and protects the spinal cord. It is an articulate structure made up joints allowing for motion of the head relative to the torso, and so it is the main concentration point of whiplash injury. The four basic motions of cervical spine are flexion (i.e. forward bending), extension (i.e. rearward bending), lateral (i.e. sideward) bending and axial rotation which are described in the following sections.

### 1.4 Phases of Whiplash Injury

As discussed in previous sections, if the biological system deforms beyond a tolerable limit which results in damage to anatomical structures and/or alteration in normal function, physical injury will take place during the rear end collision[14]. The mechanism involved is called "injury mechanism". In the rear end collisions, the head and neck are exposed to the inertia and contact forces, which may load or deform the tissues in the neck beyond tolerable limits, resulting in injury.

During a rear end automobile collision, the occupant body goes through an extremely rapid and intense acceleration and deceleration. In fact, a whiplash injury during the rear end collision occurs in less than 500 milliseconds. This duration can be divided into four phases in which different forces acting on the body that contributes to the overall injury. In order to explain these phases clearly, some critical snapshots from the high speed videos of whiplash tests performed during the study is presented in Figure 1.3 and the phases are described as follows:

Phase 1 (Retraction Phase)

The snapshots shown as Instance 1 and Instance 2 in Figure 1.3 are the starting and ending instances of retraction phase respectively. The vehicle is first pushed or accelerated forward, and is essentially pushed out from under the occupant as occupant's back forces into the seat. The upper torso is pushed forward by the seat back while the occupant’s head remains nearly stationary. As a result, an abnormal S-curve develops in the occupant cervical spine while the upper cervical spine gets into flexion and lower cervical spine gets into extension as occupant's seat back rebounds forward adding to the forward acceleration of the torso. This phase ends

when the maximum relative translation of the head and torso is reached as shown in Instance 2 of Figure 1.3.

Phase 2 (Extension Phase)

The snapshots shown as Instance 2 and Instance 3 in Figure 1.3 are the starting and ending instances of extension phase respectively. This phase starts after the head reaches the maximum translation with respect to the torso and then head rotates rearwards. During this phase, occupant's head moves backward into extension, creating a powerful shearing force in the neck. This shearing, combined with the compression of the spine in the neck causes substantial injury. As a result of this rotation some extensive orientations between the upper and lower motion segments of the spine occur. This phase ends when the head touches to the head restraint.

Phase 3 (Rebound Phase)

The snapshots shown as Instance 3 and Instance 4 in Figure 1.3 are the starting and ending instances of rebound phase respectively. This is probably the most damaging phase of the whiplash phenomenon. This phase starts after the head touches the head restraint and then the head bounds to the front. This bounce from the head restraint may cause the maximum head translational acceleration occurring through all phases. This phase ends when the torso of the dummy is stopped by the seat belt.

Phase 4 (Protraction Phase)

The snapshots shown as Instance 4 and Instance 5 in Figure 1.3 are the starting and ending instances of protraction phase respectively. The protraction phase occurs when differential motion between the head and torso are reversed. In this fourth phase, occupant's torso is stopped by the seat belt and the head is free to move forward without any restraint. This results in a violent forward-bending motion of the neck, straining the muscles and ligaments, tearing fibers in the spinal discs, and forcing vertebrae out of their normal position. Occupant's spinal cord and nerve roots get stretched and irritated, and the brain can strike the inside of the skull. When head reaches the maximum translational distance with respect to torso, the phase ends.

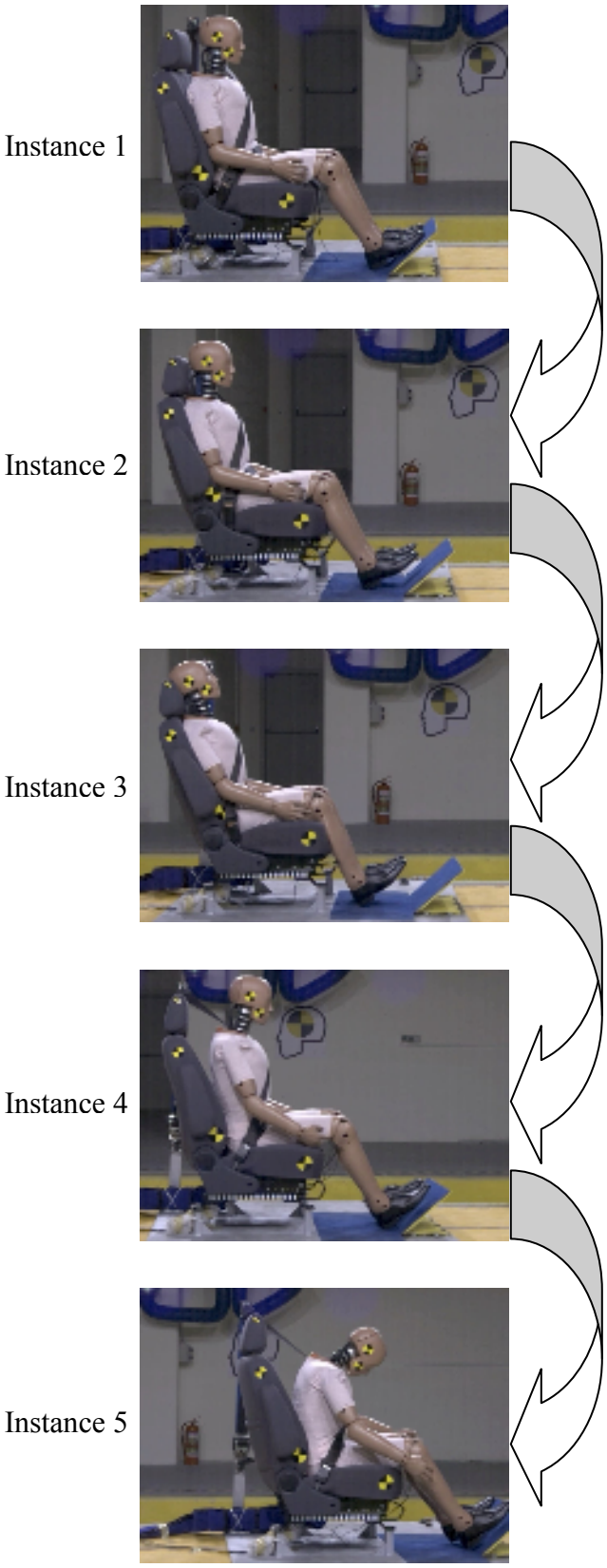


**Figure 1.3 Phases of Whiplash Injury**

In relation to the phases of whiplash injury, there are many hypotheses which explain the whiplash injury mechanisms. To understand the details of the whiplash injury, some of these whiplash injury mechanism hypotheses are also given in Appendix A.

### 1.5 Medical and Economical Importance of Whiplash Injuries

At the end of the 1970s WADs represented nearly 30% of all disabling injuries in motor vehicle collisions in Sweden [15]. The incidence of WADs has risen in the United Kingdom in 1982 from 7.7 % of all emergency accidents to 57% in 1995. According to Ono and Kanno [2], based on 1993 insurance statistical data in Japan, 50% of all car to car collisions particularly at low impacts velocities resulted in WADs and the number of WADs still increasing over time. In the years between 1999-2004, there occurs up to 3.000.000 whiplash associated cases annually in USA and it is estimated that there are 15,500,000 Americans who have chronic whiplash in 2004 [5].

Hell et al. [16] identified risk factors and the population at risk of WADs; using a large database of old insurance data material covering 15000 car to car collisions in Germany in 1990 involving injured occupants. In about 54% of these cases the pattern was a rear end collision, in correspondence with the Japanese findings by Ono and Kanno [2]. In order to obtain an overview of the real scenarios, 517 rear end collisions were analyzed medically and technically. Females were generally at higher risk, and older people showed higher risk for high-grade cervical spine distortion injuries.

In depth collision analysis by Boström et al. also indicated higher risk for females [17]. The fact that women generally have smaller values of neck circumference suggests that this may relate to the actual risk factor, although more research in this area should be performed [16].

Although classified as a minor injury whiplash-associated disorders are very costly to the society. The costs to the society of WADs in the early nineties have been estimated to be 700 million Euro in Germany and 210 million Euro in Sweden [9]. Based on these data a cost estimate for the European society for neck injuries in rear

end impacts is in the order of 5-10 billion Euros per year. The incidence of new WAD patients due to automotive accidents in the Netherlands is estimated to be more than 15,000 per year with total costs to the Dutch society of more than 300 million Euro based on the insurance data in 1994 [3] . In addition to this data, the socio-economic losses for rear end collisions are increasing year by year [16]. Based on another study performed in 1996, it is again estimated that whiplash injuries cost for Europe 10 billion Euro per annum [18]. With respect to the 2004 insurance data, whiplash claims cost for UK insurers 1.6 billion GBP and US insurers pay 10 billion USD per annum [4].

### 1.6 Some Previous Studies on WADs with Crash Test Dummies

Several previous studies have been conducted about whiplash related subjects. Some of these studies have been concentrated mainly on the biomechanical part of it such as finding new whiplash injury criteria, creating a new cervical spine model for whiplash and so on. However there are also other studies concentrated more on the mechanical part of whiplash like a new seat design against whiplash, finding the effects of whiplash on different crash test dummy types and so on. Since it is basically aimed to perform some low speed rear impact (whiplash) tests with crash test dummies in this thesis, some studies related to this thesis are explained in this section. All the detailed information about the crash test dummies which are Hybrid III 5th, 50th, and 95th percentile dummies, BioRID II, RID2 are given in Appendix B.

In the study of Davidsson, Lövsund, Ono, Svensson and Inami, a comparison between BioRID P3 (the earliest version of BioRID II) and Hybrid III performance in rear impacts is presented. The BioRID P3 was compared with human volunteer test data in a rigid and a standard seat without head restraints. The dummy kinematics performance, pressure distribution between subject and seatback, neck loads and accelerations were compared with those of ten human volunteers and a Hybrid III. The BioRID P3 provided repeatable test results and its response was very similar to that of the average volunteer in rear impacts at velocity difference of 9 km/h [19].

Linder, Svensson and Viano have evaluated the BioRID P3 and the Hybrid III in pendulum impacts to the back with respect to the human subject test data. This study evaluates both BioRID P3 dummy for rear impacts and the Hybrid III dummy by means of a recently available set of human subject data. The BioRID P3 and the Hybrid III were evaluated by means of pendulum impacts to the back and compared with the data from previously run cadaver tests. Seated dummies were struck with a pendulum with a mass of 23 kg and an impact velocity of 4.6 m/s at the level of the 6th thoracic vertebra. The results showed that peak values and temporal responses of the BioRID P3 was closer to that of the corridor of the cadavers than the Hybrid III in terms of horizontal, vertical, and angular displacement of the head and of the head relative to first vertebra of thoracic spine (T1) [20].

Philippens et al. from TNO Automotive, Netherlands compared the biofidelity of BioRID II and RID 2 crash test dummies in low speed rear end impacts with respect to each other also compared both of them with respect to Hybrid III dummy. They have used a rigid seat without a head restraint. The results show that both rear impact dummies are capable of simulating rear impact responses, especially the head-neck kinematics. A difference in load pattern was found, which could be relevant when injury criteria will be based on neck forces and/or torques. Moreover, the dummies show a different interaction with the seat back, illustrated by the differences in first thoracic vertebrae (T1) kinematics: BioRID II shows larger first thoracic vertebrae (T1) rotation and more ramping up than RID2, while spine straightening is comparable for both dummies. The current study showed good scores for both dummies in the setup on which they are based. The biofidelity score of BioRID II is slightly better than for RID2, while the performance of the Hybrid III is relatively poor. However, repeatability, reproducibility and handling are not part of the evaluation, even though they are important for the practical use of the dummies [21].

Viano and Davidsson have proposed a new whiplash injury criterion by evaluating neck displacements of 10 volunteers, BioRID P3 and Hybrid III from sled tests at 8.6 km/h with a standard seat and 9.3 km/h with a rigid seat in their study. They have used the film analysis method to determine the rotation, and x and z displacements of

the occipital condyles (OC), the base of the skull, with respect to first thoracic vertebrae (T1). For the volunteers, average and standard deviations were determined and cross-plotted as OC rotation versus x-displacement, and z-displacement versus x-displacement of OC-T1. These responses have provided corridors for the natural range of neck motion in rear impacts. For these parameters, BioRID P3 and Hybrid III have closely simulated the volunteer neck kinematics. Tests of the Saab SAHR (SAAB Active Head Restraint) and standard head restraints showed differences in neck displacements that are consistent with field whiplash rates. A Neck Displacement Criterion (NDC) has been proposed to assess whiplash risks. By using the BioRID P3 and Hybrid III responses in sled tests and knowing the whiplash rates for the Saab SAHR and standard head restraints, initial working targets for NDC are proposed for consideration [22].

In the study of Derosia, Yoganandan and Pintar they have compared rear impact responses of different sized adult Hybrid III dummies. Rear impact sled tests were conducted using 5th, 50th, and 95th percentile Hybrid III dummies to evaluate proposed injury criteria. Different head restraint heights (750, 800 mm) and backset positions (0, 50, 100 mm) which is the distance between the back of the head and front of the head restraint were used to determine axial and shear forces, bending moments, and some injury criteria. The time sequence to attain each parameter was also determined. Three events were identified in the response. Event I was coincident with the maximum rearward motion of the torso, Event II occurred at the time of the peak upper neck flexion moment, and Event III occurred at the time of the maximum rearward motion of the head. Parameters such as backset position, head restraint height and seat-head restraint interaction affected impact responses. Head rotations increased with increasing backset position and increasing head restraint height. However, some injury criteria did not exhibit such clear trends. The 50th percentile dummy responded with consistent injury criteria values (e.g., the magnitude of the injury criteria increased with backset position increase or head restraint height decrease). However, the 5th and 95th percentile dummies did not demonstrate such trends [23].

Kim et al. from Rear Impact Dummy Evaluation Task Group of the Occupant Safety Research Partnership/USCAR (United States Council for Automotive Research) have made a comparison of the BioRID II, Hybrid III and RID2 in low-severity rear impacts. The BioRID II, 50th percentile Hybrid III and RID2 crash test dummies, all representing a mid-size adult male, were subjected to the rear impact sled tests. Their measured and calculated responses were used to evaluate their sensitivity to sled velocity, head restraint position, and other test setup parameters. Three test series were conducted using different sled acceleration pulses and different types of seats. For conditions where three identical tests were conducted, repeatability was evaluated. In Series A, the effect of sled velocity on the Hybrid III and RID2 was evaluated. For the RID2, the effect of the initial backset position was also evaluated in this series. In Series B, the head restraint position and the sled velocity were changed to see how the performances of the BioRID II, Hybrid III and RID2 were affected. In Series C, the effect of sled velocity changes and head restraint position on the Hybrid III and RID2 were again evaluated, and repeatability was assessed [24].

In the study of Kuppa, Saunders and Stammen from National Highway Traffic Safety Administration, a new whiplash injury criterion is proposed by performing some rear impact sled tests using Hybrid III dummy for "FMVSS No 202 Head Restraints" regulation tests. The injury risk curve, based on the head-to-torso rotation of the Hybrid III dummy, was developed using insurance claims data, and the rear impact sled tests with the Hybrid III dummy. The feasibility of the application of this injury criterion in rear impact vehicle crash tests and sled tests has also been performed. The sled test results indicate that the developed whiplash injury criterion correctly predicts improved performance of head restraint and seat systems [25].

### 1.7 Scope of the Thesis

Although there are many different whiplash test protocols used in the vehicle safety testing, the most recent one is the Euro NCAP (European New Car Assessment Programme) Whiplash Test Protocol [26] which is first issued on February 2009. It is described to use a BioRID II crash test dummy during the whiplash tests in the Euro

NCAP Whiplash Test Protocol. Using a special rear crash test dummy, BioRID II, is more appropriate in whiplash tests if it is possible. However, this dummy is very rare and expensive and it is not possible for this study to buy such an expensive dummy. Additionally, as it is clearly seen from the previous studies, the Hybrid III family crash test dummies are very commonly used in the whiplash related research studies. It is also decided in this study to perform the whiplash tests by using an instrumented Hybrid III family 50th percentile male adult crash test dummy according to the most recent whiplash test protocol, Euro NCAP Whiplash Test Protocol to get the required data and to gain experience about the whiplash testing.

In this study, the effect of three different head restraint positions with respect to the head of the occupant at three different impact velocities, totally nine configurations will be examined by performing the sled crash tests using the crash simulation system available in METU-BILTIR Center Vehicle Safety Unit Sled Test Facility. In order to perform these sled crash tests a test sample consisting of a particular seat, a three point generic seat belt, a hybrid III family 50th percentile male adult crash test dummy, has been prepared according to the Euro NCAP Whiplash Test Protocol.

As it is stated previously there are other low speed rear impact test protocols like IIWPG (International Insurance Whiplash Prevention Group) [27], FOLKSAM [28], and ADAC [29] and these will be explained in Chapter 2. Euro NCAP Whiplash Test Protocol which is used in this study will also be explained in Chapter 2.

Preparation of the test sample, positioning of the crash test dummy in the test sample, preparation of the required test pulses and so the test procedure based on the Euro NCAP Whiplash Test Protocol will be explained in Chapter 3.

Test data which are obtained from the crash test dummy sensors and the high speed videos taken during the tests and their assessments by using the defined whiplash injury criteria will be presented in Chapter 4. The behavior of the seat in each test according to the whiplash injury criteria scores defined in Euro NCAP Assessment Protocol [39] will also be discussed in the same chapter.

Finally, in Chapter 5, conclusions and suggestions for future works will be presented.

# CHAPTER 2

# LOW SPEED REAR IMPACT TEST PROTOCOLS

There are several organizations, mainly from the field of consumer information and insurance institutes, working on the development of test procedures and assessment criteria regarding to WADs. The most active ones are Thatcham from UK and IIHS (The Insurance Institute for Highway Safety) from USA which are united in the group of IIWPG (International Insurance Whiplash Prevention Group), SNRA (Swedish National Road Administration) and Folksam from Sweden, and ADAC (Allgemeiner Deutscher Automobil-Club) from Germany. Although these organizations have their own low speed rear impact test protocols, they are also integrated in the preparatory activities of Euro NCAP for the assessment of whiplash injuries [30]. Below a summary of the most common test protocols other than Euro NCAP Whiplash Test Protocol is presented.

## 2.1 IIWPG Test Protocol

International Insurance Whiplash Prevention Group (IIWPG) test protocol [27] describes a standard for evaluating and rating the ability of seats and head restraints to prevent neck injury in moderate and low-speed rear-end crashes. The evaluation procedure is a two-stage process, starting with the measurement and rating of the static geometry of head restraints and followed by a dynamic evaluation in a simulated rear-end crash of those seats that meet certain geometric criteria.

A head restraint prevents neck injury in a rear-end crash by supporting an occupant's neck and head so they can be accelerated together with the torso as the seat and head restraint are driven forward. To accomplish this, a vehicle's head restraint needs to

be tall enough so that the top of the head restraint is above the center of gravity of the tallest expected seat occupant's head. In addition, the top of the head restraint should be close to the back of an occupant's head so that it can contact and support the head early. The farther the restraint is from the head, the less support it can provide and, consequently, the more the head and torso will tend to move separately, creating potentially injurious forces on the neck.

A head restraint design with a geometric rating of acceptable or good will be tested in a simulated 16 km/h rear impact to determine a dynamic rating of how well the restraint supports the torso, neck, and head. The final overall rating of the seat will be a combination of its geometric and dynamic ratings. A seat design with a geometric rating of marginal or poor automatically will receive an overall rating of poor. It will not be subjected to dynamic testing because its geometry is inadequate to protect anyone taller than an average-size adult male.

### 2.1.1. Measurement and Rating of Static Head Restraint Geometry

Static geometric evaluations are based on measurements of height and backset positions that are made with a manikin representing an average-size adult male. To be rated at least "marginal" which corresponds to the "Zone 3" in Figure 2.1, the top of a restraint should be no lower than the center of gravity of the head (no more than 10 cm below the top of the head) and no farther than 11 cm behind the head. Otherwise, the head restraint geometric evaluation is "poor" and it is shown by "Zone 4" in Figure 2.1. Higher head restraints provide protection for even taller occupants, and closer head restraints can reduce the time the head is unsupported in a rear crash. An "acceptable" geometric rating implies a head restraint no farther than 8 cm below the top of the head and no farther than 9 cm behind it which corresponds to the "Zone 2" in Figure 2.1. "Good" geometry implies a head restraint no further than 6 cm below the top of the head and no farther than 7 cm behind it as it is sown as "Zone 1" in Figure 2.1.

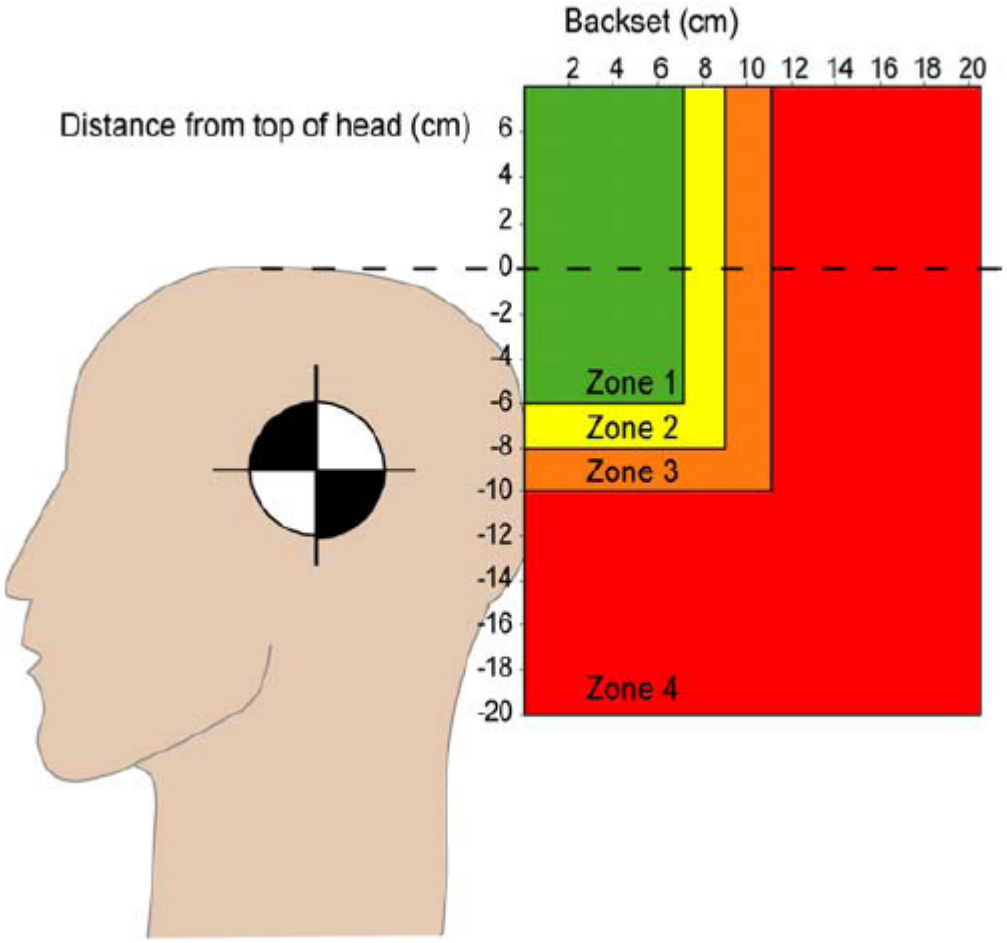


**Figure 2.1 Diagram of Geometric Head Restraint Ratings**

The seats with fixed geometry are rated using the measured height and backset when the seat is adjusted according to the RCAR (Research Council for Automotive Repairs) procedure. The seats with adjustable head restraints that cannot be locked into the adjusted position are rated based on measurements from the unadjusted (lowest and rearmost) position of the head restraint. Seats with locking head restraint adjustments are rated using the midpoint between the lowest/rearmost adjustment and the highest/foremost adjustment.

For head restraints with marginal or poor geometry, the overall rating is poor. Head restraints with good or acceptable geometry undergo the dynamic testing.

### 2.1.2 Dynamic Testing

The dynamic test consists of a rear crash simulation in which a BioRID II dummy is positioned in the seat to be tested. The seat is attached to a crash simulation sled and accelerated/decelerated to represent a rear crash with a velocity change of 16 km/h. The acceleration profile is in Figure 2.2.

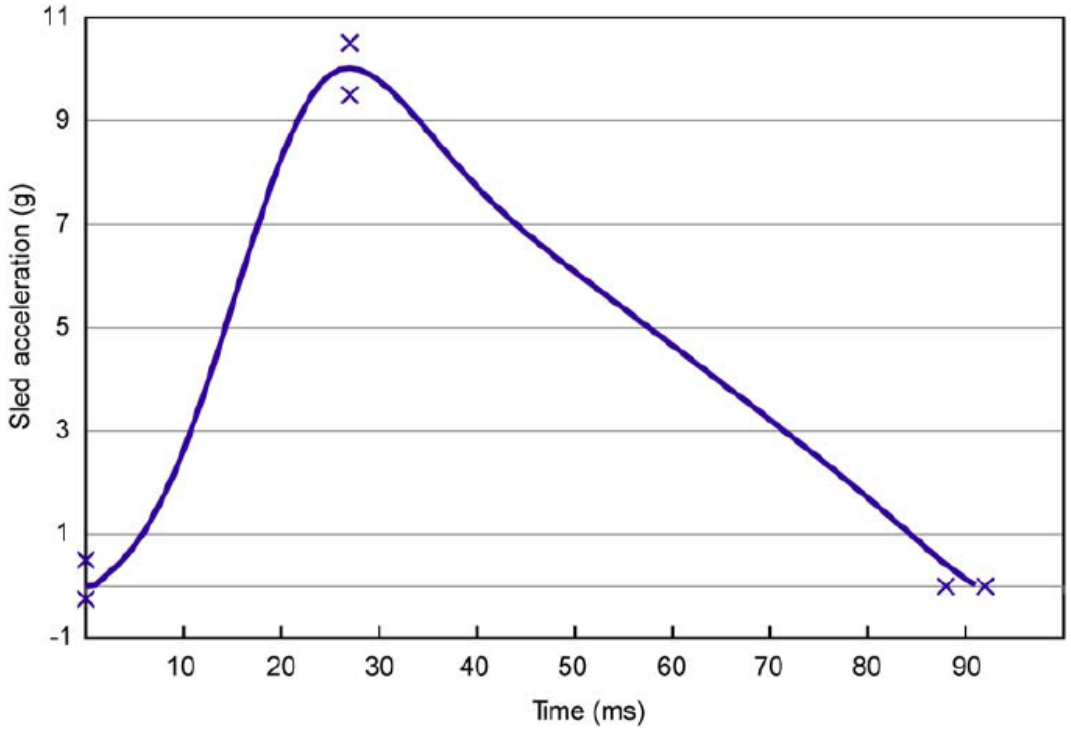


**Figure 2.2 Target Sled Acceleration and Specification Corridors in IIWPG Test Protocol**

The dynamic test consists of a simulated rear crash on a sled device using a BioRID II crash dummy to represent a human occupant. The IIWPG procedure will use a sled test with the standard real crash pulse rather than a full-vehicle crash test. In theory, full-vehicle test results could include the effect that a vehicle's rear structure might

have on seat performance. However, in real-world rear crashes, vehicles experience impacts with a wide range of vehicle types at a variety of speeds. Thus, the seats in rear struck vehicles can experience a wide range of crash pulses. This IIWPG procedure is designed specifically to assess the performance of seats and head restraints, not rear-end structures, the designs of which are driven by many factors other than neck injury prevention.

The performance criteria for the dynamic test are divided into two groups: two seat design parameters and two test dummy response parameters. The first seat design parameter, time-to-head-restraint-contact, requires that the head restraint or seatback contact the seat occupant's head early in the crash. The main purpose of requiring a head restraint to have only a small distance behind the head is to reduce the time until the head is supported by the restraint. Thus, the time-to-head-restraint-contact parameter assures that initially good or acceptable static geometry is not made irrelevant by poor seat design.

Some seats are designed to absorb some of the crash energy so that occupants experience lower forward accelerations. This aspect of performance, the second seat design parameter, is measured by the forward acceleration of the seat occupant's torso (T1 acceleration). In some cases, these designs may result in later head contact times. To assure that earlier head contact or lower T1 acceleration actually results in better support for the head.

In addition to these seat design parameters, two dummy response parameters also are measured: neck shear force and neck tension force. The critical values of the neck forces are set according to the distribution of neck forces observed in current seats with good geometry.

To receive a "good" dynamic rating, a head restraint must pass at least one of the seat design parameters and also have low neck forces. If neck forces are moderate or high, then the dynamic rating is only "acceptable" or "marginal". If neck forces are high and neither seat design parameter is passed, then the dynamic rating falls to "poor".

## 2.2 SNRA and Folksam Test Protocol

SNRA (Swedish National Road Administration) and Folksam test protocol [28] includes only the dynamic testing of the seats and it is created by performing the dynamic tests using in market seats. Three series of crash tests have been performed aimed at assessing whiplash injury risk in rear-end crashes. The first series of test was conducted in year 2003 with 13 seats tested. In 2004 another 14 seats were tested and in 2005, 9 additional seats were tested. In the tests, seats get points when certain limits in dummy readings have been exceeded. A highest possible point is “15” and best is “0”. A seat is regarded as ”good” if it gets up to 5 points, ”average” between 5.1 and 10, and ”poor” above 10 points.

All seats are mounted on a test sled. The crash simulations are made at three crash severities to measure the protective effect at several crash conditions. Based on the results from the real crash recorders, three test conditions at different velocity and acceleration are chosen as seen in Table 2.1. The three crash simulations covers that area, 4.5 g represents low risk but where many real crashes occur, 5.5 g represents medium risk and medium exposure, while 6.5 g represents high risk but low exposure.

**Table 2.1 Test Speed and Acceleration**

| Test | Speed | Mean Acceleration |
|---|---|---|
| Low Severity | 16 km/h | 4,5g |
| Mid Severity | 16 km/h | 5,5g |
| High Severity | 24 km/h | 6,5g |

The crash pulses of the test series, 2003, 2004 and 2005, are presented in Figures 2.3 and 2.4. The 2nd test pulse is changed after the first test series from the trapezoidal shape to the triangular shape, but with the same test speed and mean acceleration. The test series should not be directly compared because of this change. However, the results should be very close to one another.

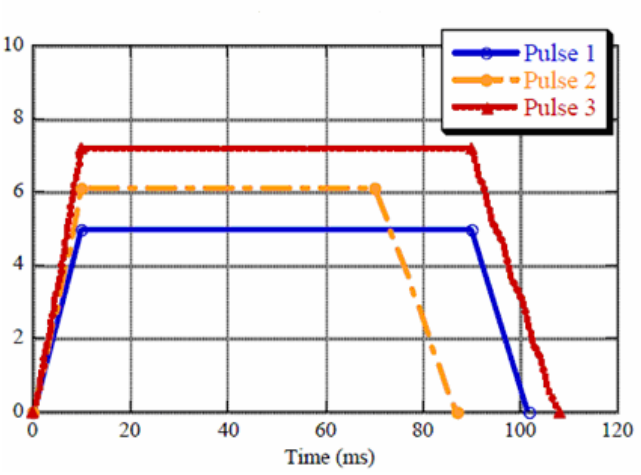


**Figure 2.3 Pulses Used in the first Test Series in 2003**

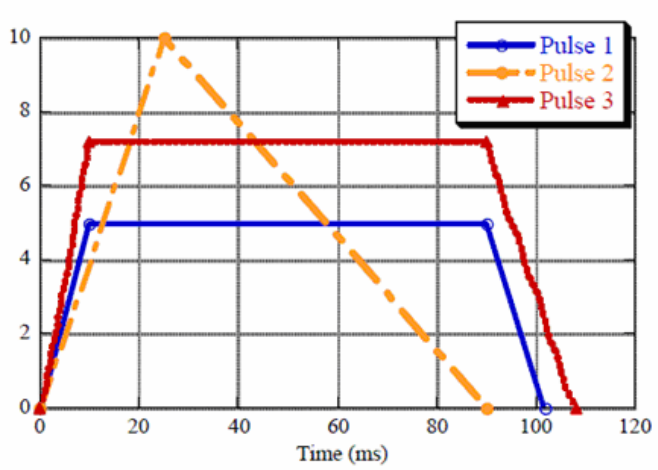


**Figure 2.4 Pulses Used in the Test Series in 2004 and 2005**

Other important test specifications are:

- Dummy: BioRID
- Measurements: Acceleration in head, chest, T1 and pelvis, forces and moments in upper and lower neck, belt load, head and chest velocity from the film analysis.
- Head restraint in mid positions.
- Seat back angle: 25 degrees using an H-Point Manikin
- Seat belt: Generic seat belt (non-car specific but geometry close to car geometry).

To rate the various seats regarding risk of whiplash injury three parameters were measured and used, which are $NIC_{max}$, $N_{km}$ and head rebound velocity [31]. The $NIC_{max}$ is expressed by the relative acceleration and velocity between the upper and lower neck. $N_{km}$ corresponds to the four neck injury criteria which are $N_{fa}$ (neck flexion anterior), $N_{ea}$ (neck extension anterior), $N_{fp}$ (neck flexion posterior) and $N_{ep}$ (neck extension posterior). These four criteria are calculated by adding the standardized shear forces and standardized corrected bending moments of neck. Head rebound velocity is the relative velocity of the head with respect to the sled velocity. The more detailed definitions of these parameters are given in Chapter 4. The overall rating is based on point scores. In the calculation of points, the seats got points if each measured parameter exceeded critical limits as described in Table 2.2. Two limits per injury criteria were used and maximum 2 points for $NIC_{max}$ and $N_{km}$ and were given, while maximum 1 point was given for head rebound velocity. High point scores indicate poor protection levels.

**Table 2.2 Critical Limits**

| Criterion | Lower limit | Upper limit | Green Low Risk | Yellow Medium risk | Red High Risk |
|---|---|---|---|---|---|
| $NIC_{max}$ | > 15 $m^2/s^2$ | > 18 $m^2/s^2$ | ≤ 15 $m^2/s^2$ | 15< $NIC_{max}$≤18 | > 15 $m^2/s^2$ |
| $N_{km}$ | > 0,3 | > 0,4 | ≤ 0,3 | 0,3< $NIC_{max}$≤0,4 | > 0,4 |
| Rebound velocity | > 4,5 m/s | > 6,0 m/s | ≤ 4,5 m/s | 4,5< $NIC_{max}$≤6,0 | > 6,0 m/s |

## 2.3 ADAC Test Protocol

The ADAC protocol [30] is separated into two parts as neck injury protection tests and seat stability tests.

### 2.3.1 Neck Injury Protection Test Procedure

The ADAC neck injury protection test procedure including type of dummy, set up procedure, seat and dummy positioning and pulse shape is mainly equivalent to the IIWPG procedure. The most important divergence of ADAC procedure from IIWPG procedure is as follows:

Sled Test Acceleration Pulse: ADAC uses the triangular pulse of velocity change of 16 km/h according to the IIWPG requirements to examine the neck injury protection of a vehicle seat. Additionally one test with a higher severity, velocity change of 25 km/h, is carried out and can be seen in Figure 2.5.

Assessment Criteria: For the neck injury assessment the measuring results from BioRID II dummy of the 16 km/h and 25km/h test are used. For final neck injury rating five criteria are used as in Table 2.3. The Lower Neck Load Index (LNL) is calculated from the moments and forces of lower neck.

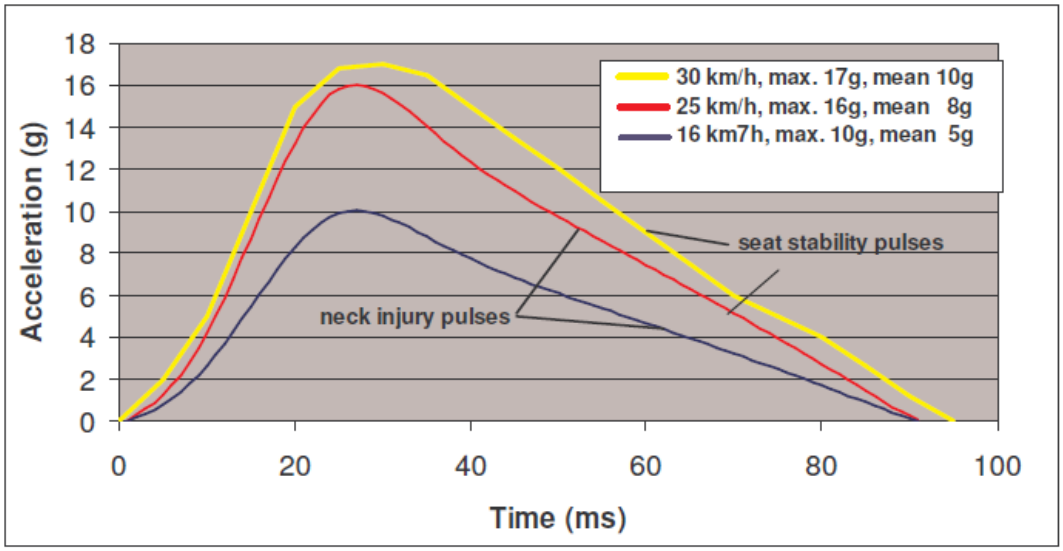


**Figure 2.5 Pulses for Neck Injury and Seat Stability Tests**

**Table 2.3 Criteria for Neck Injury Assessment**

| Criteria | Lower Limit | Upper Limit |
|---|---|---|
| NIC | 10 | 20 |
| $N_{km}$ | 0,3 | 0,5 |
| LNL | 1,5 | 3 |
| Extension Rotation | 5 | 25 |
| Retraction | 10 | 15 |

Additionally other important effects such as failure of active head rest, dummy ramping and fractures of the seat are monitored. The figures in the table indicate the lower/upper limits for the scaling: The lower limits apply to the best possible mark 0.6, the upper limits to the worst possible mark 5.5. Within these limits a sliding scale is used. An arithmetic mean of all these five criteria grades is taken and the

mean mark of the test is calculated for both 16 km/h and 25km/h tests. The overall neck injury protection mark is calculated as the mean of the 16 km/h and 25km/h tests.

### 2.3.2 Seat Stability Test Procedure

For seat stability evaluation ADAC procedure uses the maximum dynamic seat back angle result from the 25 km/h neck injury test. Additionally a separate test with a 30 km/h pulse and a Hybrid III 95th percentile dummy is carried out as in Figure 2.5.

Other important conditions of this additional test are:

- Dummy: Hybrid III 95th percentile
- Set-up: Equivalent to neck injury testing
- Pulses: Triangular maximum 17g, mean 10g, 30km/h and triangular maximum 16g, mean 8g, 25km/h

Assessment Criteria: For the evaluation of the maximum dynamic back rest angle a sliding scale with 15 deg lower limit and 35 deg upper limits are used and the lower limits apply to the best possible mark 0.6, the upper limits to the worst possible mark 5.5. The overall seat stability rating is calculated as the mean of 25 km/h and 30 km/h test marks.

### 2.3.3. Overall Quality Assessment

The total rating is based on the overall neck injury protection rating and the overall seat stability rating. Neck injury protection is weighted with 70%, and seat stability with 30%. If one of the marks of neck injury or seat stability is greater than 4.5, a penalty of 1 mark is applied. Table 2.4 shows the ranges of overall marks and their classification.

**Table 2.4 Ranges of Marks and Their Classification in ADAC Test Protocol**

| Mark | Classification | |
|---|---|---|
| 0,6 - 1,5 | ++ | very good |
| 1,6 - 2,5 | + | good |
| 2,6 - 3,5 | 0 | sufficient |
| 3,6 - 4,5 | θ | marginal |
| 4,6 - 5,5 | - | poor |

## 2.4 Euro NCAP Whiplash Test Protocol

Established in 1997, the European New Car Assessment Programme (Euro NCAP) provides consumers with a safety performance assessment for the majority of the most popular cars in Europe. By performing its specific crash tests, Euro NCAP has rapidly become the driver of major safety improvements to new cars. Rather than focusing exclusively at life threatening injuries, the intention from the start has been to encourage manufacturers to make improvements in all areas and to avoid concentrating attention on any individual area of the car [32].

So far, Euro NCAP has assessed the protection for car occupants in frontal and side impact as well as the protection afforded by the car's front to pedestrians. However, it has not included a rear impact test up to 2009. The interest to actively address the problem of "whiplash" associated neck injuries was first raised in 2000 as part of Euro NCAP future development strategy and in February 2009 the new Euro NCAP Whiplash Test Protocol [26] has been started to be used. The tests performed during this study are also based on the Euro NCAP Whiplash Test Protocol.

Although this protocol is used in this thesis, a modification on it is done because of the available technical conditions in the laboratory. This difference is the test dummy used in the test. In the Euro NCAP testing protocol, the BioRID II dummy which is a

special dummy produced for the neck injury assessments is used during the tests. However, since this dummy is not available in the laboratory and it is very expensive to purchase it for the time being, the Hybrid III 50th percentile male dummy is used during the study. There are some important points which justify usage of this dummy. First of all, the objective of this study is to see how the head restraint position with respect to the head of the occupant affects the whiplash injury at different impact conditions. Since there will be a relative comparison between different head restraint positions and impact conditions, either usage of the Hybrid III 50th percentile male dummy or BioRID II dummy will give a correct result to make the comparison. Secondly, the BioRID II dummy is a dummy based and improved on the Hybrid III 50th percentile male dummy. Except the spine region, the dummy is the same with the Hybrid III 50th percentile male dummy. The main difference known is that the spine region of the Hybrid III 50th percentile male dummy behaves stiffer than the BioRID II one. Thirdly, there are still some regulations like United States "FMVSS 202 Head Restraints" regulation [33] and plenty of previous studies [19-25] which uses the Hybrid III 50th percentile male dummy in the approval and research tests since it gives a good result to make the assessments and comparisons.

# CHAPTER 3

## TEST SAMPLE PREPERATION ACCORDING TO EURO NCAP WHIPLASH TEST PROTOCOL

There are many whiplash testing protocols described in Chapter 2, however, the recent one is the Euro NCAP Whiplash Test Protocol [26] which started to be used in February 2009. Almost all of the organizations, who have worked on the older testing protocols, are integrated in the preparatory activities of Euro NCAP for the assessment of the whiplash injuries. So Euro NCAP protocol is based on the all previous experiences gained through older protocols. If it is seen from the website of Euro NCAP organization that more than 30 different car seats have been tested according to the Euro NCAP Whiplash Test Protocol in the period of February-April 2009, use of this protocol in this study is self evident.

In this study a whiplash test sample is prepared according to the Euro NCAP Whiplash Test Protocol. Main elements of this test sample are;

- A “steel plate” which simulates the floor of the vehicle.
- A “toe board” which is a small board oriented 45° from the horizontal on which dummy's feet rest when dummy sits in the seat.
- A “seat” on which the dummy sits during test.
- A “3 point generic seat belt” which holds the dummy on seat during the test.

The whiplash tests of this test sample have been realized on the IST Crash Simulation System and the details of this system is given in Appendix D. In order to

connect the test sample to the acceleration sled of the IST Crash Simulation System, the steel plate has been used. The steel plate has been securely connected to the sled by the help of M16 and M24 size of bolts. Other test sample elements which are seat, seat belt and toe board have also been connected on this steel plate. When everything has been connected to the sled, the crash test dummy has been sat in the seat. During the positioning of the dummy in the seat, two important equipments which are H-Point Manikin and Head Restraint Measuring Device (HRMD) used. Technical details of these devices are given in Appendix C. After the dummy has been positioned in the seat, the tests are ready to be realized. The details of the test sample preparation according to the Euro NCAP Whiplash Test Protocol [26], will be given in the following sections.

## 3.1 Preparation of Test Sample

### 3.1.1 Coordinates of Measurements

During the preparation of the test sample, Cartesian coordinate system is used. The sign convention for the coordinate system is as follows: Positive x direction is horizontally forward from dummy face and parallel to seat rails, positive y direction is to the dummy's left-hand side and positive z axis is vertically upward as in Figure 3.1.

The origin of all measurements done during this preparation work is located on the upper surface of the right hand rear seat mounting bolt hole, in the stationary part of the seat runner according to the Euro NCAP Whiplash Test Protocol and shown in Figure 3.2. This common origin will provide a means of comparing seat positions across test laboratories, when required. In the first instance, the right hand rear mounting hole is used as chosen in this study. If this is not present, the next available fixation point is chosen, considering available options in the following order: left hand rear, left hand front, right hand front according to the Euro NCAP Whiplash Test Protocol.

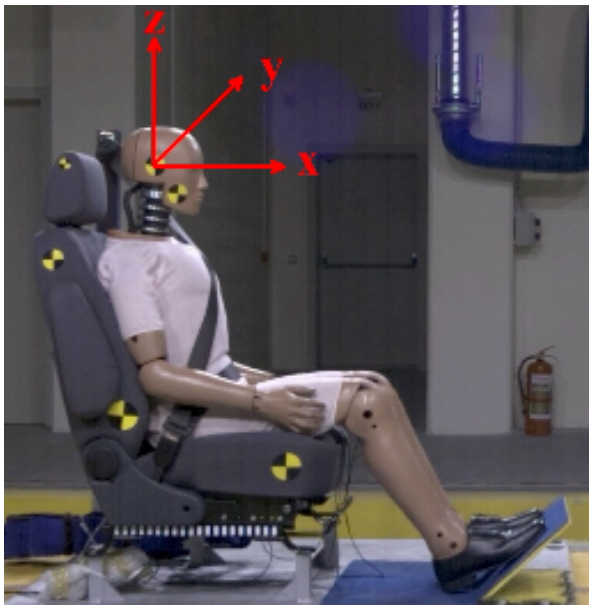


**Figure 3.1 Coordinates of Measurements**


**Figure 3.2 Origin of the Measurements**

### 3.1.2 Seat Positioning and Mounting on the Sled

All the base seat set-up specifications described in the following paragraphs is achieved within an angular tolerance of 0.2° and linear tolerance of 5 mm, with the exception of seat belt attachments.

A seat structure reference point is chosen in addition to the coordinate system origin (i.e. origin of the measurements). This is defined as a fixed point on the seat structure which stays in the same position relative to the vehicle, independent of any seat adjustment. In this thesis, the seat reference point is chosen as the front left bolt hole as in Figure 3.3, however, other non-moving parts of the seat mounting structure are acceptable according to the protocol. The seat structure reference point is chosen such that the relationship of the seat to the vehicle floor can be accurately reproduced on the sled.


**Figure 3.3 Seat Structure Reference Point**

There is a toe board which is the simulated floor of the vehicle and consisting of a horizontal section sufficiently large to rest the dummy's feet and connected to a section oriented 45° from the horizontal. Both surfaces of it are covered with the short-piled carpet as seen in Figure 3.4.

In order to define the height difference between seat and vehicle floor, a point named "heel rest point" is used. This point is found in the vehicle with removable floor mats not fitted and by using the accelerator pedal as follows (Figure 3.5):

- The geometric center point of the accelerator pedal contact surface is found (both laterally and vertically).
- A straight edge (i.e. edge of metal ruler in Figure 3.5) between the accelerator pedal center point and the fixed carpeting on the vehicle floor is placed such that the straight edge is tangential to the accelerator pedal surface at the center point.
- The heel rest point location is then the contact point of the straight edge on the vehicle floor.

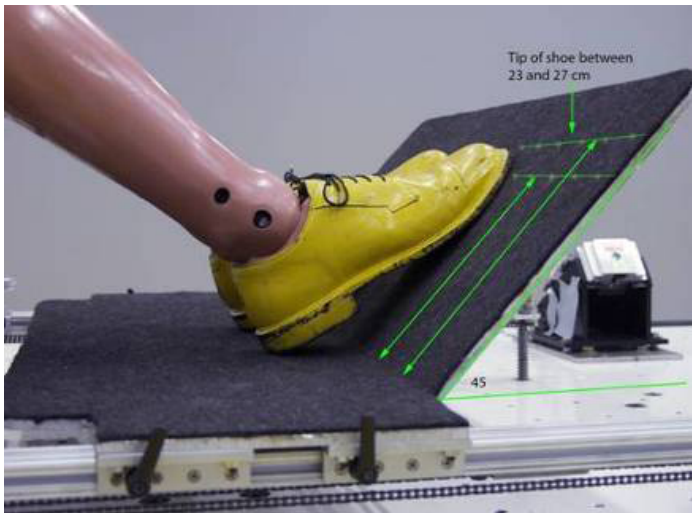


**Figure 3.4 Toe Board [26]**

After the heel rest point location is defined with respect to the origin of the measurements (i.e. right hand rear seat mounting bolt hole in this study), the height difference between it and the seat is measured and this is satisfied when mounting the seat to the sled.

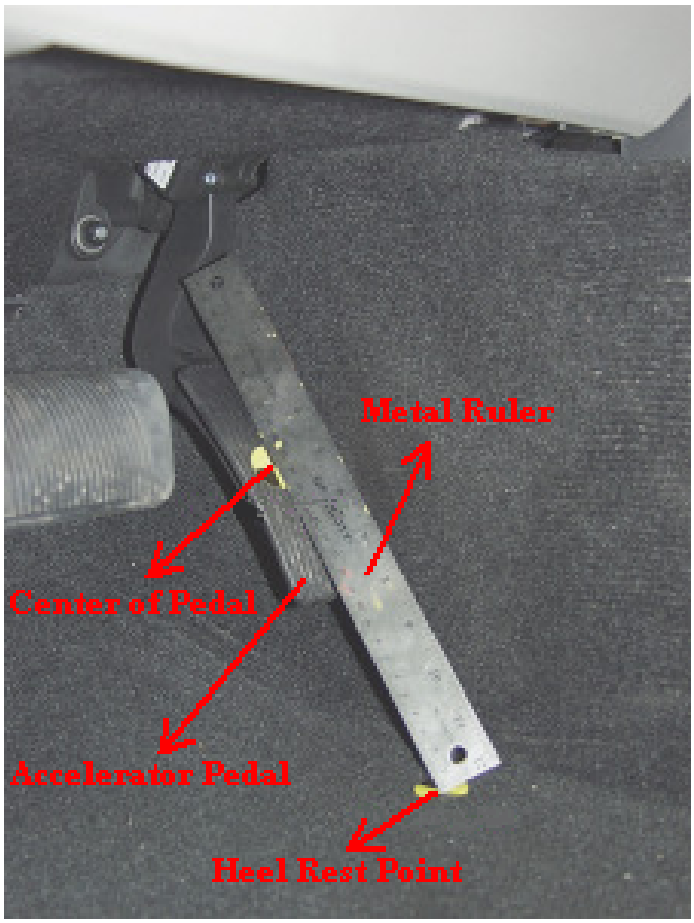


**Figure 3.5 Determination of Heel Rest Point on the Vehicle [26]**

After determination of origin, seat structure reference point and heel rest point have been completed, the process of mounting the seat to the 1400 x 1400 mm steel plate is realized. The seat, including all of its adjustment mechanisms and hardware that

normally connects it to the vehicle floor (e.g. longitudinal adjustment rails), is securely fastened to the steel plate with M10 bolts as seen in Figure 3.6. The attachment is made so that the seat's orientation relative to the horizontal is the same as it would be in its vehicle as defined by the physical vehicle measurements. The actual height of the seat from the steel plate may be different from its height above the vehicle floor, however, these heights are adjusted as the same in this study.


**Figure 3.6 Seat Mounted to the Steel Plate**

The toe board is also attached to the sled platform as in Figure 3.7. The horizontal floor portion is mounted at the same height relative to the seat bolts/rails as the heel

rest point. Seat mounts are rigid and non-deformable. The seat mount interface to the seat in the test sample is approximate that of the interface to the vehicle floor where the seat is mounted to floor by four M10 bolts in both cases.


**Figure 3.7 Toe Board Attached to the Steel Plate**

### 3.1.3 Seat Adjustment

Adjustments of the seat by using seat adjustment mechanisms before the test are explained in this subsection. However, to prevent information mess, only the adjustments of the existing mechanisms of the seat used in this thesis is explained. Other information about the own positioning of the seat can be found in the Euro NCAP Whiplash Test Protocol V2.9 [26].

The seat used in this thesis study is the driver (front left) seat of a light commercial vehicle as in Figure 3.8. This seat has the adjustment mechanisms of seat track, seatback tilt, cushion tilt, lumbar support and arm rest.


**Figure 3.8 Seat Used in the Thesis Study**

Because the setting of some adjustments may affect the adjustment range of other adjustments, the seat is set by following the order of the procedure outlined. Since the seat used in the thesis is new and has never been sat on, a person with a mass of 75 kg ± 10 kg should sit in the seat for 1 minute, twice, to flex the cushions as required in the Euro NCAP Whiplash Test Protocol [26]. This is done by the author of this study who has a mass of 83 kg. Additionally, the seat should be left at room temperature for more than six hours and not loaded for more than one hour previous to the initial installation of the H-Point Manikin which is explained in detail in

Appendix C. In the study, the seat is left at room temperature and not loaded for two days.

The seat track is initially taken in its most rearward locking position. The cushion tilt is set to the extreme of its range that puts the cushion angle (α) closest to zero (horizontal). The lumbar support is set to its most rearward position. The arm rest is set in the stowed position as shown in Figure 3.9. Then, the measurement of cushion angle of the seat is started. A point on the forward edge of the top surface of the seat cushion and midway between the right and left edges of the cushion is marked (Point 1 in Figure 3.9). A second point that is 400mm rearward from the first point and on a line parallel to the direction of the sled movement is marked (Point 2 in Figure 3.9). The cushion angle is the reading from a digital inclinometer sitting on the surface of the seat with the rearmost end on the rear seat mark as in Figure 3.9.


**Figure 3.9 Cushion Angle (α)**

The next step is to position the seat on the seat track as seen in Figure 3.10. For this purpose, two points are marked on the seat track on both sides when the seat is in the most backward position (Point 1 in Figure 3.10). Similarly, another two points are marked on both sides of the seat track when the seat is in the most forward position (Point 2 in Figure 3.10). On both sides of the seat, the distances between the two points are measured and the midways between these points are defined (Point 3 in Figure 3.10). Since the seat used in the thesis has an incremental adjusting seat track and it can be adjusted to the midway in the tolerance of ± 2mm, it is adjusted to the midway. If this tolerance is not possible to achieve, the seat track is adjusted to the first incremental position rearward of the calculated midrange position.


**Figure 3.10 Seat Track Adjustment**

### 3.1.4 Seat Belt Mounting

A generic three point lap-shoulder seat belt equipped with an inertia reel (i.e. rotating locking mechanism) shown in Figure 3.11 is used during the tests.

**Figure 3.11 Seat Belt Used in the Tests**

It is placed in such a way that the when belt is worn by the dummy it lies across the torso, clavicle and pelvis. Any anchorages not attached to the seat are positioned as shown in Figure 3.12.

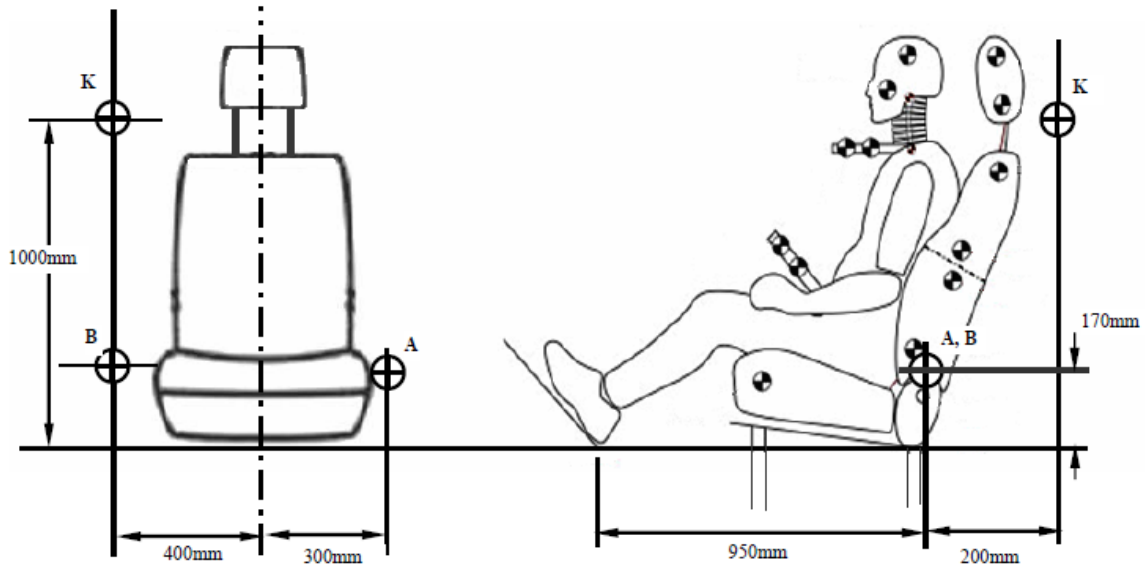


**Figure 3.12 Generic Seat Belt Anchorage Mounting [26]**

The marks, which correspond to the arrangement of the anchorages, show where the ends of the belt are to be connected to the sled. The anchorages are the points A, B and K. The tolerance on the position of the anchorage points is such that each anchorage point is situated at most at 50 mm from corresponding points A, B and K indicated in Figure 3.12.

The structure carrying the anchorages is rigid and constructed such that no permanent deformation occurs in the parts supporting the anchorages during the tests. Figure 3.13 shows the seat belt mounted to the test sample.

**Figure 3.13 Seat Belt Mounted to the Test Sample**

### 3.2 Crash Test Dummy Positioning

In order to sit Hybrid III 50th percentile crash test dummy in the seat, two important equipments are required. First and the most important one is the “H-Point Manikin”. Technical details about the H-Point Manikin are given in Appendix C. This device is a metal dummy consisting of a body, legs and metal weights. This manikin has adjustable body parts in different dimensions and masses. With respect to the test regulation or protocol used, the required dimensions and masses of this manikin is adjusted. In this study it is adjusted as defined in Euro NCAP Whiplash Test Protocol [26] and the required steps of installation of the manikin in the seat is performed. After it is seated another device called “Head Restraint Measuring Device (HRMD)”

which is a metal head form is used. This device can be connected to the H-Point Manikin as the head of it and it is used to measure the dimensions between the head of the dummy and the head restraint of the seat. When both devices are connected and seated, the H-Point locations of the seat are measured from the H-Point marks of the H-Point Manikin by using a mobile coordinate measuring machine (CMM).

### 3.2.1 H-Point Manikin Installation

The H-point (or hip-point) is the relative vertical location of an occupant's hip, specifically the pivot point between the torso and upper leg portions of the body, either relative to the floor of the vehicle or relative to the height above pavement level as shown in Figure 3.14 [27].

Before positioning the crash test dummy in the seat, this point is defined relative the origin by using the device called "H-Point Manikin". Similarly, the H-Point Manikin is also used in this thesis study before the tests and the H-Points on both sides of the crash test dummy are measured by using a mobile coordinate measuring machine (CMM) as shown in Figure 3.15. The procedure for using H-Point Manikin and finding the H-Point location of the seat is given in detail in Appendix C.

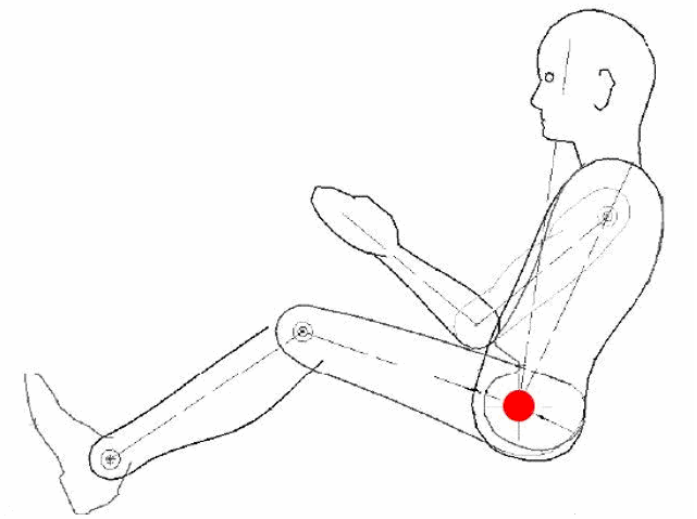

**Figure 3.14 H-Point on Test Dummy [27]**


**Figure 3.15 Measuring H-Point Locations from H-Point Manikin**

### 3.2.2 HRMD Installation

In order to measure the position the head of the crash test dummy with respect to the head restraint of the seat, a device called “Head Restraint Measuring Device (HRMD)” is used. This device is simply a special metal head form, which has the backset and height probes on it. By the help of these probes, the position of this head form relative to the head restraint is measured. When positioning the crash test dummy in the seat, these measurements are used. Detailed information about the technical details of HRMD and the procedure of installation of HRMD according to the Euro NCAP Whiplash Test Protocol is given in Appendix C. The installed HRMD in the test seat can be seen in Figure 3.16.

**Figure 3.16 HRMD Installed in the Seat**

### 3.2.3 Head Restraint Positions

There are two parameters that define the head restraint position with respect to the dummy head. These are “distance from top of the head, h,” and “backset, b,” “Distance from top of the head” is defined as the vertical measurement between height probe of the HRMD and the top of the head restraint as seen in Figure 3.17. “Backset” is defined as the horizontal measurement between the back surface of the HRMD head and the front surface of the head restraint as measured by the backset probe of the HRMD as seen in Figure 3.17.

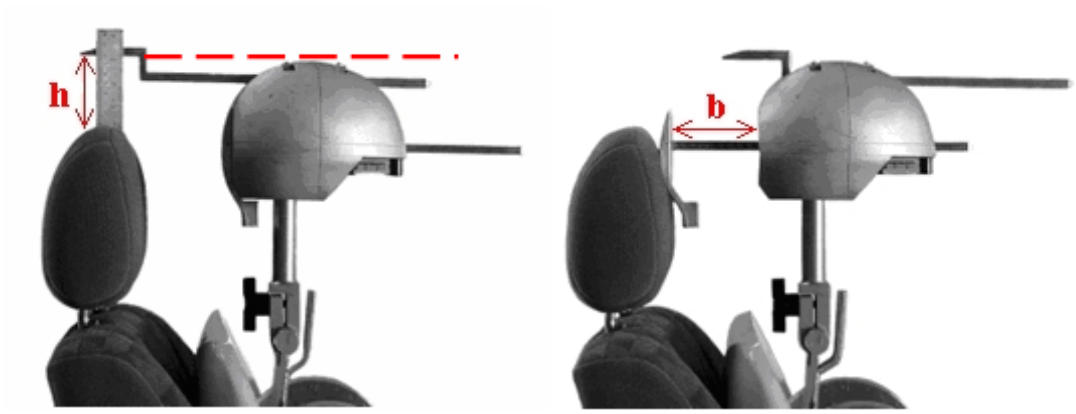


**Figure 3.17 Distance From Top of the Head (h) and Backset (b)**

After all of these positioning procedures, although the head of the dummy has a specific position with respect to the head restraint of the seat, it is aimed to see how head restraint position affects the whiplash injury with different test pulses in this study. So, three different head restraint positions have been used in the tests of this study.

One of these positions is already obtained after all of the installation procedures of H-Point Manikin and HRMD have been performed. After the HRMD is installed in

the seat, the distance from top of the head and the backset is measured from HRMD and this is the standard position found for the Euro NCAP Whiplash Test Protocol. Apart form it is thought to see how the position extremities of the head restraint affects the whiplash injury. So another two positions are defined as the nearest and furthest positions of the head restraint to the dummy head. Since the H-Point location of the dummy is preserved in this dummy positioning, there is a limited range for backset arrangement. Additionally the distance from top of the head arrangement directly depends on the height movement range of head restraint. The nearest position is the point that the head restraint is at its maximum height adjustment. In other words the head is in its nearest position to the head restraint in z direction. Additionally, the crash test dummy is sat in the seat such that its head is also nearest to the head restraint in x direction. The furthest position is the point that the head restraint is at its minimum height adjustment. Therefore, the head is in its furthest position to the head restraint in z direction and additionally the dummy is sat in the seat such that its head is also furthest to the head restraint in x direction. The nearest position is taken as "Position 1", the standard position obtained from the Euro NCAP Whiplash Test Protocol is taken as "Position 2" and the furthest position is taken as "Position 3".

Positions are given in “cm” as used in the test protocol;

- Position 1: Distance from top of the head, h, is 1 cm (above dummy head).

  Backset, b, is 2 cm.

- Position 2: Distance from top of the head, h, is -4 cm (below dummy head).

  Backset, b, is 4 cm.

- Position 3: Distance from top of the head, h, is -7 cm (below dummy head).

  Backset, b, is 7 cm.

These three different head restraint positions are tested with three different test pulses. So totally nine different tests have been performed as discussed in Chapter 4 in this study.

### 3.2.4 Dummy Positioning

After removing the H-Point Manikin from the seat, the seat is allowed to recover for 15 minutes with nothing in it before installing the Hybrid III 50th percentile crash test dummy.

Then the Hybrid III dummy is sat in the seat and its symmetry plane lying on x and z directions are aligned with the centerline of the seat. The seat belt is placed across the dummy and locked as normal leaving sufficient slack in the belt to allow positioning of Hybrid III. The instrumentation platform in the head is also aligned to be laterally leveled. The pelvis angle of the dummy is aligned to 26.5º from horizontal with a tolerance of ± 2.5º. The H-Point of the dummy is aligned such that its horizontal position is 20 mm forward with a tolerance of ± 10 mm and at the same z-height with a tolerance of ± 10 mm as the location recorded with CMM on H-Point Manikin previously, while keeping the pelvis angle at 26.5º with a tolerance of ± 2.5º. Another device called as H-Point Tool is used on the crash test dummy to find the H-Point location of the crash test dummy by the help of H-Point hole is used as in Figure 3.18. The H-Point hole of this device shows the H-Point of the crash test dummy. So the dummy is positioned in the seat such that both right and left H-Points of the dummy is coincided with the previously founded H-Points of the seat within the given tolerances and conditions by using CMM.

Spacing of the legs is adjusted so that the centerline of the knees and ankles is 200 mm with a tolerance of ±10 mm apart and the knees are leveled using an inclinometer. The horizontal position of the toe board is adjusted so that the heel of Hybrid III's shoe is resting on the heel surface. The tip of the shoe is rested on the toe pan between 230 mm and 270 mm from the intersection of the heel surface and toe board, as measured along the surface of the toe board. Hybrid III's arms are positioned so that the upper arms are as close to the torso sides as possible. The rear

of the upper arms contact the seatback and the elbows are bent so that the small fingers of both hands are in contact with the top of the vehicle seat cushion with the palms facing the dummy's thighs (i.e. upper legs). The instrumentation plane of the head (i.e. front/rear and left/right directions) is leveled to within ± 1°. The electronic tilt sensors are used to perform this check. After all of these adjustments, the Hybrid III dummy is positioned in the seat as in Figure 3.19.

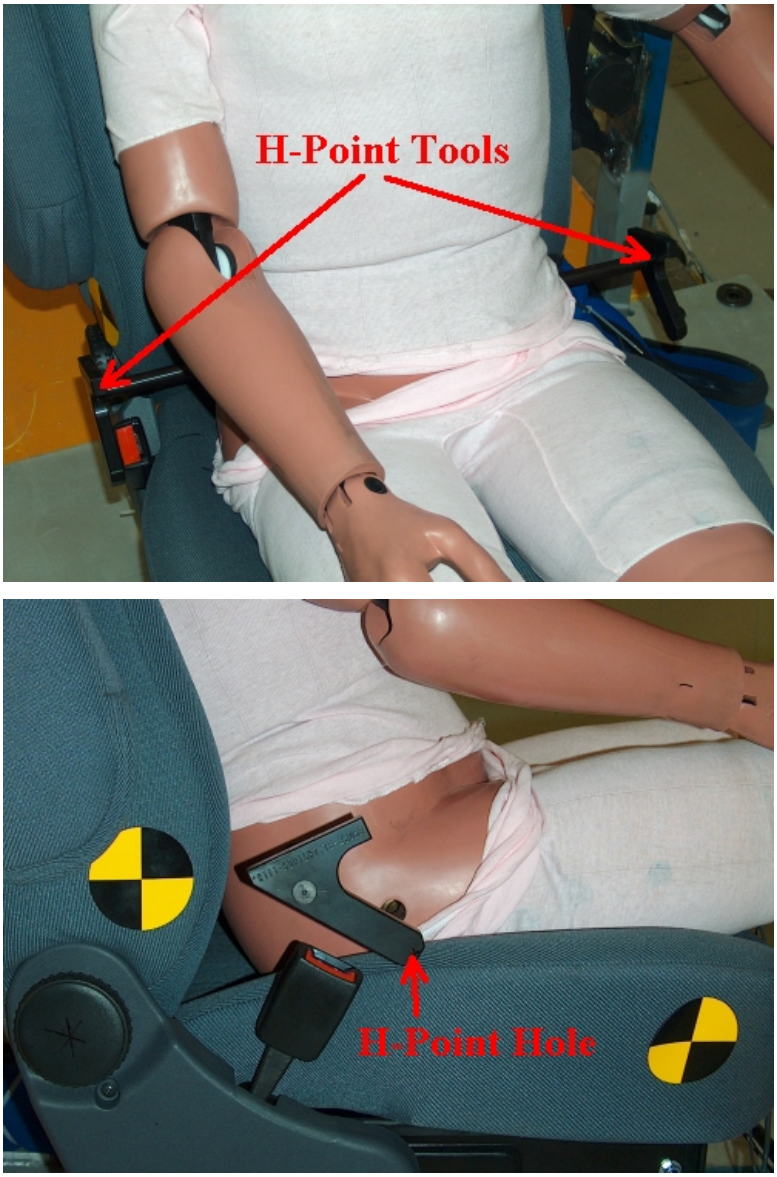


**Figure 3.18 H-Point Tool**

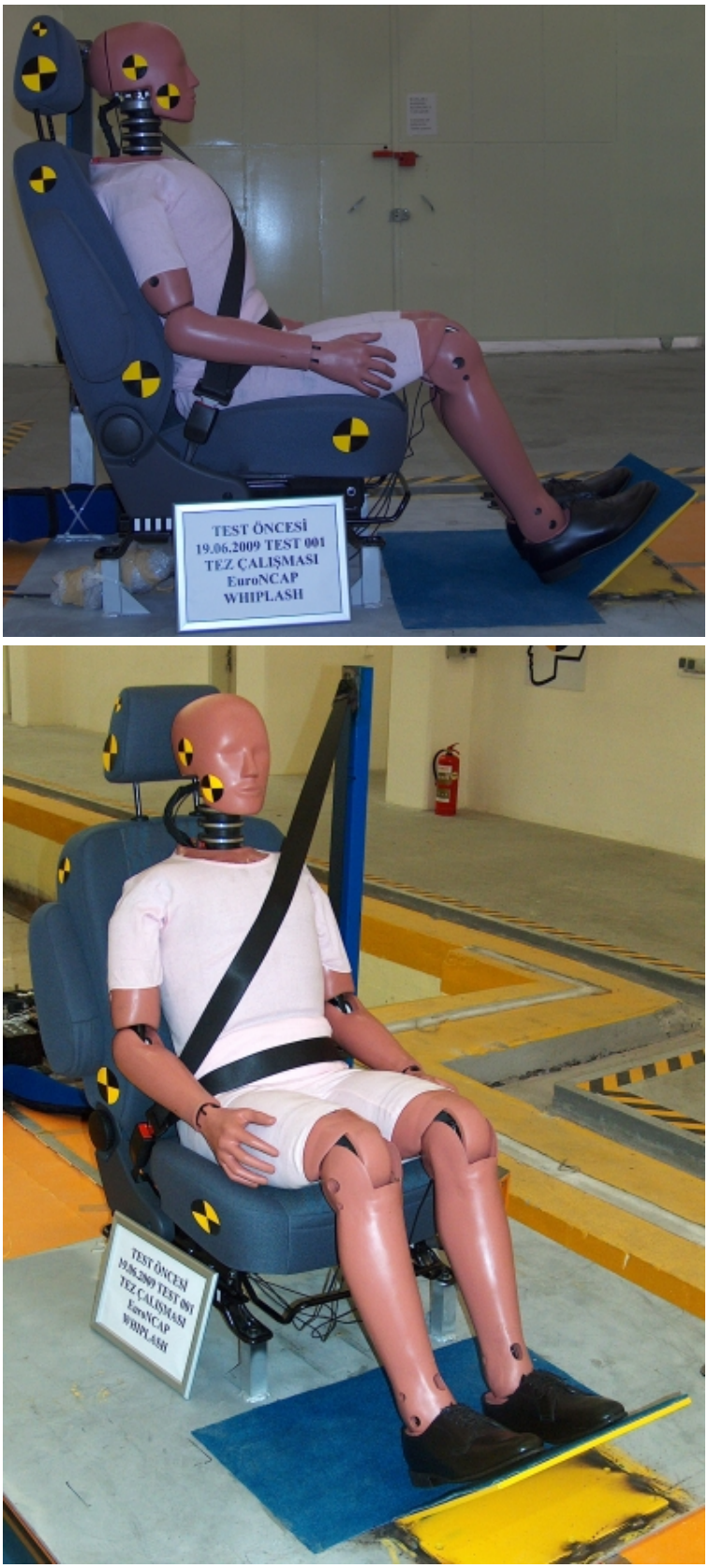


**Figure 3.19 Positioned Dummy in the Seat**

### 3.3 Preparation of the Test Pulses

As it is stated previously in Section 3.2.3, three different test pulses are used in this study. Those pulses are “low severity pulse”, “medium severity pulse” and “high severity pulse” of the Euro NCAP Whiplash Test Protocol [26]. To obtain the required test pulses and to perform the related tests, IST Crash Test Simulation System, which is described in detail in Appendix D, is used.

Before starting the test pulse creation process, the prepared test sample including the crash test dummy and other connection elements is taken onto the digital scale and its mass is measured. The mass of the test sample is measured as 298 kg. A 300 kg standard mass which is known as the dummy mass is loaded on the sled of the crash simulation system as in Figure 3.20. This dummy mass represents the test sample mass during the test pulse creation process and so the test sample is prevented to get any damage during this process. It is possible to use a standard dummy mass which is in the tolerance of ± 50 kg of the test sample mass in order to create the test pulse.

**Figure 3.20 Dummy Mass Loaded on the Sled**

After loading the standard dummy mass onto the sled, it is required to create the test pulses in the RS SigEdit software [33] of the crash simulation system so that the system can reproduce the pulses as it requires. As an example, creation of the low severity test pulse on the RS SigEdit software is defined as follows:

The low severity pulse of the Euro NCAP Whiplash Test Protocol which is the red curve in Figure 3.21 and its acceptance corridors which are the green curves in Figure 3.21 are given in Figure 3.21. Other details about all of these test signals can be found in detail in Euro NCAP Whiplash test Protocol [26].

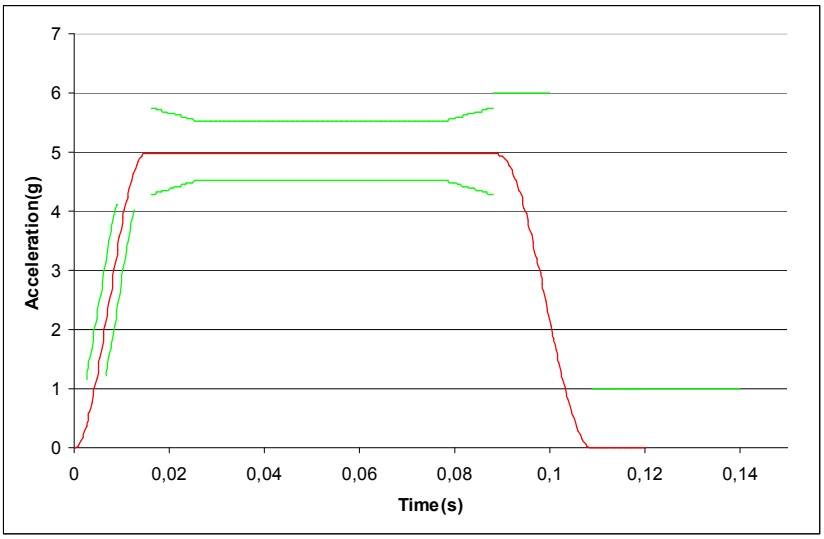


**Figure 3.21 Low Severity Pulse of the Euro NCAP Whiplash Test Protocol [26]**

In order to get this test pulse into the RS SigEdit software, it is required to digitize this graph as consisting of many data points. To perform this job, a special graph digitizing software, "UN-SCAN-IT" [35], is used. First, the signal is scanned using a scanner and then it is digitized using the UN-SCAN-IT software. The digitized test pulse is opened in the RS SigEdit software as in Figure 3.22 using a sampling rate of 2500 Hz which is the highest sampling rate of the software and the recommended

sampling rate given by the manufacturer of the crash simulation system. In order to make sure that there is no additional acceleration at the beginning of the signal before the crash simulation system is triggered, which results in a non-zero velocity profile, it is required to offset this acceleration signal. This signal offset is related with the trigger logic of the crash simulation system. The crash simulation system used in the tests has a 14 ms delay after it gets the trigger of the shot. So we add 14 ms long zero acceleration to the start of the signal to have the right trigger time for the test shot.

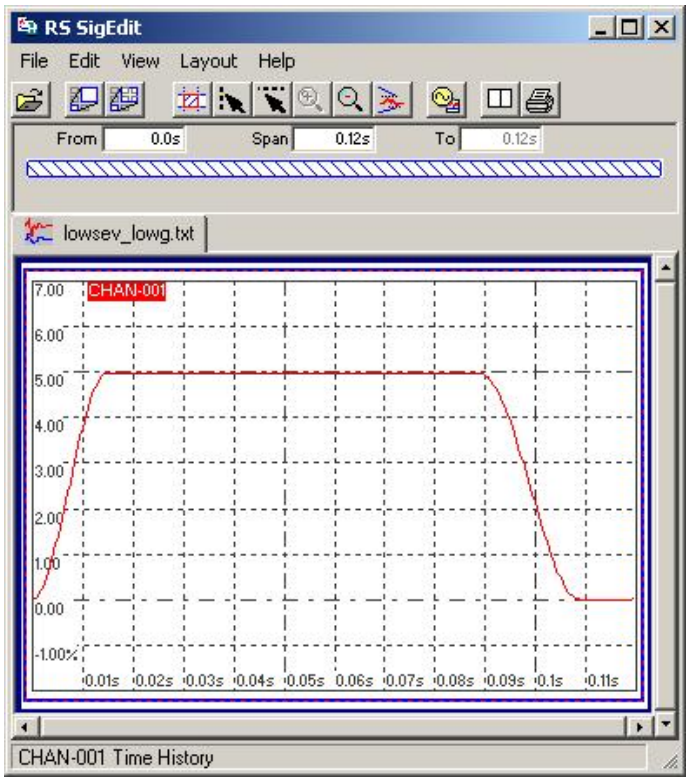


**Figure 3.22 Low Severity Pulse in RS SigEdit**

After that, this signal data is filtered using a 4 poles Butterworth filter so that the crash simulation system controller can perform the iterations on this acceleration

signal data. Finally, the part where the signal reaches zero acceleration level after the starting point is deleted from the signal as it is required by Euro NCAP Whiplash Test Protocol. The final signal which is the target iteration signal of the low severity test is as in Figure 3.23.

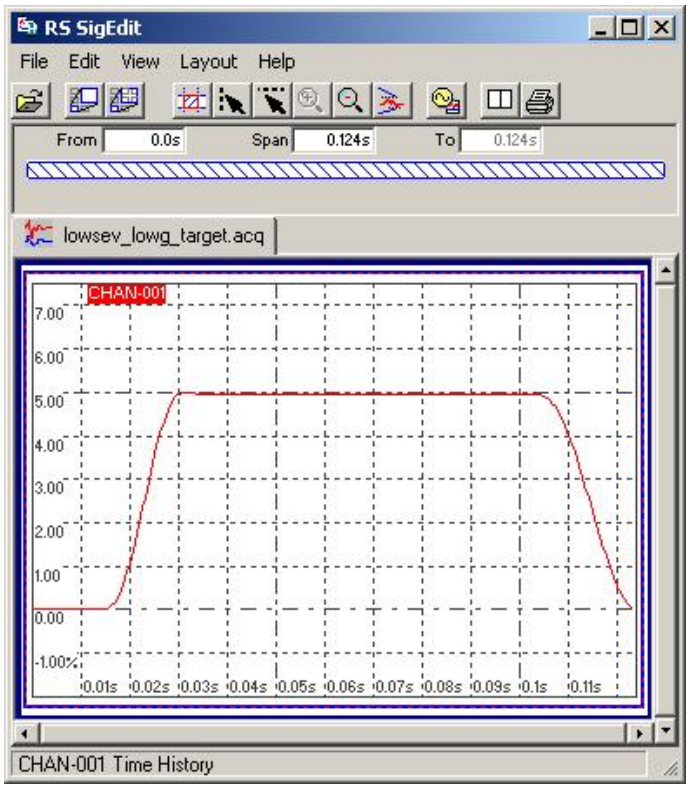


**Figure 3.23 Target Iteration Signal of Low Severity Pulse**

Crash simulation system can iterate this signal up to the best iteration it can perform now. To perform this iteration process the iteration module of another software called RS CrashSim [36] is used. In this iteration module, the previously obtained target iteration signal is given as the target and by performing crash tests using the sled loaded with the dummy mass, the nearest signal to the target is obtained. After each of the tests performed with dummy mass, a correction factor is applied to the

iteration module as in Figure 3.24. This factor makes the iteration model of the software understand how far the acquired signal during the test is away from the target iteration signal.

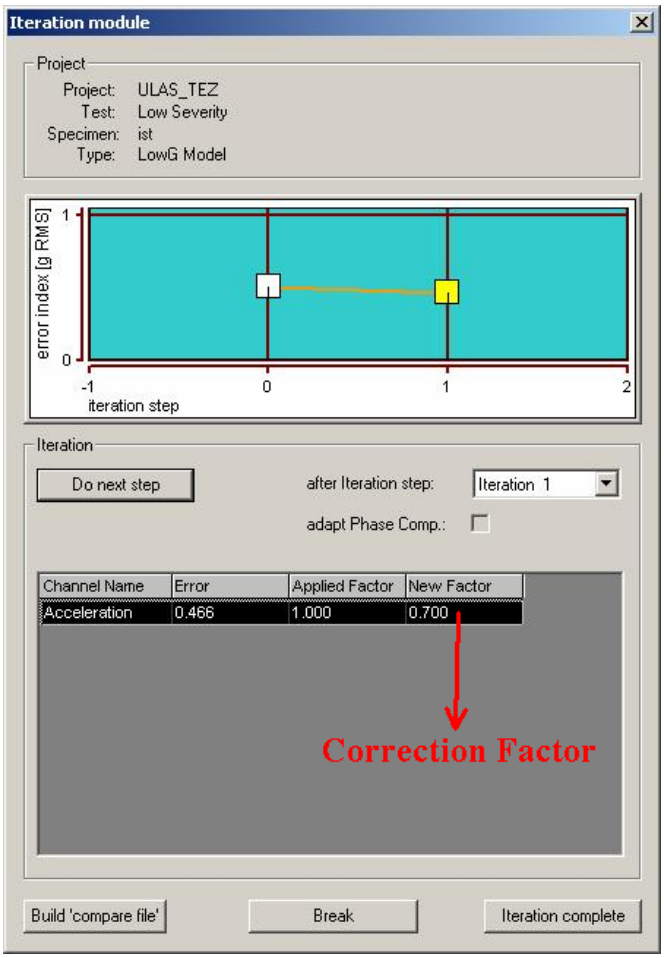


**Figure 3.24 Correction Factor of Target Signal Iteration**

After the iterations have been finished in the guide of correction factors, the target signal for low severity test is obtained. The target signals for medium severity and high severity tests have also been obtained by using the same procedure. All the three target signals obtained are shown in Figure 3.25.

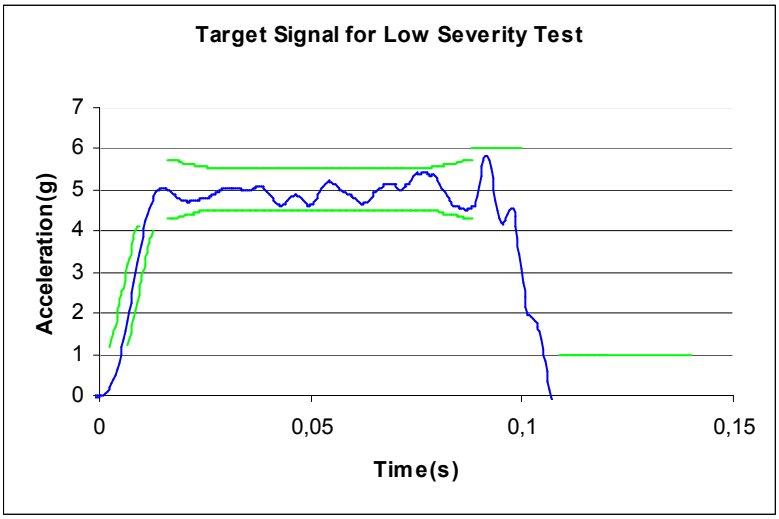


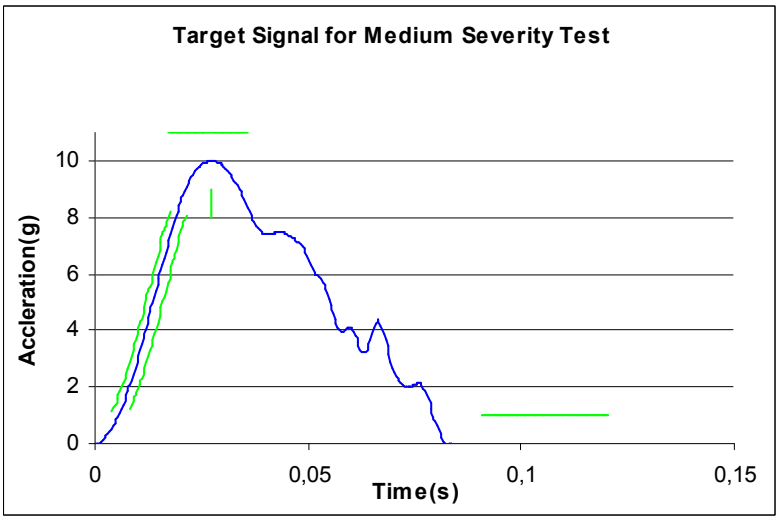


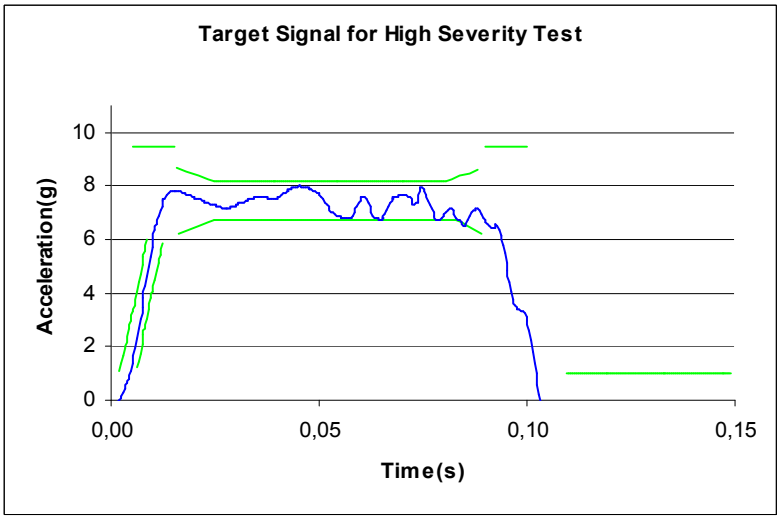


**Figure 3.25 Target Signals of the Tests**

As it is stated in previous sections, all of these three different target signals corresponds to the different impact velocities. The velocity and mean acceleration requirements of the test signals according to the Euro NCAP Whiplash Test Protocol are shown in Table 3.1.

**Table 3.1 Velocity and Mean Acceleration Requirements of the Test Signals [26]**

| Test Type | Mean Acceleration ($m/s^2$) | Velocity Difference (km/h) |
|---|---|---|
| **Low Severity** | 42.35 ± 4.50 | 16.10 ± 0.80 |
| **Medium Severity** | 47.85 ± 4.00 | 15.65 ± 0.80 |
| **High Severity** | 63.15 ± 4.85 | 24.45 ± 1.20 |

# CHAPTER 4

# PERFORMING TESTS AND ANALYSIS OF TEST RESULTS

Technical information and details about the performed tests and how the data gathered during tests are used to make the assessments about the whiplash injury criteria are described in this chapter.

## 4.1 Tests Performed

Nine tests, which correspond to three different head restraint positions and three different test pulses as explained in Section 3.2.3 in detail, are performed during this study. Table 4.1 shows these test parameters.

These tests are performed with the IST Crash Test Simulation System and the technical details of the system are presented in Appendix D. The impact velocities acquired during the tests are presented in Table 4.2. Apart from this acceleration sled system, i.e. IST Crash Test Simulation System, other important elements of the tests are instrumented Hybrid III 50th percentile male crash test dummy, Weinberger Vision Visario G2 high speed camera and Kayser Threde Minidau Advanced data acquisition system. Detailed information about the high speed camera and the data acquisition system can also be found in Appendix D.

**Table 4.1 Test Parameters**

| | Impact Type | Distance From Top of the Head (cm) | Backset (cm) |
|---|---|---|---|
| **Test 1** | High Severity | 1 | 2 |
| **Test 2** | High Severity | -4 | 4 |
| **Test 3** | High Severity | -7 | 7 |
| **Test 4** | Medium Severity | 1 | 2 |
| **Test 5** | Medium Severity | -4 | 4 |
| **Test 6** | Medium Severity | -7 | 7 |
| **Test 7** | Low Severity | 1 | 2 |
| **Test 8** | Low Severity | -4 | 4 |
| **Test 9** | Low Severity | -7 | 7 |

**Table 4.2 Impact Velocities of the Tests**

| | Impact Type | Velocity Difference (km/h) |
|---|---|---|
| **Test 1** | High Severity | 23.89 |
| **Test 2** | High Severity | 23.67 |
| **Test 3** | High Severity | 24.03 |
| **Test 4** | Medium Severity | 15.49 |
| **Test 5** | Medium Severity | 15.47 |
| **Test 6** | Medium Severity | 15.56 |
| **Test 7** | Low Severity | 17.03 |
| **Test 8** | Low Severity | 16.41 |
| **Test 9** | Low Severity | 16.50 |

The dummy used in the tests is instrumented as in the Table 4.3. It is defined in the Euro NCAP Whiplash Test Protocol [26] that a sampling rate of 10 kHz or higher must be used for the data acquisition channels used during the tests. In this study, the data is taken over all of the channels of the dummy from -200 ms to +500 ms time with the sampling rate of 10 kHz during the test by using the data acquisition system. This data is evaluated with a special software called EVAluation [38] and the required calculations for whiplash injury criteria are performed with this software. In addition to this data taken, a high speed camera is used to take the high speed video of test instance. This camera is used with 1000 frames/second as defined in the Euro NCAP Whiplash Test Protocol [26] with the resolution of 1536 x 1024 pixels and a sample of these frames is presented in Figure 4.1.

**Table 4.3 Dummy Instrumentation Used in Tests**

| Dummy Part | Sensor Type |
|---|---|
| **Head** | Triaxial Accelerometer – $A_x$, $A_y$, $A_z$ |
| | 2-Axis Tilting Sensor |
| **Neck** | 6-Axis Upper Neck Load Cell - $F_x$, $F_y$, $F_z$, $M_x$, $M_y$, $M_z$ |
| **Chest** | Triaxial Accelerometer – $A_x$, $A_y$, $A_z$ |
| | Chest Displacement Transducer – $D_x$ |
| **Pelvis** | Triaxial Accelerometer – $A_x$, $A_y$, $A_z$ |
| | 2-Axis Tilting Sensor |
| **Femur** | Uniaxial Femur Load Cell – $F_z$ (per leg) |
| **Knee** | Knee Slider Potentiometer – $D_x$ (per knee) |

**Figure 4.1 Some of the High Speed Video Frames of Test Instance**

## 4.2 Assessment Criteria

All of the tests performed are analyzed using some of the whiplash assessment criteria. The ones used in this study are head restraint contact time, chest x-acceleration, upper neck shear force ($F_x$) and upper neck tension ($F_z$), head rebound velocity and $N_{km}$. However NIC (Neck Injury Criterion) and T1 x-acceleration have not been used in this study since the required data to calculate these criteria is not available on the Hybrid III 50th percentile male crash test dummies.

### 4.2.1 Head Restraint Contact Time

The head restraint contact time is calculated from the high speed video taken during the tests. The starting of head restraint contact time, $T\text{-}HRC_{(start)}$, is defined as the time of the first contact between the rear of the dummy head and the head restraint, where the subsequent continuous contact duration exceeds 40ms. For the purposes of assessment, $T\text{-}HRC_{(start)}$ is rounded to the nearest millisecond. Minor breaks in the contact time (up to 1ms) are permissible if it can be proven that these are not due to biomechanical phenomena such as dummy ramping, head restraint or seatback collapse, or 'bounce' of the head during non-structural contact with the head restraint. For the subsequent criteria, the end of head restraint contact is also found; $T\text{-}HRC_{(end)}$. This is defined as the time at which the head first loses contact with the head restraint, where the subsequent continuous loss of contact duration exceeds 40ms. As an example, the $T\text{-}HRC_{(start)}$ and $T\text{-}HRC_{(end)}$ times of Test 1 is shown in Figure 4.2.

### 4.2.2 Chest X-Acceleration

Hybrid III 50th percentile male crash test dummy is fitted with a three channel accelerometer on the chest. Like this accelerometer, all of the sensor channels of the crash test dummy are filtered after the data is taken over them. The most common filters used in the vehicle safety area from the family of channel frequency class (CFC) filters. Similarly, Euro NCAP Whiplash Test Protocol uses this family of filters and the technical details of these filters are given in SAE J211 standard [37]. The data channel acquired from chest accelerometer is filtered to channel frequency

class (CFC) 60 as defined by SAE J211 [37]. The most common CFC filter types and their parameters are given in Table 4.4.

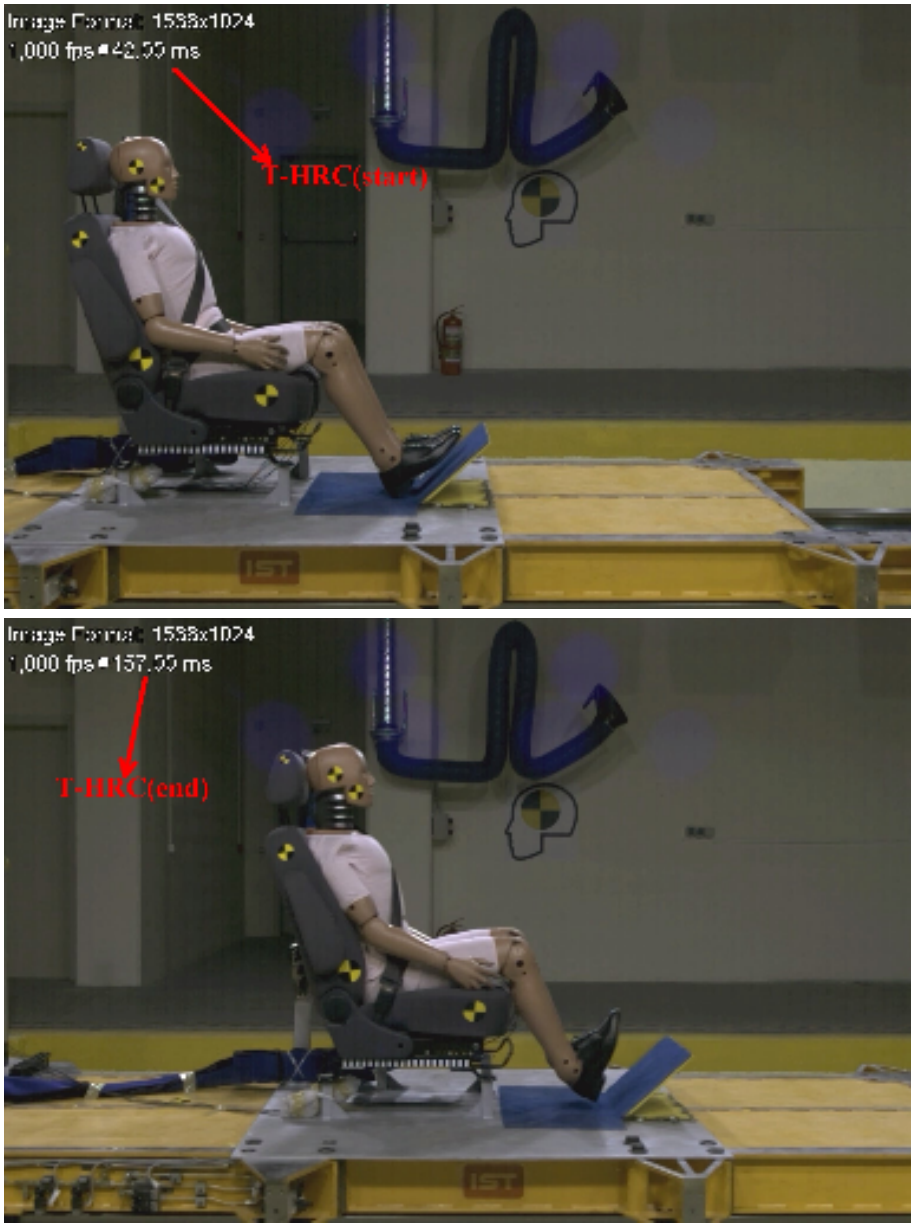


**Figure 4.2 T-HRC$_{(start)}$ and T-HRC$_{(end)}$ Times of Test 1**

**Table 4.4 Most Common CFC Filter Types [37]**

| Filter | Filter Parameters | |
|---|---|---|
| **CFC 60** | 3 dB Limit Frequency | 100 Hz |
| | Stop Damping | -30 dB |
| | Sampling Frequency | at least 600 Hz |
| **CFC 180** | 3 dB Limit Frequency | 300 Hz |
| | Stop Damping | -30 dB |
| | Sampling Frequency | at least 1800 Hz |
| **CFC 600** | 3 dB Limit Frequency | 1000 Hz |
| | Stop Damping | -40 dB |
| | Sampling Frequency | at least 6 kHz |
| **CFC 1000** | 3 dB Limit Frequency | 1650 Hz |
| | Stop Damping | -40 dB |
| | Sampling Frequency | at least 10 kHz |

The maximum acceleration is generated from the chest acceleration in the x-direction, considering only the portion of data from T-zero which is defined as the time before the CFC 60 filtered sled acceleration reached 1.0g level until T-$HRC_{(end)}$. As an example maximum chest acceleration in Test 1 is shown in Figure 4.3.

### 4.2.3 Upper Neck Shear Force and Upper Neck Tension

The upper neck load cell of the Hybrid III 50th percentile male crash test dummy records both shear and tensile forces. Since the instrumentation is configured in accordance with SAE J211, positive shear is indicative of a head-rearwards motion and positive tension is associated with pulling the head upwards, generating a tensile force in the neck as shown in Figure 4.4. Firstly, both the upper neck shear force, $F_x$, and the upper neck tension force, $F_z$, channels are filtered at CFC 1000. The peak

values, $Fx_{max}$ and $Fz_{max}$, are then determined for each of the forces, considering only the portion of data from T-zero until $T\text{-}HRC_{(end)}$ as done for the chest acceleration.

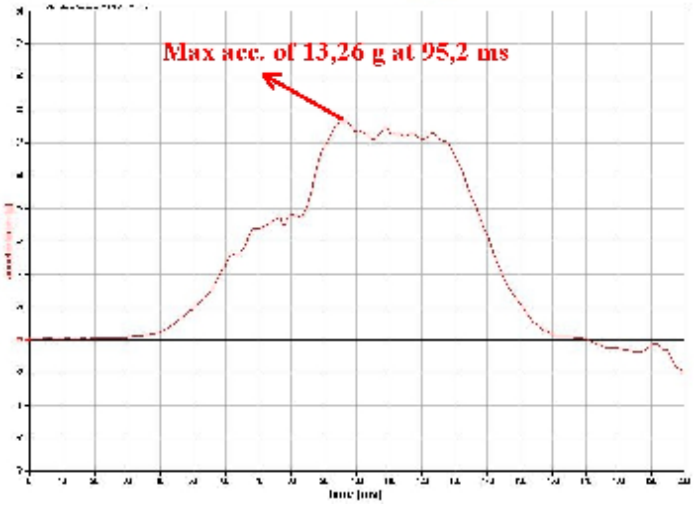


**Figure 4.3 Maximum Chest Acceleration of the Dummy in Test 1**

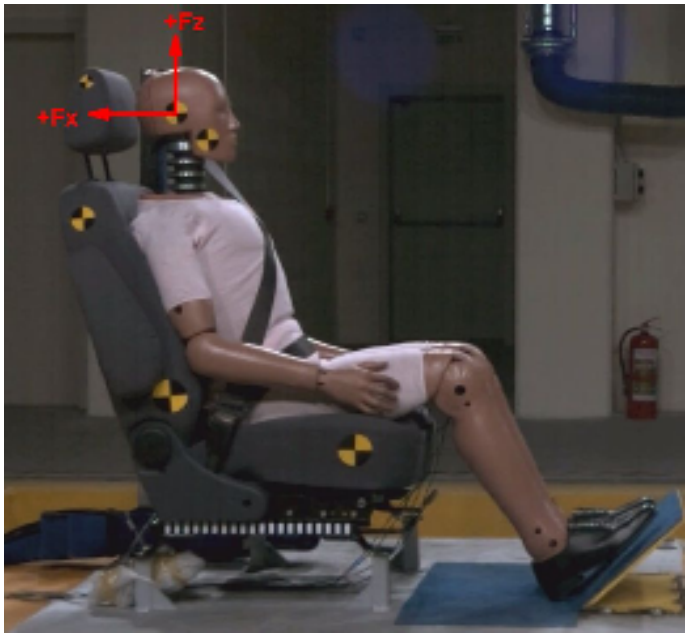


**Figure 4.4 Positive Upper Neck Shear and Tension Forces**

### 4.2.4 Head Rebound Velocity

The head rebound velocity in the horizontal (i.e. x direction) is calculated using high speed videos and the head accelerometer data in the x direction and the sled accelerometer. Theoretically, the peak rebound velocity should occur due to the elastic energy release from the seat assembly, after the peak sled acceleration has occurred. In the case of usage of the acceleration sled, this should also be prior to the sled braking, which at the earliest should occur from 300ms. The rebound velocity of the crash test dummy is usually generated due to the release of stored elastic energy within the seat structure, suspension and foam. The time of occurrence of peak rebound velocity is the maximum horizontal component of head rebound velocity calculated between T-zero and T=300ms. By parallel assessment of high speed videos and the head accelerometer data, the time when this rebound occurs is determined. The rebound velocity of the head which is the relative velocity of the head with respect to the sled velocity is calculated by using this occurrence time.

### 4.2.5 $N_{km}$

The following definition is provided following the commonly accepted convention that derives the "Anterior/ Posterior" directions from the torso motion relative to the head. Consequently, torso forward motion relative to the head would be referred to as 'anterior' (head rearward relative to the torso), and providing SAE J211 compliant instrumentation is used, would produce an associated positive upper neck shear force, $F_x^{upper}$.

Conversely, the movement of the torso rearward relative to the head is referred to as 'posterior' and produces the opposite sign of shear force.

The $N_{km}$ criterion is based on a combination of moment and shear forces, using critical intercept values for the load and moment. The shear force intercept value is identical for anterior or posterior values, being 845 N in both directions of loading. However, the critical intercept value for the bending moment depends on the direction of loading, having a value of 47.5 Nm in extension (head rotation rearwards), but a value of 88.1 Nm in flexion (head rotation forwards).

Two channels are required to perform the $N_{km}$ calculation, the upper neck shear force $F_x^{upper}$, in N and moment, $M_y^{upper}$ in Nm. Typically the shear force is acquired in kN, and so in those cases, a conversion from kN to N is required.

Once it has been confirmed that both shear force and moment are in the correct units, $M_y^{upper}$ is filtered at CFC 600, according to SAE J211. To allow combination of the $M_y^{upper}$ and $F_x^{upper}$ channels, another $F_x^{upper}$ channel is produced and filtered at CFC 600.

Due to the construction of the dummy, a correction must then be made to convert the actual moment measured by the upper neck load cell into the moment about the occipital condyle (OC) which is the connection point between the skull and the cervical spine. The corrected moment, $M_y^{OC}$ is equal to the upper neck shear force $F_x^{upper}$ multiplied by a constant, D, then subtracted from the measured moment, $M_y^{upper}$. The moment about the OC is calculated as follows;

$$M_y^{OC}(t) = M_y^{upper}(t) - DF_x^{upper}(t) \tag{4.1}$$

Where D=0.01778 in meters.

The four components of $N_{km}$ are then calculated using the upper neck shear force $F_x^{upper}$ and the corrected moment about the OC, $M_y^{OC}$. Each channel first needs to be separated into its positive or negative-going components by generating four new channels as follows:

Two new channels, $F_{xa}$ ($F_x$ in anterior motion) and $F_{xp}$ ($F_x$ in posterior motion), based on $F_x^{upper}$ force channel are generated.

Two new channels, $M_{yf}$ ($M_y$ in flexion) and $M_{ye}$ ($M_y$ in extension), based on the $M_y^{OC}$ moment channel are generated.

Each of the new channels should contain only selected positive or negative-going portions of the respective $F_x$ or $M_y$ channels, with all unwanted data points being replaced by null or zero value, as defined by:

$F_{xa}$ channel contains only the positive portion of the $F_x^{upper}$ force channel as follows:

If $F_x^{upper}(t) > 0$, then $F_{xa}(t) = F_x^{upper}(t)$, else $F_{xa}(t) = 0$

$F_{xp}$ channel contains only the negative portion of the $F_x^{upper}$ force channel as follows:

If $F_x^{upper}(t) < 0$, then $F_{xp}(t) = F_x^{upper}(t)$, else $F_{xp}(t) = 0$

$M_{yf}$ channel contains only the positive portion of the $M_y^{OC}$ moment channel as follows:

If $M_y^{OC}(t) > 0$, then $M_{yf}(t) = M_y^{OC}(t)$, else $M_{yf}(t) = 0$

$M_{ye}$ channel contains only the negative portion of the $M_y^{OC}$ moment channel as follows:

If $M_y^{OC}(t) < 0$, then $M_{ye}(t) = M_y^{OC}(t)$, else $M_{ye}(t) = 0$

The four components of $N_{km}$ are then defined as:

a) Neck Extension Posterior ($N_{ep}$)

It is the combined negative-going portions of the shear force channel ($F_{xp}$) and negative-going portions of the moment channel ($M_{ye}$), as defined by:

$$N_{ep}(t) = \frac{F_{xp}(t)}{F_{x\text{-}int}} + \frac{M_{ye}(t)}{M_{ye\text{-}int}} \tag{4.2}$$

where $F_{x\text{-}int} = -845$ N and $M_{ye\text{-}int} = -47.5$ Nm. The int stands for critical intercept value.

b) Neck Extension Anterior ($N_{ea}$)

It is the combined positive-going portions of the shear force channel ($F_{xa}$) and negative-going portions of the moment channel ($M_{ye}$), as defined by:

$$N_{ea}(t) = \frac{F_{xa}(t)}{F_{x\text{-}int}} + \frac{M_{ye}(t)}{M_{ye\text{-}int}} \tag{4.3}$$

where $F_{x\text{-}int}$ = 845 N and $M_{ye\text{-}int}$ = -47.5 Nm.

c) Neck Flexion Posterior ($N_{fp}$)

It is the combined negative-going portions of the shear force channel ($F_{xp}$) and positive-going portions of the moment channel ($M_{yf}$), as defined by:

$$N_{fp}(t) = \frac{F_{xp}(t)}{F_{x\text{-}int}} + \frac{M_{yf}(t)}{M_{yf\text{-}int}} \tag{4.4}$$

where $F_{x\text{-}int}$ = -845 N and $M_{yf\text{-}int}$ = 88.1 Nm.

d) Neck Flexion Anterior ($N_{fa}$)

It is the combined positive-going portions of the shear force channel ($F_{xa}$) and positive-going portions of the moment channel ($M_{yf}$), as defined by:

$$N_{fa}(t) = \frac{F_{xa}(t)}{F_{x\text{-}int}} + \frac{M_{yf}(t)}{M_{yf\text{-}int}} \tag{4.5}$$

where $F_{x\text{-}int}$ = 845 N and $M_{yf\text{-}int}$ = 88.1 Nm.

Each of the four components should be calculated as a new data channel, using only the positive-going or negative-going portions of the $F_x$ and $M_y$ channels as appropriate, and the relevant critical intercept values. Maxima for each of the four components should be calculated, considering only the portion of data from T-zero until T-$HRC_{(end)}$, as follows:

$$N_{ep(max)} = \underset{T\text{-}HRC(end)}{Max} \left[ N_{ep}(t) \right] \quad (4.6)$$

$$N_{ea(max)} = \underset{T\text{-}HRC(end)}{Max} \left[ N_{ea}(t) \right] \quad (4.7)$$

$$N_{fp(max)} = \underset{T\text{-}HRC(end)}{Max} \left[ N_{fp}(t) \right] \quad (4.8)$$

$$N_{fa(max)} = \underset{T\text{-}HRC(end)}{Max} \left[ N_{fa}(t) \right] \quad (4.9)$$

The $N_{km}$ value is taken as the maximum value reached by any one of the four components $N_{ea}$, $N_{ep}$, $N_{fa}$ and $N_{fp}$. It should be noted which component of the four reached the maximum value and the time at which this occurred.

### 4.3 Test Results

In order to define the analysis intervals of the whiplash assessment criteria, the T-$HRC_{(start)}$, T-$HRC_{(end)}$ and T-zero are used. Definitions of T-$HRC_{(start)}$ and T-$HRC_{(end)}$ was given in the earlier sections of this chapter . However T-zero is defined as the time before the filtered sled acceleration reaches 1.0g and the relevant times for the low, medium and high severity pulses are 4.6ms, 5.8ms and 3.7ms. The assessment criteria calculated for all of the tests are given in Tables 4.5, 4.6, 4.7, 4.8, 4.9 and 4.10.

**Table 4.5 Head Restraint Contact Time**

| | T-HRC$_{(start)}$ (ms) | T-HRC$_{(end)}$ (ms) |
|---|---|---|
| **Test 1** | 42 | 157 |
| **Test 2** | 46 | 151 |
| **Test 3** | 66 | 152 |
| **Test 4** | 46 | 140 |
| **Test 5** | 49 | 134 |
| **Test 6** | 68 | 138 |
| **Test 7** | 47 | 157 |
| **Test 8** | 50 | 155 |
| **Test 9** | 74 | 155 |

**Table 4.6 Chest X-Acceleration**

| | Maximum Acceleration (g) | Occurence Time (ms) |
|---|---|---|
| **Test 1** | 13.26 | 95.20 |
| **Test 2** | 16.47 | 92.15 |
| **Test 3** | 18.11 | 94.85 |
| **Test 4** | 13.88 | 92.40 |
| **Test 5** | 15.26 | 93.65 |
| **Test 6** | 16.17 | 93.30 |
| **Test 7** | 10.68 | 102.80 |
| **Test 8** | 10.63 | 105.70 |
| **Test 9** | 11.52 | 104.30 |

**Table 4.7 Upper Neck Shear Force ($F_x$) and Upper Neck Tension Force ($F_z$)**

| | Maximum $F_x$ (N) | Maximum $F_z$ (N) |
|---|---|---|
| **Test 1** | -135.5 | 475.2 |
| **Test 2** | -225.5 | 466.9 |
| **Test 3** | -291.7 | 455.7 |
| **Test 4** | -198.7 | 371.8 |
| **Test 5** | -295.4 | 710.8 |
| **Test 6** | -284.5 | 1059.0 |
| **Test 7** | -187.4 | 358.9 |
| **Test 8** | -193.0 | 446.8 |
| **Test 9** | -254.6 | 875.7 |

**Table 4.8 Head Rebound Velocity**

| | Rebound Velocity (m/s) | Occurence Time (ms) |
|---|---|---|
| **Test 1** | 4.12 | 147.9 |
| **Test 2** | 4.31 | 147.2 |
| **Test 3** | 4.74 | 158.6 |
| **Test 4** | 3.32 | 143.3 |
| **Test 5** | 4.23 | 139.1 |
| **Test 6** | 4.40 | 144.9 |
| **Test 7** | 3.73 | 172.6 |
| **Test 8** | 3.82 | 170.6 |
| **Test 9** | 3.97 | 162.0 |

**Table 4.9 Maximum Component of $N_{km}$**

| | Maximum $N_{km}$ | Component | Occurence Time (ms) |
|---|---|---|---|
| **Test 1** | 0.2831 | $N_{fp}$ | 122.0 |
| **Test 2** | 0.4562 | $N_{fp}$ | 97.1 |
| **Test 3** | 0.6453 | $N_{fp}$ | 101.2 |
| **Test 4** | 0.3272 | $N_{fp}$ | 85.8 |
| **Test 5** | 0.5987 | $N_{fp}$ | 100.4 |
| **Test 6** | 0.6130 | $N_{fp}$ | 103.1 |
| **Test 7** | 0.3238 | $N_{fp}$ | 97.3 |
| **Test 8** | 0.3325 | $N_{fp}$ | 110.8 |
| **Test 9** | 0.5202 | $N_{fp}$ | 115.3 |

**Table 4.10 Other Components of $N_{km}$**

| | Maximum $N_{ep}$ | Maximum $N_{ea}$ | Maximum $N_{fa}$ |
|---|---|---|---|
| **Test 1** | 0.1063 | 0.1001 | 0.0051 |
| **Test 2** | 0.0726 | 0.0273 | 0.0104 |
| **Test 3** | 0.0062 | 0.0323 | 0.0350 |
| **Test 4** | 0.1734 | 0.0082 | 0.0011 |
| **Test 5** | 0.1082 | 0.0153 | 0.0109 |
| **Test 6** | 0.1773 | 0.2565 | 0.0173 |
| **Test 7** | 0.0072 | 0.0106 | 0.0024 |
| **Test 8** | 0.0082 | 0.0122 | 0.0141 |
| **Test 9** | 0.1610 | 0.0228 | 0.0255 |

### 4.4. Discussion of the Test Results

Results of the tests are calculated according to the Euro NCAP Whiplash Test Protocol [26] as described in the Section 4.2 and discussions about the test results are given according to the values presented in Tables 4.5, 4.6, 4.7, 4.8, 4.9 and 4.10 are as follows:

- It has been seen that increasing the impact velocity during the tests creates earlier T-HRC$_{(start)}$ times for the same head restraint position. However, T-HRC$_{(end)}$ times have different trends. The medium severity tests have the earliest T-HRC$_{(end)}$ times for the same head restraint position. However, T-HRC$_{(end)}$ times of the low and high severity tests are close to each other but later than the T-HRC$_{(end)}$ times of the medium severity tests for the same head restraint position. The high severity and low severity signals creates longer and very close total contact times (i.e. T-HRC$_{(end)}$- T-HRC$_{(start)}$) to each other with respect to the medium severity signal. This is a result of triangular shape of the medium severity signal whereas the others have trapezoidal shapes. Since the medium severity signal has a single peak acceleration while the others keep the peak accelerations continuously for a while, such total contact times have been occurred.

- There seems a 3-4 ms delay in the T-HRC$_{(start)}$ times from the first head restraint position in tests 1, 4, 7 to the second head restraint position in tests 2, 5, 8. However, this delay reaches the 15-20 ms level when the head restraint position changes from the second position to the third position in tests 3, 6, 9.

- Increasing the impact velocity creates higher maximum chest accelerations in the x-direction for the same head restraint position. However, it is seen that this increase is more from the low to medium severity impacts and less from medium to high severity impacts respectively.

- When the first head restraint position is changed to the second one, the maximum chest acceleration in the x-direction increases for the same impact

velocities. Similarly, the same effect has been seen from the second position to the third position. This increase gets more when the severity of the test pulse gets harder.

- The maximum chest acceleration occurs at 95, 93 and 105 milliseconds for high, medium and low severity signals respectively.

- The maximum upper neck shear force, $F_x$, obtained in the entire tests has negative sign that means it occurs during the forward motion of the head.

- The trend in charge of the maximum upper neck shear force is not clear when the head restraint positions are the same and impact velocities are different. The maximum shear force increases from the low to medium severity tests for all head restraint positions, however, it increases from the medium to the high severity tests just only for the third head restraint position and decreases for the first and second head restraint positions.

- There is an increasing trend in the upper neck shear force when impact velocities are the same and the head restraint positions are changing from the first to the second and the second to the third positions.

- The maximum upper neck tensile force, $F_z$, obtained in the tests has positive sign that means it occurs during the upwards pulling of the head.

- Similar to the shear force, the trend in the maximum upper neck tensile force is not clear when the head restraint positions are the same and the impact velocities are different. The maximum tensile force increases form the low to the medium severity tests, however, it increases from the medium to the high severity tests just only for the first head restraint position and decreases for the second and third head restraint positions.

- The maximum upper neck tensile force increases from the first to the second and the second to the third head restraint positions for the low and medium impact velocities and decreases for the high impact velocity.

- The maximum head rebound velocity increases from the first to the second and the second to the third head restraint positions for the same impact velocities.

- The maximum head rebound velocity generally increases with the increasing impact velocities for the same head restraint positions. The only exception occurs for first head restraint position from the low to the medium severity.

- Occurrence times of the maximum head rebound velocity are the earliest for the medium severity and the latest for the low severity pulses. This is a result of the triangular shape of the medium severity pulse.

- The maximum of all of the four parts of the $N_{km}$ has been the neck flexion posterior ($N_{fp}$) in the tests. So the $N_{km}$ is taken as the $N_{fp}$ which is the combined negative-going portions of the shear force channel ($F_{xp}$) and positive-going portions of the moment channel around y axis ($M_{yf}$) as described in Equations 4.4 and 4.8.

- $N_{fp}$ value is increasing from the first to the second and the second to the third head restraint positions for the same impact velocities.

There are higher performance and lower performance limits described in the Euro NCAP Assessment Protocol [39], which corresponds to the higher and lower scores respectively for some of the whiplash assessment criteria used in this study. Although these limits are originally for BioRID II dummy, it is useful to see how the Hybrid III dummy behaves in these limits. The higher performance limit corresponds to the maximum score of 0.5 whereas lower performance limit corresponds to the minimum score of 0 for each criterion. All the scores calculated for these criterion are presented in Tables 4.11, 4.12, 4.12, 4.14 and 4.15. The first and the second columns of these tables show the higher and lower performance limits of the injury criteria as given in the Euro NCAP Assessment Protocol [39]. The third columns show the calculated injury criteria value and the fourth columns show the calculated score of the injury criteria.

The discussion on the performance of the particular seat according to the Euro NCAP Assessment Protocol [39] by the "T-HRC$_{(start)}$" time, "Upper Neck Shear Force ($F_x$)" and "Upper Neck Tension Force ($F_z$)", "Head Rebound Velocity" and "$N_{km}$" are also presented as follows:

- The higher and lower performance limits for the T-HRC$_{(start)}$ time of the high severity test are 53 ms which corresponds to the maximum score of 0.5 and 80 ms which corresponds to the minimum score of 0 respectively. So, the defined T-HRC$_{(start)}$ values for Test 1 which is 42 ms and Test 2 which is 46 ms correspond to the highest score of 0.5. However, Test 3, which has a 66 ms T-HRC$_{(start)}$ time, stays between the higher and lower performance limits of the injury criteria. In such a case, a linear interpolation between the higher and lower performance limits is used to find the corresponding score of the injury criteria value of the test. This linear interpolation logic is the same for each injury criterion used in the tests. So score of the Test 3 is found as the 0.26 by linear interpolation. Similarly the higher and lower performance limits for the T-HRC$_{(start)}$ time of medium severity and low severity tests are 57 ms - 82 ms and 61 ms - 83 ms respectively. So, Test 4 (46 ms) and Test 5 (49 ms) correspond to the highest score of 0.5 and Test 6 (68 ms) corresponds to the score of 0.32. Similarly, Test 7 (47 ms) and Test 8 (50 ms) correspond to the highest score of 0.5 and Test 9 (74 ms) corresponds to the score of 0.20. All scores of the T-HRC$_{(start)}$ time are presented in Table 4.11.

**Table 4.11 Scores of the Particular Seat for T-HRC$_{(start)}$**

| | Higher Performance Limit (ms) | Lower Performance Limit (ms) | T-HRC$_{(start)}$ (ms) | Score for T-HRC$_{(start)}$ |
|---|---|---|---|---|
| **Test 1** | 53 | 80 | 42 | 0.50 |
| **Test 2** | 53 | 80 | 46 | 0.50 |
| **Test 3** | 53 | 80 | 66 | 0.26 |
| **Test 4** | 57 | 82 | 46 | 0.50 |
| **Test 5** | 57 | 82 | 49 | 0.50 |
| **Test 6** | 57 | 82 | 68 | 0.32 |
| **Test 7** | 61 | 83 | 47 | 0.50 |
| **Test 8** | 61 | 83 | 50 | 0.50 |
| **Test 9** | 61 | 83 | 74 | 0.20 |

- The higher and lower performance limits for the Upper Neck Shear Force ($F_x$) of high severity test are 30 N and 210 N respectively. So, Test 1 (135.5 N) corresponds to the score of 0.21. Test 2 (225.5 N) and Test 3 (291.7 N) correspond to the lowest score of 0. Similarly the higher and lower performance limits for the Upper Neck Shear Force ($F_x$) of medium severity and low severity tests are 30 N - 190 N and 30 N - 110 N respectively. So, Test 4 (198.7 N), Test 5 (295.4 N) and Test 6 (284.5 N) correspond to the lowest score of 0. Similarly, Test 7 (187.4 N), Test 8 (193.0 N) and Test 9 (254.6 N) also correspond to the lowest score of 0. All scores of the Upper Neck Shear Force ($F_x$) are presented in Table 4.12.

**Table 4.12 Scores of the Particular Seat for Upper Neck Shear Force ($F_x$)**

| | Higher Performance Limit (N) | Lower Performance Limit (N) | $F_x$ (N) | Score for $F_x$ |
|---|---|---|---|---|
| **Test 1** | 30 | 210 | 135.5 | 0.21 |
| **Test 2** | 30 | 210 | 225.5 | 0 |
| **Test 3** | 30 | 210 | 291.7 | 0 |
| **Test 4** | 30 | 190 | 198.7 | 0 |
| **Test 5** | 30 | 190 | 295.4 | 0 |
| **Test 6** | 30 | 190 | 284.5 | 0 |
| **Test 7** | 30 | 110 | 187.4 | 0 |
| **Test 8** | 30 | 110 | 193.0 | 0 |
| **Test 9** | 30 | 110 | 254.6 | 0 |

- The higher and lower performance limits for the Upper Neck Tension Force ($F_z$) of high severity test are 470 N and 770 N respectively. So, Test 1 (475.2 N) corresponds to the score of 0.49. Test 2 (466.9 N) and Test 3 (455.7 N) correspond to the highest score of 0.5. Similarly the higher and lower performance limits for the Upper Neck Tension Force ($F_z$) of medium severity and low severity tests are 360 N - 750 N and 270 N - 610 N respectively. So, Test 4 (371.8 N) corresponds to the score of 0.48 and Test 5 (710.8 N) corresponds to the score of 0.05. Test 6 (1059.0 N) corresponds to the lowest score of 0. Similarly, Test 7 (358.9 N) corresponds to the score of 0.37 and Test 8 (446.8 N) corresponds to the score of 0.24. Test 9 (875.7 N) corresponds to the lowest score of 0. All scores of the Upper Neck Tension Force ($F_z$) are presented in Table 4.13.

**Table 4.13 Scores of the Particular Seat for Upper Neck Tension Force ($F_z$)**

| | Higher Performance Limit (N) | Lower Performance Limit (N) | $F_z$ (N) | Score for $F_z$ |
|---|---|---|---|---|
| **Test 1** | 470 | 770 | 475.2 | 0.49 |
| **Test 2** | 470 | 770 | 466.9 | 0.50 |
| **Test 3** | 470 | 770 | 455.7 | 0.50 |
| **Test 4** | 360 | 750 | 371.8 | 0.48 |
| **Test 5** | 360 | 750 | 710.8 | 0.05 |
| **Test 6** | 360 | 750 | 1059.0 | 0 |
| **Test 7** | 270 | 610 | 358.9 | 0.37 |
| **Test 8** | 270 | 610 | 446.8 | 0.24 |
| **Test 9** | 270 | 610 | 875.7 | 0 |

- The higher and lower performance limits for the Head Rebound Velocity of high severity test are 4.1 m/s and 5.5 m/s respectively. So, Test 1 (4.12 m/s) corresponds to the score of 0.49. Test 2 (4.31 m/s) and Test 3 (4.74 m/s) correspond to the scores of 0.43 and 0.27 respectively. Similarly the higher and lower performance limits for the Head Rebound Velocity of medium severity and low severity tests are 3.2 m/s - 4.8 m/s and 3.0 m/s - 4.4 m/s respectively. So, Test 4 (3.32 m/s) corresponds to the score of 0.46. Test 5 (4.23 m/s) and Test 6 (4.40 m/s) correspond to the scores of 0.18 and 0.13 respectively. Similarly, Test 7 (3.73 m/s) corresponds to the score of 0.24. Test 8 (3.82 m/s) and Test 9 (3.97 m/s) correspond to the scores of 0.21 and 0.15 respectively. All scores of the Head Rebound Velocity are presented in Table 4.14.

**Table 4.14 Scores of the Particular Seat for Head Rebound Velocity**

| | Higher Performance Limit (m/s) | Lower Performance Limit (m/s) | Head Rebound Velocity (m/s) | Score for Head Rebound Velocity |
|---|---|---|---|---|
| **Test 1** | 4.1 | 5.5 | 4.12 | 0.49 |
| **Test 2** | 4.1 | 5.5 | 4.31 | 0.43 |
| **Test 3** | 4.1 | 5.5 | 4.74 | 0.27 |
| **Test 4** | 3.2 | 4.8 | 3.32 | 0.46 |
| **Test 5** | 3.2 | 4.8 | 4.23 | 0.18 |
| **Test 6** | 3.2 | 4.8 | 4.40 | 0.13 |
| **Test 7** | 3.0 | 4.4 | 3.73 | 0.24 |
| **Test 8** | 3.0 | 4.4 | 3.82 | 0.21 |
| **Test 9** | 3.0 | 4.4 | 3.97 | 0.15 |

- The higher and lower performance limits for the $N_{km}$ of high severity test are 0.22 and 0.47 respectively. So, Test 1 (0.2831) and Test 2 (0.4562) correspond to the scores of 0.37 and 0.03 respectively. Test 3 (0.6453) corresponds to the lowest score of 0. Similarly the higher and lower performance limits for the $N_{km}$ of medium severity and low severity tests are 0.15 - 0.55 and 0.12 - 0.35 respectively. So, Test 4 (0.3272) corresponds to the score of 0.28. Test 5 (0.5987) and Test 6 (0.6130) correspond to the lowest score of 0. Similarly, Test 7 (0.3238) and Test 8 (0.3325) correspond to the scores of 0.06 and 0.04 respectively. Test 9 (0.5202) corresponds to the score of lowest score of 0. All scores of the $N_{km}$ are presented in Table 4.15.

Total scores of the seat for each test are calculated by summation of each injury criteria score. Since five injury criteria have been used in the tests, the maximum score of the seat is 2.5 points. These total scores are presented in Table 4.16.

**Table 4.15 Scores of the Particular Seat for $N_{km}$**

| | Higher Performance Limit | Lower Performance Limit | $N_{km}$ | Score for $N_{km}$ |
|---|---|---|---|---|
| **Test 1** | 0.22 | 0.47 | 0.2831 | 0.37 |
| **Test 2** | 0.22 | 0.47 | 0.4562 | 0.03 |
| **Test 3** | 0.22 | 0.47 | 0.6453 | 0 |
| **Test 4** | 0.15 | 0.55 | 0.3272 | 0.28 |
| **Test 5** | 0.15 | 0.55 | 0.5987 | 0 |
| **Test 6** | 0.15 | 0.55 | 0.6130 | 0 |
| **Test 7** | 0.12 | 0.35 | 0.3238 | 0.06 |
| **Test 8** | 0.12 | 0.35 | 0.3325 | 0.04 |
| **Test 9** | 0.12 | 0.35 | 0.5202 | 0 |

**Table 4.16 Total Score of the Seat for each Tests**

| | Impact Type | Distance From Top of the Head (cm) | Backset (cm) | Total Score |
|---|---|---|---|---|
| **Test 1** | High Severity | 1 | 2 | 2.06 |
| **Test 2** | High Severity | -4 | 4 | 1.46 |
| **Test 3** | High Severity | -7 | 7 | 1.03 |
| **Test 4** | Medium Severity | 1 | 2 | 1.72 |
| **Test 5** | Medium Severity | -4 | 4 | 0.73 |
| **Test 6** | Medium Severity | -7 | 7 | 0.45 |
| **Test 7** | Low Severity | 1 | 2 | 1.17 |
| **Test 8** | Low Severity | -4 | 4 | 0.99 |
| **Test 9** | Low Severity | -7 | 7 | 0.35 |

Although the seat dynamic performance score in the Euro NCAP Whiplash Protocol [26] is different since there used more injury criteria to find the score of the seat, it is very meaningful to get the total score of the seat for the tests performed in this study. The effect of changing head restraint position and changing impact pulse on the behavior of the seat in a whiplash injury case can be seen from the whiplash injury criteria values.

As it is stated in previous sections, the original head restraint position of the particular seat for the Euro NCAP Whiplash Test Protocol is the position 2 which has a distance from top of the head of 1 cm and a backset of 4 cm. So, the tests 2, 5 and 8 are the original Euro NCAP whiplash tests for the particular seat. The sum of the scores of the particular seat for these three tests is 3.18 over the maximum possible score of 7.5. So the general performance of the particular seat against whiplash is classified as “marginal” according to the Euro NCAP Assessment Protocol whiplash seat performance classifications.

The test series for head restraint position 1, tests 1, 4 and 7, and head restraint position 3, tests 3, 6 and 9, has a total score of 4.95 and 1.83 over 7.5 respectively.. So the general performance of the particular seat for position 1 and position 3 against whiplash is classified as “marginal” and “poor” respectively according to the Euro NCAP Assessment Protocol whiplash seat performance classifications.

It has been clearly seen that when the impact severity increases from low to medium and medium to high severity, the performance of the seat gets better for the first and third head restraint positions. However, for the second head restraint position the performance score of the seat decreases from low to medium severity and increases from medium to high severity.

It is also shown that a seating position where the head of the passenger is nearer to the head restraint in both vertical and longitudinal directions increase the performance score of the seat for the same severity pulses.

# CHAPTER 5

# CONCLUSIONS AND FUTURE WORK

## 5.1 Conclusions

In this study, effects of the relative head restraint position with respect to the head of the occupant changing in both vertical and longitudinal directions and impact pulse on whiplash injury have been analyzed by performing the sled crash tests. The test sample used in the tests has been prepared according to the Euro NCAP Whiplash Test Protocol as explained in Chapter 3. The sled tests are performed for three different head restraint positions and three different impact pulses in the METU-BILTIR Center Vehicle Safety Unit Sled Test Facility. During these tests an acceleration sled, a Hybrid III 50th percentile instrumented adult male dummy, a three point generic seat belt and a driver seat are used as the main parts of the test sample. The test data are obtained from the high speed video and the sensors of the crash test dummy through the data acquisition system.

Results of the tests are calculated according to the Euro NCAP Whiplash Test Protocol [26] and conclusions about the tests and their results are given as follows:

- It has been shown that the performance of the particular seat in terms of the resistance to the whiplash injury can also be analyzed and discussed by using the instrumented Hybrid III crash test dummy which is available in METU-BILTIR Center Vehicle Safety Unit Sled Test Facility.

- A study with the most recent whiplash test protocol which is first issued on February 2009 has been performed. This is why this study can't be compared with any previous studies.

- The test sample which can be used for whiplash tests has been prepared according to the most recent whiplash test protocol during the study.

- Important experience has been gained about the Euro NCAP Whiplash Test Procedure and usage of equipments related to the whiplash testing.

During the test sample preparation stage, the followings have been observed and experienced:

- It is seen that using a mobile coordinate measuring machine is hard to use in some narrow spaces since it is not possible to reach those spaces. Different coordinate measuring devices with the laser pointers would be more suitable for this application.

- Although the toe board used is fixed on to the steel plate in this study, a toe board, moveable and fixable in the x-direction whenever desired, would be better for different seats and dummies.

- The anchorages of both the seat and seat belt are specially produced for this test sample. Using more flexible fixtures which have more connections points for the anchorages would be easier to use for different seats and seat belts.

During the test signal preparation stage, the following has also been observed and experienced:

- It has been seen that producing medium severity target test signal is easier with respect to the low severity and high severity ones for the IST Crash Simulation System. This may show the crash simulation system is better on triangular pulses rather than trapezoid ones for the low speed impacts. With respect to the previous experiences of the author on the particular crash

simulation system, small mass of the test sample (298 kg) may have a negative effect on the target signal production.

The followings have also been concluded according to the results of the performed tests:

- It has been shown that increasing the impact severity for the first and third head restraint positions, decreases the possibility of having the whiplash injury for the occupant. However, there is not a such clear trend for the second head restraint position.

- It has also been shown that a seating position where the head of the passenger is closer to the head restraint in both vertical and longitudinal directions decreases the possibility to have the whiplash injury for the same test pulses.

- It is shown that maximum $N_{km}$ is obtained for the combined negative-going portions of the shear force channel and positive-going portions of the moment channel around y axis.

### 5.2 Future Work

Future work can be suggested for this particular study as follows:

- Different types of the rear impact crash test dummies, i.e. BioRID II or RID2 crash test dummies can be used in the tests and a comparison between the current thesis study and the new study may be done.

- Different types of the Hybrid III family crash test dummies, i.e. Hybrid III 5th percentile female and Hybrid III 95th percentile male crash test dummies can be used in the tests and a comparison between the current thesis study and the new study may be done.

- A finite element analysis for the thesis study can be performed and a comparison between the test results and finite element analysis results may be done.

- Additional tests can be performed by taking backset of the head restraint as fixed and distance from top of the head as changing and vice versa for the current study. So the effect of both parameters on whiplash injury can be seen separately.

- Different head restraint positions and impact pulses can be used in the tests and a comparison between the current thesis study and the new study may be done.

- The seat parameters such as the seat cushion and foam stiffness, the seat back inclination etc. may be proposed in addition to the performed study especially for the product development tests.

- An optimization for the seat performance can be performed according the changing parameters of the tests.

- The study can be performed with different seats, head restraints and seat belts to see their behaviors and to make a comparison.

- The tests can be performed with airbags and their effects on the injury can be analyzed.

- A new seat or head restraint mechanism against whiplash may be developed or some improvements may be proposed for seats in the light of test results.

# REFERENCES

[1] N. Yoganandan, F.A. Pintar, “Frontiers in Whiplash Trauma, Clinical and Biomechanical”, IOS Press, Amsterdam, 2000.

[2] K. Ono, M. Kanno, “Influences of the Physical Parameters on the Risk to Neck Injuries in Low Impact Speed Rear-End Collisions”, International IRCOBI Conference on the Biomechanics of Impacts (1993), 201-212.

[3] J. S. H. M. Wismans, C. G. Huijskens, “Incidence and Prevention of the Whiplash Trauma”, TNO Crash Safety Centre, Delft, The Netherlands, 1994.

[4] Aspen Insurance UK, 2004 Data, web site: “www.aspen.bm”, last accessed: 22 January 2009.

[5] T. Burton, “Whiplash Injury and Cervical Spine X-rays”, The Leeds Teaching Hospitals, Yorkshire, England, 2004.

[6] H. E. Crow, “Injuries to the Cervical Spine”, Western Orthopaedic Association, San Francisco, 1928.

[7] R.W. Evans, “Some Observation on Whiplash Injuries”, Neurol Clin(1992), 975-997.

[8] W. O. Spitzer, M. L. Skovron, L. R. Salmi, J. D. Cassidy, J. Duranceau, S. Suissa, E. Zeiss, “Scientific Monograph of the Quebec Task Force on Whiplash-Associated Disorders: Redefining ‘Whiplash’ and Its Management”, Spine(1995), 2-73.

[9] M. J. V. D. Horst, “Human Head Neck Response in Frontal, Lateral and Rear End Impact Loading: Modelling and Validation”, PhD Thesis, Technische Universiteit Eindhoven, Eindhoven, 2002.

[10] L. Barnsley, S. Lord, N. Bogduk, “Clinical Review: Whiplash Injury”, Pain (1994), 58(283-307).

[11] M. Sturzenegger, G. DiStefano, B. P. Radanov, A. Schnidrig, “Presenting Symptoms and Signs After Whiplash Injury: The Influence of Accident Mechanisms”, Neurology (1994), 44(688-693).

[12] S. Suissa, S. Harder, M. Veilleux, “The Relationship Between Initial Symptoms and Signs and the Prognosis of Whiplash”, European Spine Journal (2001), 10(44-49).

[13] United States National Library of Medicine, web site: “www.nlm.nih.gov”, last accessed: 07 July 2009.

[14] J. S. H. M. Wismans, E.G. Janssen, M. Beusenberg, W. P. Koppens, R. Happee,, P.H.M. Bovendeerd, “Injury Biomechanics Course Notes”, Eindhoven University of Technology, Eindhoven, The Netherlands, 2000.

[15] A. Nygren, “Injuries to Car Occupants, Some Aspects of the Interior Safety of Cars”, 1984.

[16] W. Hell, S. Schick, K. Langwieder, “Epidemiology of Cervical Spine Injuries in Rear-End Collisions and Influence of Different Anthropometric Parameters in Human Volunteer Tests”, Frontiers in Whiplash Trauma, Clinical and Biomechanical (2000), 146-169.

[17] O. Boström, M. Krafft, B. Aldman, A. Eichberer, R. Fredriksson, Y. Haland, P. Lovsund, H. Steffan, M. Y. Svensson, C. Tingvall, “Prediction of Neck Injuries in

Rear Impacts Based on Accident Data and Simulations", International IRCOBI Conference on the Biomechanics of Impacts Proceedings, 1997, 251-264.

[18] B. P. Radanov, J. Dvorak, "Impaired Cognitive Functioning After Whiplash Injury of the Cervical Spine", Spine (1996), 92-397

[19] J. Davidsson, P. Lövsund, K. Ono, M. Y. Svensson, S. Inami, "A Comparison of Volunteer, BioRID P3 and Hybrid III Performance in Rear Impacts", International IRCOBI Conference, 1999, Spain.

[20] A. Linder, M. Svensson, D. Viano," Evaluation of the BioRID P3 and the Hybrid III in Pendulum Impacts to the Back: A Comparison with Human Subject Test Data", Traffic Injury Prevention(April 2002),159-166.

[21] M. Philippens , H. Cappon , M. Van Ratingen , J. Wismans , M. Svensson , F. Sirey , K. Ono, N. Nishimoto, F. Matsuoka, "Comparison of the Rear Impact Biofidelity of BioRID II and RID2", TNO Automotive, Delft, The Netherlands, 2002.

[22] D. C. Viano, J. Davidsson, "Neck Displacements of Volunteers, BioRID P3 and Hybrid III in Rear Impacts: Implications to Whiplash Assessment by a Neck Displacement Criterion (NDC)", Traffic Injury Prevention,(April 2002), 105-116.

[23] J. Derosia, N. Yoganandan, F. Pintar, "Rear Impact Responses of Different Sized Adult Hybrid III Dummies", Traffic Injury Prevention,(March 2004), 50-55.

[24] A. Kim, A. Sutterfield, A. Rao, K. F. Anderson, J. Berliner, J. Hassan, A. Irwin, J. Jensen, J. Kleinert, H.J. Mertz, H. Pietsch, S. Rouhana, R. Scherer, "A Comparison of the Biorid II, Hybrid III, and RID2 in Low-Severity Rear Impacts", Rear Impact Dummy Evaluation Task Group of the Occupant Safety Research Partnership/ USCAR, USA, 2005.

[25] S. Kuppa, J. Saunders, J. Stammen, A. Mallory, “Kinematically Based Whiplash Injury Criterion”, NHTSA and Transportation Research Center Inc., USA, 2005.

[26] “The Dynamic Assessment of Car Seats for Neck Injury Protection Testing Protocol”, European New Car Assessment Programme (Euro NCAP), Version 2.9, 2009.

[27] “RCAR-IIWPG Seat/Head Restraint Evaluation Protocol”, Version 3, 2008.

[28] “FOLKSAM-SNRA Assessment of Whiplash Protection in Rear Impacts”, 2005.

[29] “ADAC Dynamic Testing and Assessment Procedure of Vehicle Seats to Examine the Risk of Injury for the Neck in Rear Impacts”, 2004.

[30] “SafetyCompanion 2009”.

[31] “Crash Analysis Criteria Description”, Version 2, Arbeitskreis Messdatenverarbeitung Fahrzeugsicherheit, October 2006.

[32] C. A. Hobbs, P. J. McDonough, “Development Of The European New Car Assessment Programme (Euro NCAP)”, Proceedings of the 16th International Technical Conference on the Enhanced Safety of Vehicles (ESV), 1998.

[33] “FMVSS No. 202 Head Restraints for Passenger Vehicles” Test Regulation.

[34] “RS SigEdit Software” User Manual.

[35] “UN-SCAN-IT Software” User Manual.

[36] “RS CrashSim Software” User Manual.

[37] “SAE J211 Instrumentation for Impact Test” Standard.

[38] “EVAluation Software” User Manual.

[39] “Euro NCAP Assessment Protocol”, European New Car Assessment Programme (Euro NCAP), Version 5.0, May 2009.

[40] B. Deng, “Kinematics of Human Cadaver Cervical Spine During Low Speed Rear-End Impacts”, PhD Thesis, Wayne State University, Detroit, Michigan, 1999.

[41] C.A. Van Ee, A.L. Chasse, B.S. Myers, “Quantifiying Skeletal Muscle Properties in Cadaveric Test Speciments: Effects of Mechanical Loading, Postmortem Time, and Freezer Storage”, Journal of Biomechanical Engineering, 122(2000), 9–14.

[42] A. Eichberger, H. Steffan, B. Geigl, M. Svensson, O. Boström, P.E. Leinzinger, M. Darok, “Evuation of the Applicability of the Neck Injury Criterion (NIC) in Rear End Impacts on the Basis of Human Subject Tests”, International IRCOBI Conference on the Biomechanics of Impacts, IRCOBI, 1998, 321–333.

[43] J. N. Grauer, M. M. Panjabi, J. Cholewicki, K. Nibu, J. Dvorak, “Whiplash Produces an S-Shaped Curvature of the Neck with Hyperextension in Lower Levels Spine, 1997.

[44] Backpain-Guide, web site: “www.backpain-guide.com”, last accessed: 19 January 2009.

[45] Capitalregionspine, web site: “http://www.capitalregionspine.com”, last accessed: 22 January 2009.

[46] Ispub, web site: “www.ispub.com”, last accessed: 22 January 2009.

[47] Netterimages, website: “www.netterimages.com”, last accessed: 11 January 2009.

[48] N. Bertholon, S. Robin, J. Y. Le Coz, P. Portier, J. P. Lassau, W. Skalli, “Human Head and Cervical Spine Behaviour During Low-Speed Rear-End Impacts, PMHS Sled Tests with Rigid Seat”, International IRCOBI Conference on the Biomechanics of Impacts, 2000.

[49] J. Davidsson, C. Deutscher, W. Hell, A. Linder, P. Lövsund, M. Y. Svensson, “Human Volunteer Kinematics in Rear-End Sled Collisions”, International IRCOBI Conference on the Biomechanics of Impacts, 1998, 289-302.

[50] B.C. Geigl, H. Steffan, P. Leinzinger, P. Roll, M. Mühlbauer, G. Bauer, “The Movement of Head and Cervical Spine During Rear End Impact”, International IRCOBI Conference on the Biomechanics of Impacts, 1994, 127-134.

[51] W.E. McConnell, R. P.Howard, H.M.Guzman, J. B. Bomar, J. H. Raddin, J. V. Benedict, H. L. Smith, C. P. Hatsell, “Analysis of Human Test Subject Kinematic Responses to Low Velocity Rear End Impacts”, SAE Special Publication SP-975, Paper No. 930889.

[52] W. E. McConnell, R. P. Howard, J. Van Poppel, R. Krause, H. M. Guzman, J. B. Bomar, J. H. Raddin, J. V. Benedict, C.P. Hatsell, “Human Head and Neck Kinematics After Low Velocity Rear-End Impacts-Understanding Whiplash”, Proceedings of the 39th Stapp Car Crash Conference, 215-238.

[53] H. J. Mertz and L. M. Patrick, “Investigation of the Kinematics and Kinetics of Whiplash”, Proceedings of the 11th Stapp Car Crash Conference, 1967, 267-317.

[54] J. G. M. Thunnissen, “Analysis of Human Head-Neck Response During Low Severity Rear-End Impacts”, TNO Crash Safety Centre, Delft, The Netherlands, 1996.

[55] M. Kleinberger, “Application of Finite Element Techniques to the Study Of Cervical Spine Mechanics”, Proceedings of the 37th Stapp Car Crash Conference, 1993, 261-272.

[56] A. Van Der Kroonenberg, J. Thunnissen, J. Wismans, “A Human Model for Low-Severity Rear Impacts”, International IRCOBI Conference on the Biomechanics of Impacts, 1997, 117-32.

[57] E. Lizee, S. Robin, E. Song, N. Bertholon, J.Y. Le Coz, B. Besnault, F. Lavaste, “Development of a 3D Finite Element Model of the Human Body”, Proceedings of the 42nd Stapp Car Crash Conference, 1998, 115-138.

[58] K. Y. Yang, F. Zhu, F. Luan, L. Zhoa, P.C. Begeman, “Development of a Finite Element Model of the Human Neck”, Proceedings of the 42nd Stapp Car Crash Conference, 1998, 195–205.

[59] I. Macnab, “Acceleration Injuries of the Cervical Spine”, 1964.

[60] L. Penning, “Acceleration Injury of the Cervical Spine By Hypertranslation of the Head. Part I: Effect of Normal Translation of The Head on Cervical Spine Motion: A Radiologic Study”, European Spine Journal, 1992.

[61] L. Penning, “Acceleration Injury of the Cervical Spine By Hypertranslation of the Head. Part II: Effect of Normal Translation of The Head on Cervical Spine Motion: Discussion of Literature Data”, European Spine Journal, 1992.

[62] M. Y. Svensson, B. Aldman, H. A. Hansson, P. Lövsund, T. Seeman, A. Suneson, T. Örtengren, “Pressure Effects in the Spinal Canal During Whiplash Motion - A Possible Cause of Injury to the Cervical Spinal Ganglia”, International IRCOBI Conference on the Biomechanics of Impacts, 1993, 189-200.

[63] B. Aldman, “An Analytical Approach to the Impact Biomechanics of Head and Neck Injury”, Proceedings 30th Annual AAAM Conference, 1986, 439–454.

[64] K. Ono, K. Kaneoka, A. Wittek, J. Kajzer, “Cervical Injury Mechanism Based on The Analysis of Human Cervical Vertebral Motion and Head-Neck Torso Kinematics During Low Speed Rear Impacts”, Proceedings of the 41th Stapp Car Crash Conference, Society of Automotive Engineers, 1997. SAE Paper No 973340, 339-356.

[65] N. Yoganandan, F.A. Pintar, M. Klienberger, “Cervical Spine Vertebral and Facet Joint Kinematics under Whiplash”, Journal of Biomechanical Engineering (120), 1998, 305-307.

[66] K. Y. Yang, P. C. Begeman, M. Muser, P. Niederer, F. Walz, “On the Role of Cervical Facet Joints in Rear End Impact Neck Injury Mechanisms”, Motor Vehicle Safety Design Innovations, Society of Automotive Engineers, 1997, 127-129.

[67] T. Matsushita, T. B. Sato, K. Hirabayashi, S. Fujimura, T. Asazuma, T. Takatori, “X-Ray Study of the Human Neck Motion Due to Head Inertia Loading”, Proceedings of the 38th Stapp Car Crash Conference, 1994, 55–64.

[68] First Technology Safety Systems, website: “www.ftss.com”, last accessed: 07 July 2009.

[69] Denton ATD, website: “www.dentonatd.com”, last accessed: 07 July 2009.

[70] ECE-R17 Regulation, “Uniform Provisions Concerning The Approval of Vehicles With Regard to the Seats, Their Anchorages and Any Head Restraints”, Annex3-Appendix1.

[71] Research Council for Automotive Repairs, “A Procedure for Evaluating Motor Vehicle Head Restraints”, Issue 2, February 2001.

[72] Instron Structural Testing Systems, website: “www.instron.com/ist/”, last accessed: 08 July 2009.

[73] Weinberger Vision, website: “www.weinbergervision.com”, last accessed: 19 October 2008.

[74] KT Automotive, website: “www.kt-automotive.com”, last accessed: 08 July 2009.

# APPENDIX A

# HUMAN CERVICAL SPINE ANATOMY AND WHIPLASH INJURY MECHANISM HYPOTHESES

## A.1 Human Cervical Spine Anatomy

A summary of the human cervical spine anatomy is presented here and more detailed information can be found in literature [5, 12, 19, 20, 40, 41, 42, 43].

Three main sections of the human spine are cervical, thoracic and lumbar spine and their anterior (i.e. front), left lateral and posterior (i.e. back) views are given in Figure A.1.

The human spine constitutes bony elements which are called vertebrae. These vertebrae are connected to each other by soft tissues. Of these tissues, intervertebral discs, ligaments, uncovertebral joints, facet joints and muscles are relevant to the biomechanics of the neck as they control motion between vertebrae.

Cervical spine which consists of seven vertebrae, is the uppermost portion of the human spine and can be seen from Figure A.2.

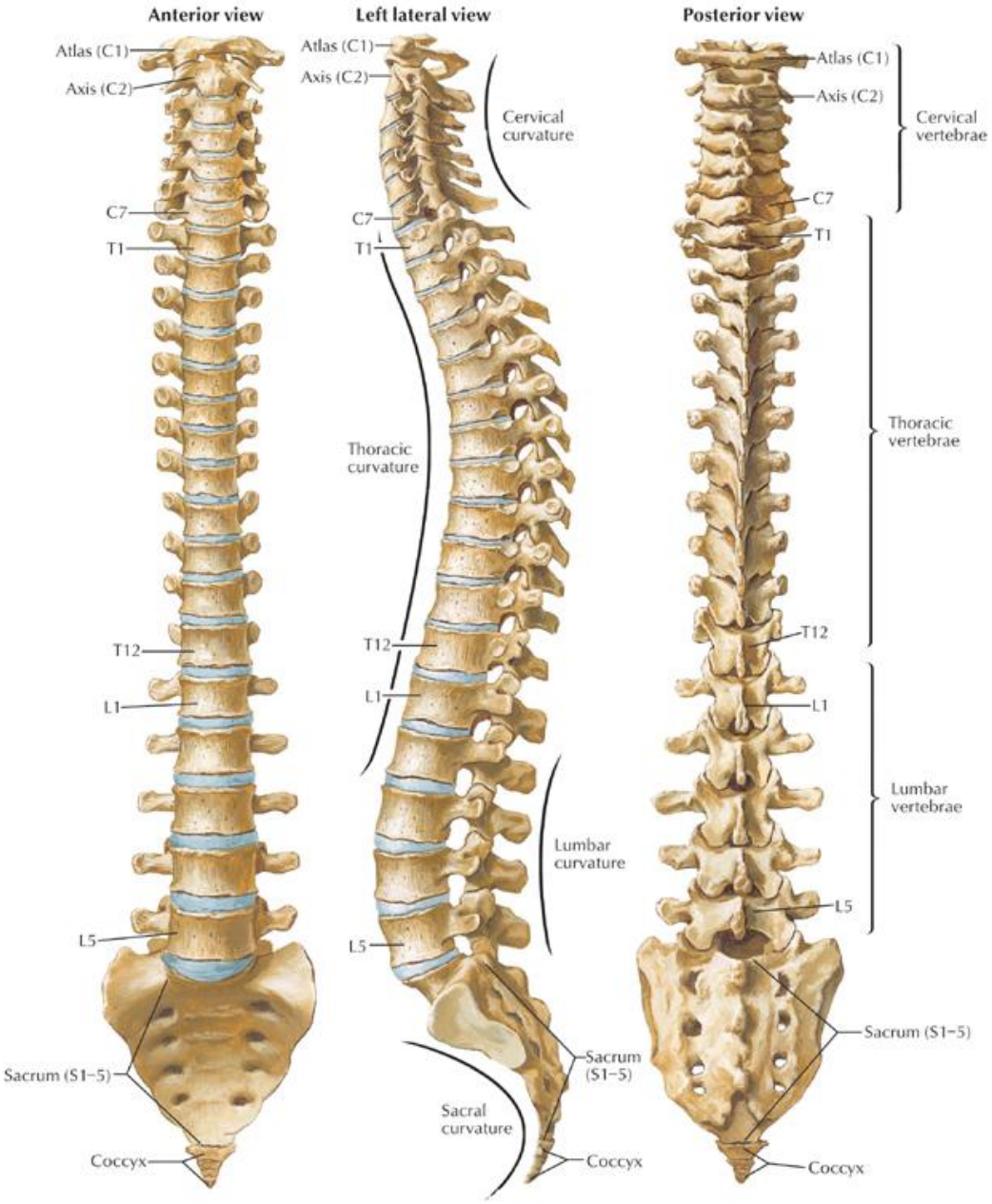


**Figure A.1 Three Views of Human Spine [44]**

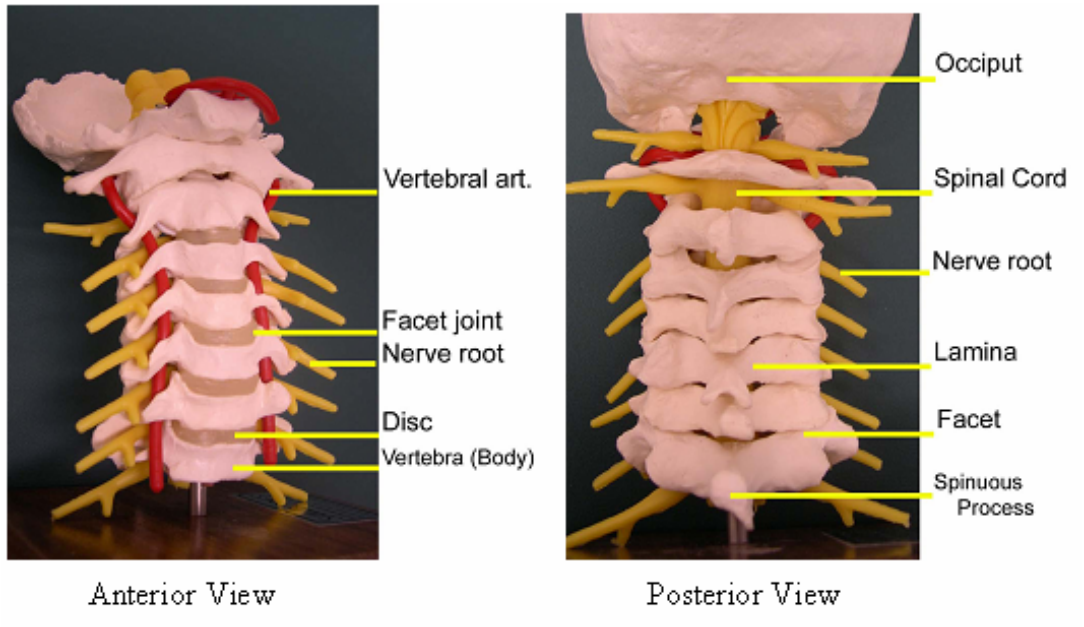


**Figure A.2 Cervical Spine [44]**

Vertebrae of the cervical spine are numbered form C1 to C7 as seen in Figure A.3. The first and second vertebrae, "atlas" and "axis" respectively, are distinct from each other and from other lower five vertebrae, which are basically the same. Due to these differences, the cervical spine can be divided into lower and upper cervical spine.

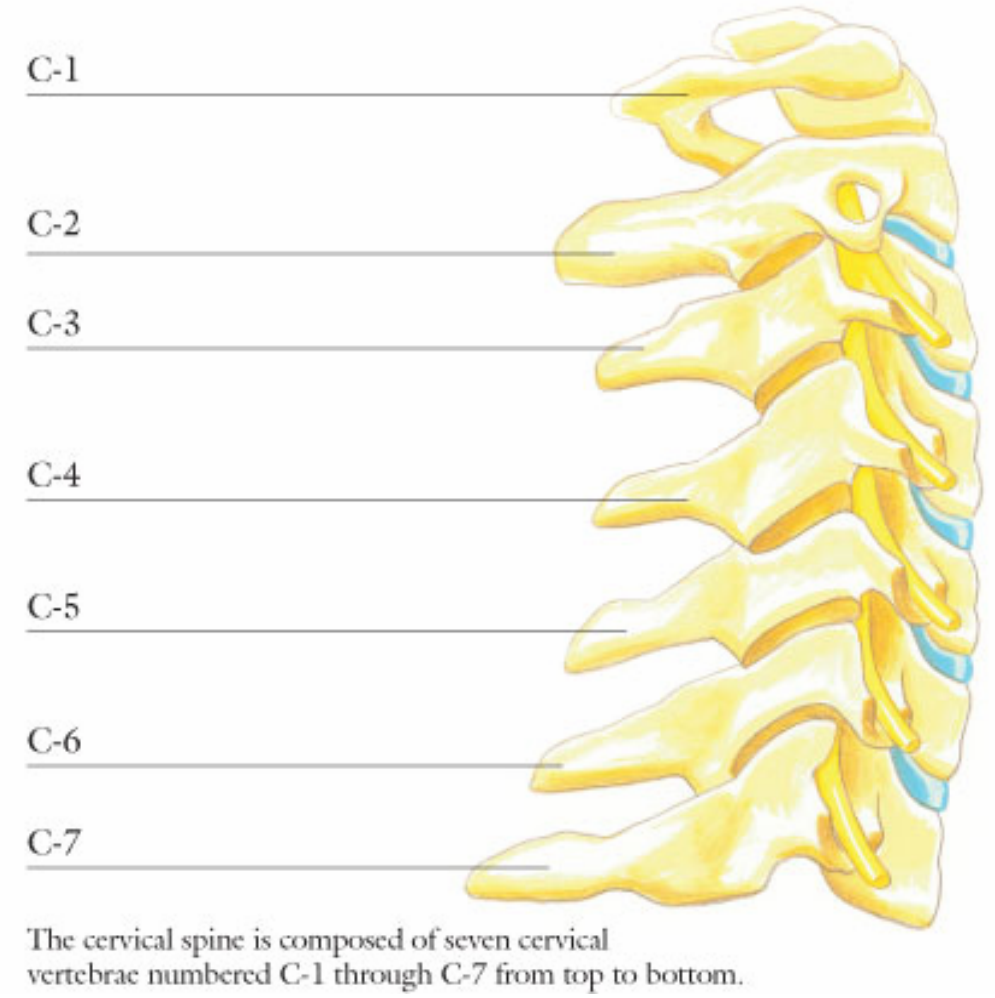


**Figure A.3 Vertebrae of Human Cervical Spine [45]**

The upper cervical spine comprises axis, atlas and occiput, and is also called the occipito-atlanto-axial region. The occiput (C0) is the base of the skull and articulates with the atlas through the occipital condyles which are convex in shape. The atlas (C1) has no vertebral body, but consists of a bony ring with anterior and posterior arches on which the articular facets and transverse processes are situated. The upper facets are large, concave and oval. Like the lower vertebrae, the axis (C2) comprises a body and an arch, but it has an additional element, the odontoid process or dens The dens points out upwards from the body of C2 and is the missing body of the atlas fused to the axis. These two vertebrae are given in Figure A.4.

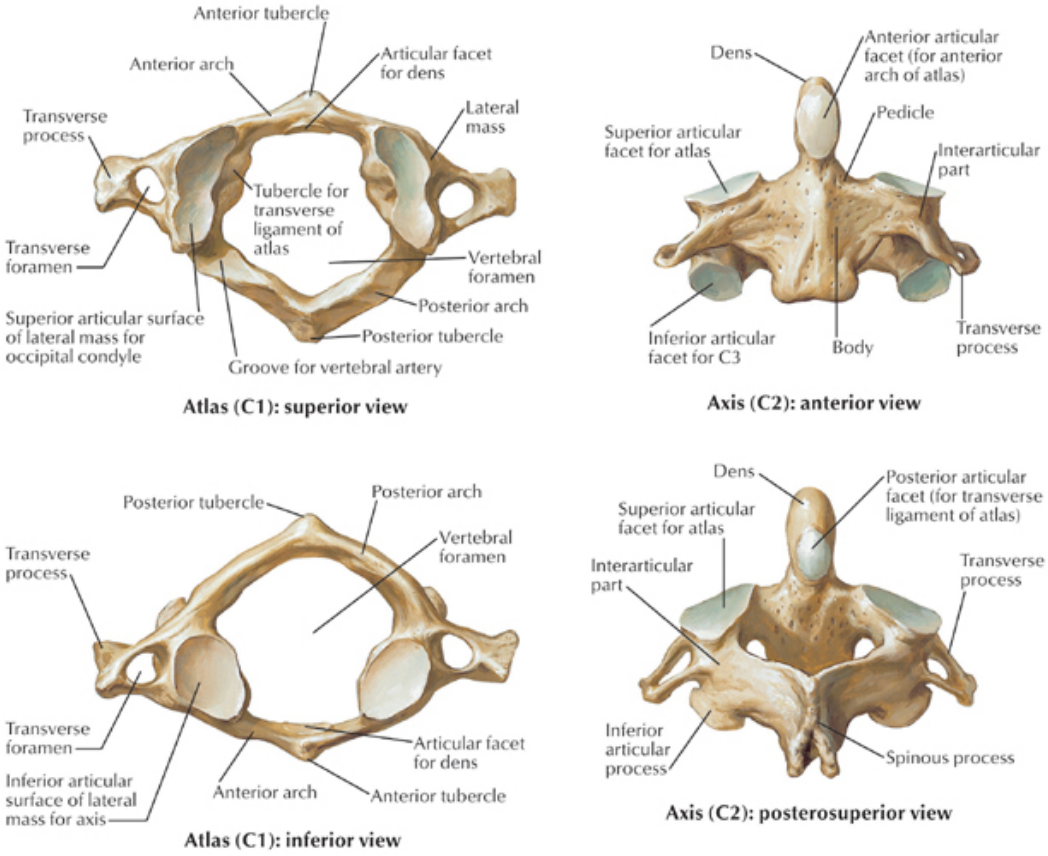


**Figure A.4 Axis and Atlas [46]**

The lower cervical spine includes vertebrae C3 through C7, each of which consists of a cylindrically shaped body and an arch as presented in Figure A.5. The lower end of the body is concave from front to back, whereas its upper end is concave from side to side and has an uncinate process on each side. The upper and lower ends of the body are covered by a thin layer of hyaline cartilage, the endplates. The arch includes two pairs of articular facets, a spinous process and two transverse processes. The articular facets are almost flat and covered with cartilage, and have a backward inclination of about 45 degrees in the horizontal plane. The transverse and spinous processes constitute attachment points for muscles and ligaments. The arch and body enclose the vertebral foramen to form the spinal canal through which the spinal cord and associated structures run.

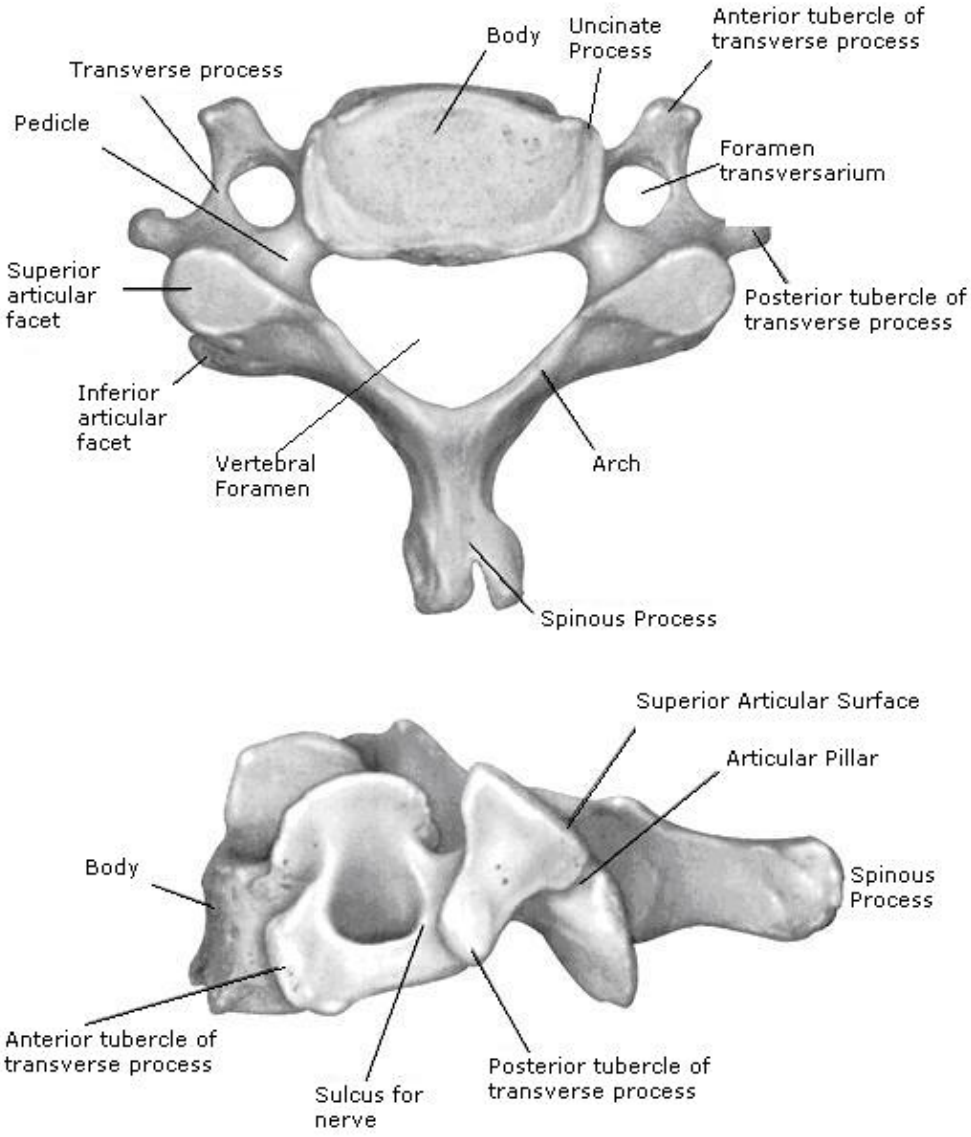


**Figure A.5 A Typical Vertebra From the Lower Cervical Spine [47]**

The joints between two adjacent vertebrae are the intervertebral disc, the facet joints and the uncovertebral joints. The disc allows for motion between vertebrae in all directions, and the uncovertebral and facet joints guide and constrain these motions. The intervertebral disc is a fibrocartilaginous joint between the endplates of each two adjacent vertebral bodies, but there are no discs between axis, atlas and occiput.

Because discs are thicker anterior than posterior, the cervical spine has an anteriorly convex curve, known as cervical lordosis. Uncovertebral joints, situated on either side of the disc, are small synovial joints between the uncinate processes of the lower vertebra and the lower endplate of the upper vertebra. Facet joints are synovial joints formed by the corresponding articular facets of adjacent vertebrae and enclosed by capsular ligaments. Usually, synovial joints allow for sliding movements only, but within the facet joints other movements are also possible due to the laxity of the capsular ligaments. The facet joints between the superior facets of the atlas and the occipital condyles allow little axial rotation and much flexion/extension. Atlas and axis articulate through the facet joints and a synovial joint between the dens and the anterior arch of the atlas, which together allow much axial rotation.

### A.2 Whiplash Injury Mechanism Hypotheses

Although the biomechanical responses in rear end impact have been investigated for many years using experimental research [48-54] as well as biomechanical models [55-58], the injury mechanisms of WADs are still unknown. Different hypotheses, offering explanations for the source of WADs are reviewed and a list of injury types and mechanisms relevant for a rear end impact are presented as follows:

The first and most simple hypothesis was based on primate studies in which head and neck extensions (bending backward) exceeded 90 degrees during a rear end impact without head restraint. During these rear impacts, neck hyperextension was suggested as the injury cause [59].

Based on similar results between experiments and literature, Penning [60] hypothesized that during a rear end impact, the injury of the head-neck system is caused by posterior hypertranslation of the head, almost immediately resulting in damaging hyperflexion (bending forward) of the upper neck joint. This is known as the "hypertranslation hypothesis".

Grauer et al. [43] assumed that intervertebral motions beyond the physiological limits have the potential to cause soft tissue injury. In correspondence with Penning's study [61], the S-shape (see Figure A.6) was identified as the injury stage. However,

injury risk at the lower cervical levels was also expected. This is in contrast with Penning's theory [61], who hypothesized that the upper cervical level, the craniovertebral junction which comprises the occiput, atlas, and axis, is the principle site of cervical trauma in a rear end impact.

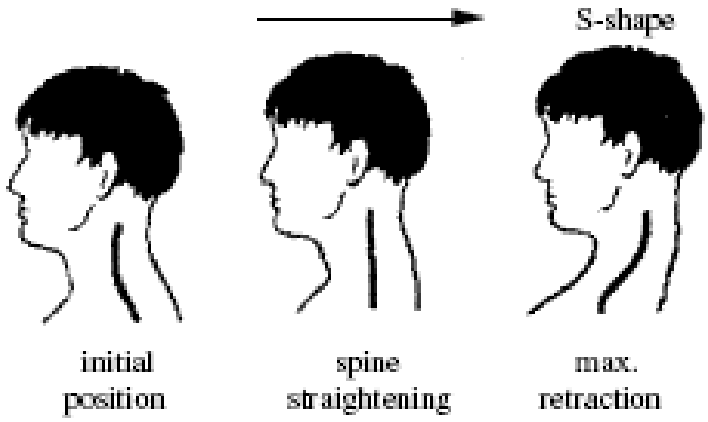


**Figure A.6 S Shape Occurred During Retraction (First) Phase [42]**

Svensson et al. [62] verified a hypothesis by Aldman [63] predicting that the volume changes inside the spinal canal during swift extension-flexion motions of the cervical spine would result in transient pressure changes in the Central Nervous System. Aldman also hypothesized that these pressure effects could induce injurious mechanical loads to the tissues in the intervertebral foramina which is known as the "pressure hypothesis". The extension motion causes a pressure rise and flexion motion causes a corresponding pressure drop. Experimental findings on pigs [62] made it sensible that the transient pressure changes induce injurious mechanical loads to the tissues inside the intervertebral foramina, according to the "pressure hypothesis".

A facet joint impingement (deformation) injury mechanism has been proposed by Ono et al. [64] and Yoganandan et al. [65]. This hypothesis is based on the assumption that during the S-shape of the neck, a portion of the facet capsule can be trapped between the facet joint surfaces and pinched, causing pain. Evidence is lacking, to show that the capsule is loose enough to be trapped between the facet joint and even if it was trapped, it is unknown if this could cause pain.

Yang et al. [66] hypothesized that axial compression in the neck, together with the shear force (the "compression-shear hypothesis"), is responsible for the higher observed frequency of neck injuries in rear end impacts versus frontal impacts of comparable severity. This axial compression occurs during the first phase of the rear end impact due to ramping up or other mechanical interactions between the seat back and the spine [67]. The axial compression reduces the shear stiffness of the cervical spine (loosening of cervical ligaments) and makes it easier for the shear type soft tissue injuries to occur.

Different theories about the cause of WADs are presented above. Any one theory does not necessarily preclude the others, as until now no single answer has been found for the mechanism causing WADs in rear end impact car accidents. Further research is needed to validate existing hypotheses and to gain understanding of the relative cervical vertebral motions, the facet joint motions and the pressure changes in the central nervous system occurring during a rear end impact.

# APPENDIX B

# TECHNICAL INFORMATION OF CRASH TEST DUMMIES

Main crash test dummies (i.e. anthropomorphic test dummies (ATDs)) used in low speed rear crash tests are Hybrid III family as 5th percentile female, 50th percentile and 95th percentile males, BioRID II and RID2 and their earlier versions.

## B.1 Technical Information of Hybrid III 5th Percentile Female Dummy

The Hybrid III 5th percentile female crash test dummy was developed by First Technology Safety Systems and the Society of Automotive Engineers (SAE) Biomechanics Subcommittees, CDC and Ohio State University [68]. The dummy represents the smallest segment of the adult population and derived from scaled data from the Hybrid III 50th dummy. Originally developed in 1988, the dummy was upgraded in 1991 to evaluate seat belt submarining. It was upgraded again in 1997 to improve the dummy's ability to evaluate airbag aggressiveness, particularly for the car driver close to the steering wheel in the "Out Of Position" (OOP) test condition.

**Figure B.1 Hybrid III 5th Percentile Female Dummy [68]**

The technical information of the dummy is given as follows:

**Table B.1 Mass of Hybrid III 5th Percentile Female Dummy [68]**

| BODY PARTS | MASS(kg) |
|---|---|
| **Head** | 3.73 |
| **Neck** | 0.91 |
| **Upper Torso** | 12.02 |
| **Lower Torso** | 13.25 |
| **Upper Arm** | 1.18 |
| **Lower Arm with Hand** | 1.18 |
| **Upper Leg** | 3.13 |
| **Lower Leg** | 4.06 |
| **Total Mass** | 49.05 |

**Table B.2 Dimensions of Hybrid III 5th Percentile Female Dummy [68]**

| BODY PARTS | DIMENSION(cm) |
|---|---|
| **Head Circumference** | 53.85 |
| **Head Breadth** | 14.22 |
| **Head Depth** | 18.29 |
| **Buttock to Knee Length** | 53.34 |
| **Knee Pivot Height** | 40.64 |
| **Hip Pivot From Backline** | 14.73 |
| **Hip Pivot Height** | 8.38 |
| **Sitting Height** | 78.74 |

## B.2 Technical Information of Hybrid III 50th Percentile Male Dummy

The Hybrid III 50th percentile male crash test dummy is the most widely used crash test dummy in the world for the evaluation of automotive safety restraint systems in crash testing [68]. Originally developed by General Motors, the Hybrid III 50th design is now maintained and developed by FTSS in conjunction with the Society of Automotive Engineers (SAE) Biomechanics Committees and the National Highway Transport and Safety Administration (NHTSA). The dummy is a regulated test device in the USA Code of Federal Regulations (Part 572, Subpart E) and also in the European ECE Regulations. It is considered to have excellent biofidelity and instrumentation capability. Recent revisions have improved the biofidelity in the femur range of motion and the ankle and foot. The dummy can also be used in many non-automotive applications such as wheelchairs and medical and sport equipment.

**Figure B.2 Hybrid III 50th Percentile Male Dummy [68]**

The technical information of the dummy is given as follows:

**Table B.3 Mass of Hybrid III 50th Percentile Male Dummy [68]**

| BODY PARTS | MASS(kg) |
|---|---|
| **Head** | 4.54 |
| **Neck** | 1.54 |
| **Upper Torso** | 17.19 |
| **Lower Torso** | 23.04 |
| **Upper Arm** | 2.00 |
| **Lower Arm** | 1.70 |
| **Hand** | 0.57 |
| **Upper Leg** | 5.99 |
| **Lower Leg** | 5.44 |
| **Total Mass** | 77.70 |

**Table B.4 Dimensions of Hybrid III 50th Percentile Male Dummy [68]**

| BODY PARTS | DIMENSION(cm) |
|---|---|
| **Head Circumference** | 57.15 |
| **Head Breadth** | 15.49 |
| **Head Depth** | 19.56 |
| **Buttock to Knee Length** | 59.2 |
| **Knee Pivot Height** | 49.3 |
| **Hip Pivot From Backline** | 13.7 |
| **Hip Pivot Height** | 8.6 |
| **Sitting Height** | 88.4 |

## B.3 Technical Information of Hybrid III 95th Percentile Male Dummy

The Hybrid III 95th percentile male dummy is currently at build level C, was originally developed by First Technology Safety Systems (then Humanetics) and the Society of Automotive Engineers (SAE) Biomechanics Subcommittees, CDC and Ohio State University [68]. The dummy represents the largest segment of the adult population and is based on USA anthropometry studies. The biomechanical impact responses are derived from scaling functions applied to the Hybrid III 50th dummy. Originally developed in 1988, the dummy is used worldwide for the evaluation of automotive and military safety restraints and particularly for seat belt integrity testing.

**Figure B.3 Hybrid III 95th Percentile Male Dummy [68]**

The technical information of the dummy is given as follows:

**Table B.5 Mass of Hybrid III 95th Percentile Male Dummy [68]**

| BODY PARTS | MASS(kg) |
|---|---|
| **Head** | 4.94 |
| **Neck** | 1.68 |
| **Upper Torso** | 22.31 |
| **Lower Torso** | 30.30 |
| **Upper Arm** | 2.81 |
| **Lower Arm with Hand** | 2.63 |
| **Upper Leg** | 8.21 |
| **Lower Leg** | 5.75 |
| **Foot** | 1.59 |
| **Total Mass** | 101.24 |

**Table B.6 Dimensions of Hybrid III 95th Percentile Male Dummy [68]**

| BODY PARTS | DIMENSION(cm) |
|---|---|
| **Head Circumference** | 57.15 |
| **Head Breadth** | 15.49 |
| **Head Depth** | 19.56 |
| **Buttock to Knee Length** | 56.90 |
| **Knee Pivot Height** | 53.34 |
| **Hip Pivot From Backline** | 14.22 |
| **Hip Pivot Height** | 10.67 |
| **Sitting Height** | 93.47 |

## B.4 Technical Information of RID2 Dummy

In 1996, TNO Crash Safety Centre made a step towards the development of the Rear Impact Dummy (RID) [68]. The TRID Neck (TNO Rear Impact Dummy neck) was presented as a biofidelic dummy neck retrofitting the Hybrid III 50th percentile. This was the first validated test tool to study the biomechanical response of the head-neck complex during low and mid-severity rear impacts. Further testing with human volunteers and post mortem human subjects (PMHS) within the whiplash program and similar tests with the RID showed that the dummy had some deficiencies. Therefore, a second phase dummy, the RID2 was developed. As part of the work for the Brite-Euram Whiplash project, a RID2 dummy has been developed. Basis for the RID2 Production Dummy still is the Hybrid III 50th percentile male. With the RID2 conversion package, the Hybrid III can be transformed into a rear-end impact dummy, which is considered necessary to evaluate the performance of seat and restraint systems in rear impact conditions. The RID2 production dummy is strictly intended to be used in low and mid-severity rear-end collision testing, either with or without head restraint systems.

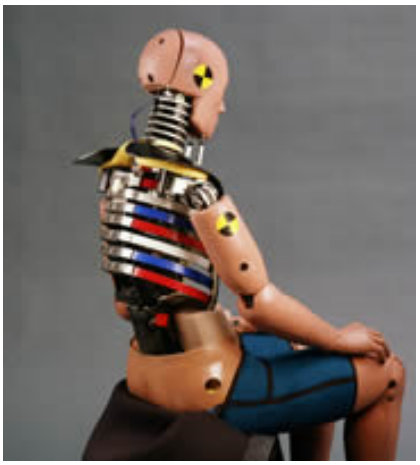

**Figure B.4 RID2 Dummy [68]**

The technical information of the dummy is given as follows:

**Table B.7 Mass of RID2 Dummy [68]**

| BODY PARTS | MASS(kg) |
|---|---|
| **Skull Cap** | 0.19 |
| **T1** | 0.06 |
| **Shoulder Assembly** | 3.89 |
| **Lower Throcacic Spine** | 3.16 |
| **Lumbar Bracket** | 6.29 |
| **Ribs** | 2.58 |
| **Pelvis** | 9.47 |
| **Total Mass** | 81.0 |

### B.5 Technical Information of BioRID II Dummy

The Biofidelic Rear Impact Dummy II (BioRID II) was developed in collaboration with Denton ATD, Inc. and the Department of Machine and Vehicle Design at Chalmers University of Technology in Götenburg, Sweden to meet the need for a testing tool to measure automotive seat and head restraint performance in rear end collisions [69]. It allows for repeatable and reproducible evaluations of neck injuries during low speed rear-end collisions.

The BioRID-II was developed as a 50th percentile male dummy to measure responses in low speed rear-end impact tests. The dummy is comprised of an articulated thoracic lumbar spine and neck made from a composite material. Each human spinal pivot point is reproduced in the BioRID-II. The torso construction includes a water filled abdomen and a pliable molding fitted around the flexible spinal assembly and attached through spine torso pins protruding outward from the central structure. Torsion bars are used in each of the thoracic-lumbar pivot joints to control the motion. The motion of the cervical vertebra assembly is controlled by a single cable attached to a damper and two cables attached to springs that act as neck-muscle substitutes. Also included between the vertebra are elastomer bumpers to control the end of travel response. The arms and legs are standard Hybrid III 50th percentile components. The molded pelvis is a modified Hybrid III 50th type with increased range of motion about the H-point. The head is a modified Hybrid III 50th.

**Figure B.5 BioRID II Dummy [69]**

The technical information of the dummy is given as follows:

**Table B.8 Mass of BioRID II Dummy [69]**

| BODY PARTS | MASS(kg) |
|---|---|
| **Head** | 4.54 |
| **Torso** | 42.41 |
| **Upper Arm** | 2.0 |
| **Lower Arm with Hand** | 2.27 |
| **Upper Leg** | 6.17 |
| **Lower Leg with Foot** | 5.44 |
| **Total Mass** | 77.70 |

**Table B.9 Dimensions of BioRID II Dummy [69]**

| BODY PARTS | DIMENSION(cm) |
|---|---|
| **H-Point Above Seat** | 8.6 |
| **H-Point From Seat Rear** | 13.7 |
| **Thigh Clearance** | 14.7 |
| **Buttock to Knee Length** | 59.2 |
| **Knee Pivot Height** | 49.3 |
| **Foot Length** | 25.9 |
| **Foot Breadth** | 9.9 |
| **Seated Height** | 88.4 |

# APPENDIX C

# TECHNICAL INFORMATION OF H-POINT MANIKIN AND HRMD

## C.1 Technical Information of H-Point Manikin

The SAE J826 standard has been prepared to provide a universal three dimensional manikin for use in defining vehicle seating accommodation. This represents the weight and contour of a 10th, 50th and 95th percentile adult male [70].

The back and seat pans are constructed of reinforced plastic and metal; they stimulate the human torso and thigh and are mechanically hinged at the "H" point. A quadrant is fastened to the probe hinged at the "H" point to measure the actual torso angle. An adjustable thigh bar, attached to the seat pan, establishes the thigh centerline and serves as a baseline for the hip angle quadrant.

Lower leg segments are connected to the seat pan assembly at the T-bar joining the knees, which is a lateral extension of the adjustable thigh bar. Quadrants are incorporated in the lower leg segments to measure knee angles. Shoe and foot assemblies are calibrated to measure the foot angle. Two spirit levels orient the device in space. Body element weights are placed at the corresponding centers of gravity to provide seat penetration equivalent to a 76 kg male. All joints of the H-Point Manikin (HPM) should be checked for free movement without encountering noticeable friction.

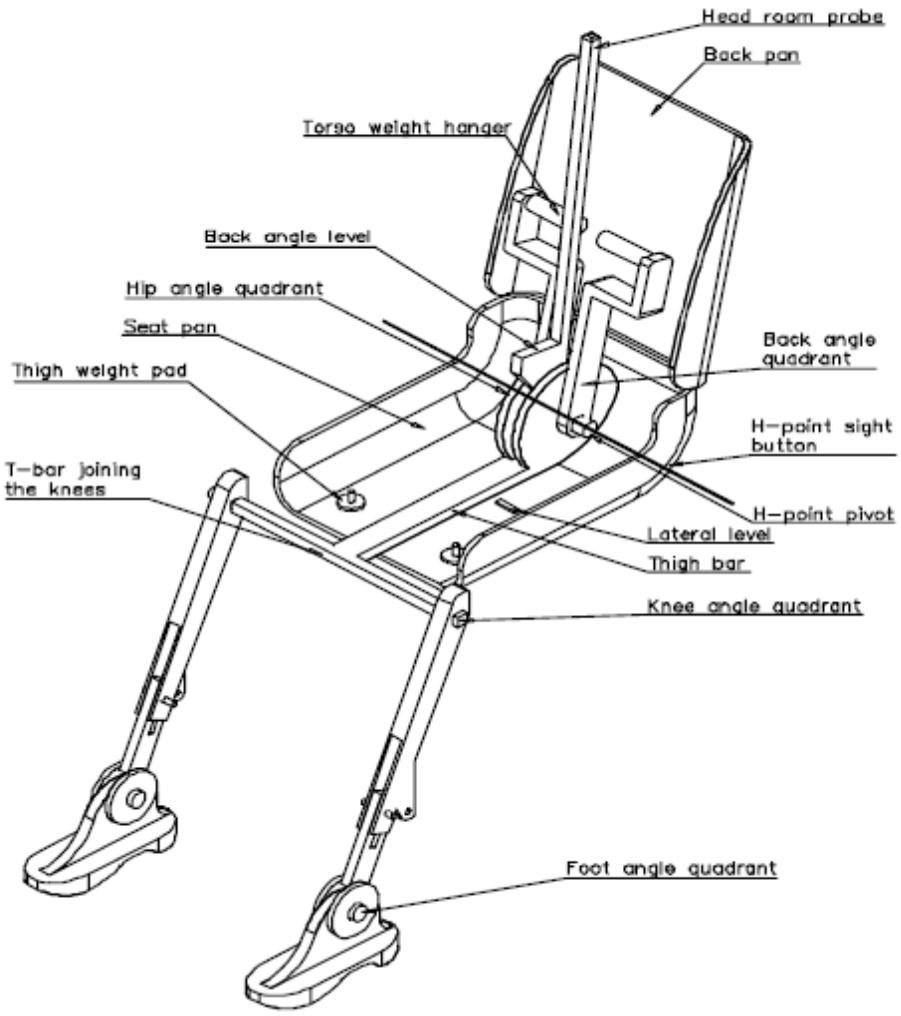


**Figure C.1 H-Point Manikin Elements Designation [70]**

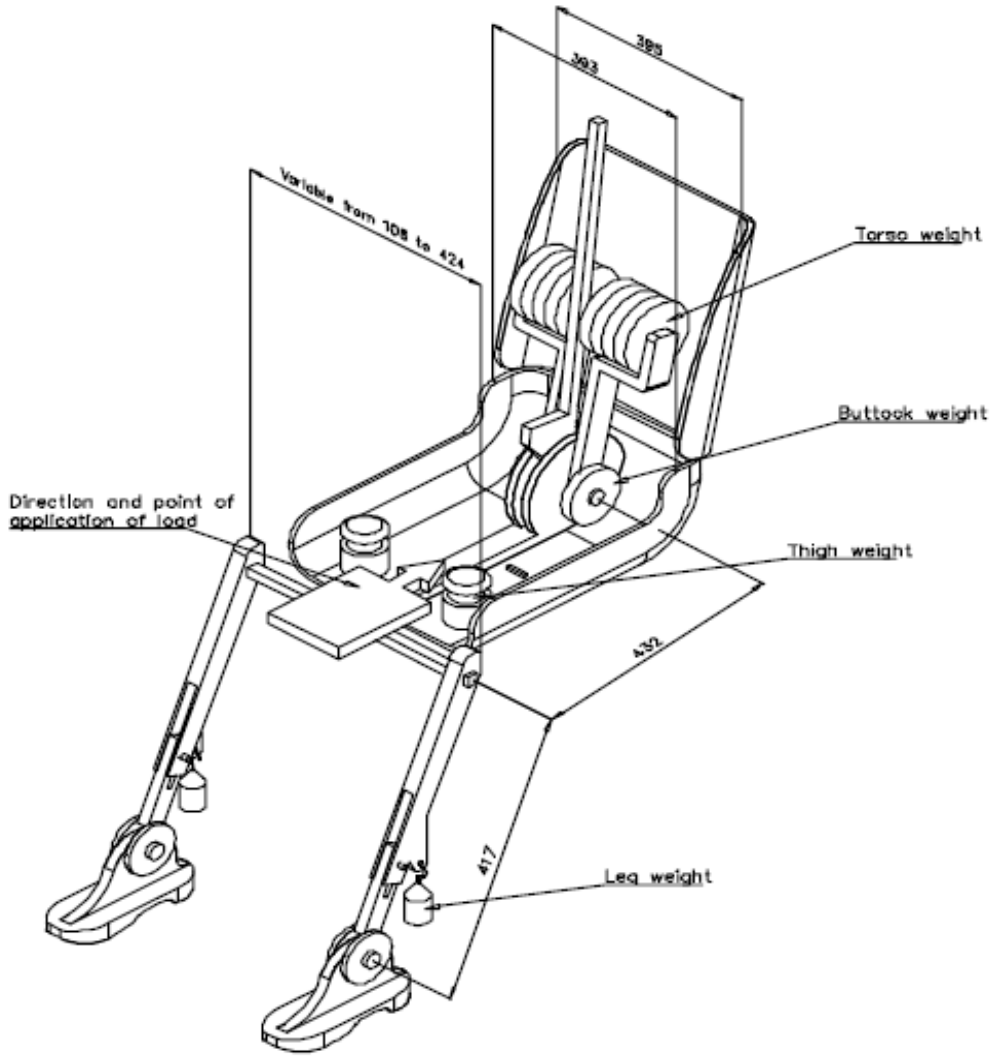


**Figure C.2 Dimensions of the H-Point Manikin Elements and Load Distribution [70]**

## C.2 H-Point Manikin Installation

The steps required to install H-Point Manikin in the seat according to the Euro NCAP Whiplash Test Protocol [26] is as follows:

- The seat shall be covered with a cotton cloth large enough to cover both cushions and seatback. The cloth shall be tucked into the seat joint by an amount sufficient to prevent hammocking of the material.

- The H-Point Manikin shall be installed in the seat.

- The lower legs shall be adjusted to the 50th percentile leg length setting, and the upper legs shall be adjusted to the 10th percentile leg length setting; these are the HPM settings closest to the Euro NCAP front and side impact protocol settings.

- The legs shall be attached to the HPM and set to the 5th position (no.5) on the knee joint T-bar, which places the knees 250mm apart.

- With the legs attached and the back pan tilted forward, the HPM shall be positioned in the seat such that its midsagittal plane coincides with the longitudinal centerline of the seat.

- The back pan shall be straightened to conform to the vehicle seat back.

- The feet shall be placed as far forward as possible, with the heels resting on the heel plane and the feet positioned at 90° to the tibias. The toe pan shall be positioned sufficiently far away so as to avoid any interaction with the feet during the HPM installation process.

- The lower leg and thigh weights shall be attached to the HPM and the assembly shall be leveled.

- The back pan shall be tilted forward to 45º from the seat back and the HPM assembly pushed rearward until the seat pan contacts the vehicle seat back. While maintaining the back pan at 45º to the seat back, a horizontal rearward force of 100N shall be applied using the plunger if present or using a force gauge pressed against the hip angle quadrant structure.

- The load application shall be repeated and, while keeping the 100N applied, the back pan shall be returned to the vehicle seat back and the load then released. As the 100N is released, a small force should be maintained on the front of the T-bar to prevent any longitudinal movement.

- A check shall be made to determine that the HPM is level, facing directly forward, and located in the centerline of the seat

- The HPM torso angle shall be measured by placing an inclinometer on the calibrated block located on the lower brace of the torso weight hanger.

- After estimating the vehicle seat back position, the right and left buttock weights shall be installed. The six chest weights (including the two larger weights) shall be installed by alternating left to right. The two larger HRMD chest weights shall be attached last, flat side down. Throughout the weight installation, maintain a light pressure to the T-bar preventing any longitudinal movement.

- Tilting the back pan forward to a vertical position, the assembly shall be rocked from side to side over a 10° arc, 5° in each direction. Where seat side bolsters prevent movement of up to 5°, the assembly should be rocked as far as permissible. This rocking shall be repeated twice, making a total of three complete cycles. Care should be taken to maintain support of the T-bar during the rocking action, and to ensure that no inadvertent exterior loads are applied. Ensure that the movements of the HPM feet not restricted during this step. If the feet change position, they should be allowed to remain in that attitude for the time being.

- Holding the T-bar to prevent the HPM from sliding forward in the seat cushion, the back pan shall be returned to the vehicle seat back, and the HPM shall be leveled.

- To ensure a stable torso position, apply and release a horizontal rearward load, not to exceed 10N, to the back pan molding at a height approximately at

the centre of the torso weights. Care shall be exercised to ensure that no exterior downward or lateral loads are applied to the HPM.

- Each foot shall be alternately lifted off the floor via the instep until no additional forward foot movement is available.

- The 45 degree plane of the toe board should be moved toward the feet such that the tip of the toe lies between the 230mm and 270mm lines taking care not to disturb the position of the HPM.

- When each foot is in its final position, the heel shall be in contact with the floor, and the sole of the foot shall be in contact with the 45 degree plane of the toe pan between the 230mm and 270mm lines.

- If the HPM is not level after the feet have been repositioned, a sufficient load shall be applied to the top of the seat pan to level it on the vehicle seat. This may be verified using the bubble gauge fitted to the manikin or alternatively by verifying with CMM that the H-point position on both sides of the machine are within ± 2.5mm of each other.

**C.3 Technical Information of Head Restraint Measuring Device**

"HRMD" (Head Restraint Measuring Device) means a separate head-shaped device used with the H-Point Manikin to measure the static geometry of a vehicle head restraint [71]. It was developed under the sponsorship of the Insurance Corporation of British Columbia (ICBC, SAE paper 1999-01-0639). The HRMD is equipped with two probes to measure head restraint height and backset. The height probe projects horizontally, level with the top of the head, to provide a reference line for the vertical measurement to the top of the restraint. The backset probe simulates the rear profile of the head and neck and projects horizontally, to provide the horizontal measurement to the restraint. (Figure C.3 and C.4).

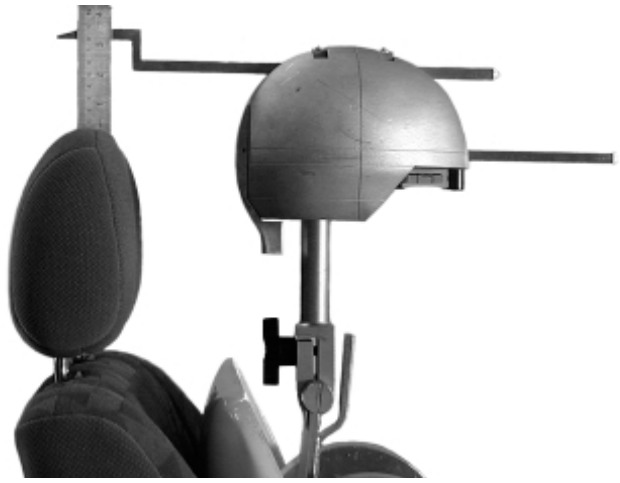

**Figure C.3 Head Restraint Height Measurement [71]**

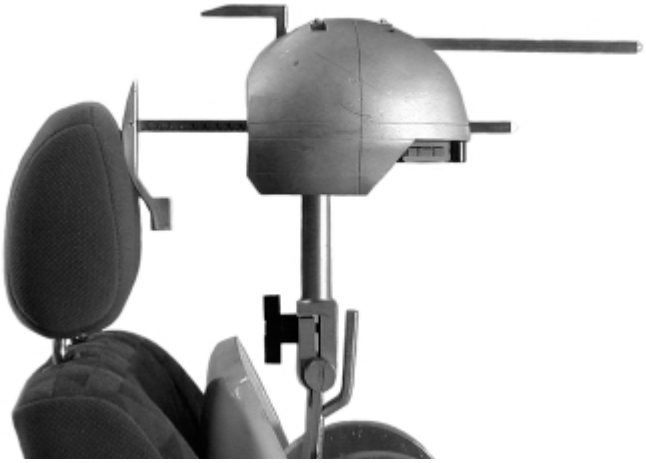

**Figure C.4 Head Restraint Backset Measurement [71]**

## C.4 HRMD Installation

The installation steps of HRMD are as follows [26]:

- The backset and height probes shall be installed and pushed against the HRMD.

- The HRMD leveling knob shall be confirmed as finger tight and the plungers which engage at the HPM to HRMD interface shall be fully loosened.

- The HRMD shall then be lowered into position on the HPM torso weight hangers and on the top edge of the channel between the hangers. During the fitment, ensure that the HRMD fits easily into place without inducing forces which might disturb the manikin position.

- The HRMD shall be leveled by loosening the leveling knob at the rear of the device and repositioning the head using the HRMD bubble level; the leveling knob shall then be retightened by hand.

- Measure the torso angle on the calibrated block attached to the weight hanger bar.

- If the measured angle is not 25°±1°, the HRMD and chest and buttocks weights shall be removed, the seat back readjusted, and the steps to position the HPM shall be repeated, beginning with tilting the back pan forward and pushing the HPM rearward.

- If more than 3 installations of the HPM and HRMD are required to ascertain a seatback angle that supports a torso angle of 25°±1°, then the seat should be allowed to recover for 15 minutes with nothing in it between each third and fourth installation.

- Some indexed seatback adjustments may have more than 2° between adjustments with none giving a torso angle between 25°±1°. In such cases, adjust the seatback to the most reclined position that supports a torso angle less than 24°.

- The torso angle shall be recorded when it falls within the allowed range.

# APPENDIX D

## TECHNICAL INFORMATION OF CRASH SIMULATION SYSTEM, HIGH SPEED CAMERA AND DATA ACQUISITION SYSTEM

### D.1 Technical Specifications of IST Crash Simulation System

The IST Crash Simulation System(Figure D.1) constitutes an important element in the development of restraint systems and their components [72].

**Figure D.1 IST Crash Simulation System**

Areas of application of the crash simulation system [72]:

- Dynamic seat testing to ECE-R17, ECE-R80
- Dynamic seat testing to AS 8049(Aerospace Standard)
- Crash simulation tests with dummies in the vehicle body or on a rigid fixture
- Dynamic testing of restraint systems to ECE-R16
- Crash Simulation tests with pyrotechnical restraint systems (belt retractors, airbags)
- Testing of cargo restraint systems to DIN 75410/2
- Child seat testing to ECE R-44
- Low speed rear end impact - seat testing
- Test pulses to US and Euro NCAP

Technical Specifications [72]:

Catapult Actuator Unit:

- 2500 kN nominal force
- 1700mm working stroke
- 140.000 l/min 4-stage Servovalf
- 2500 kg maximum payload

Sled and Rail System:

- 32m. long precise rails
- 1800 x 4100 mm sled dimensions

Hydraulic Power Pack:

- 250 l/min flow capacity
- 290 bar pressure

Performance:

- 90 g maximum acceleration
- 90 km/hr maximum velocity

## D.2 Technical Specifications of Weinberger Vision Visario G2 High Speed Camera

Based upon the world-wide proven Weinberger Vision Visario industry standard, the compact and lightweight systems of the second generation (G2) unite to provide a rare wealth of performance features. It is designed for high end operation in the fields of automotive, military and research and development [73].


**Figure D.2 Visario G2 High Speed Camera [73]**

Technical specifications of the Visario G2 camera [73]:

- High Speed APS CMOS Sensor
- 1536 x 1024 resolution at 1.000 fps
- Maximum 10.000 fps at reduced resolutions
- 10µs global electronic shutter
- Fast Gigabit Ethernet interface
- Monochrome 10 bit, color depth up to 30 bit
- 25 Watt power consumption
- Lens Mounts: C, F, Box and Custom
- Weight: 7.8 lbs.
- Size: 113 x 120 x 200 mm
- Rated at 100g's in all three axes
- Embedded LINUX operating system

### D.3 Technical Specifications of Kayser Threde Minidau Advanced Data Acquisition System

The Minidau Advanced used during test has 32 analog channels of which 16 of them can also be used as digital channels (Figure D.3). Each analog channel comprises a programmable input amplifier, bridge excitation, 16 bit A/D converter for simultaneous sampling. The amplifier gain precision is better than 0.2% and the input impedance above 10 MOhm. The gain values can be programmed in steps from 1 to 10000. An internal reference voltage is used for precise control of the amplifier setting. Neither potentiometers nor trimmers nor mechanical switches are used inside

the device. All adjustments are implemented by software, automatically or by command [74].


**Figure D.3 Minidau Advanced with 32 Channels [74]**

The bridge excitation voltage is programmable separately for each channel. All 8 channels of an amplifier board can be used for the classical voltage excitation modes. Four out of these channels can deliver extended excitation modes. This includes a high voltage mode up to 20 V and a constant current excitation mode. Bridge completion for half bridges can be switched internally.

Shunt measurement and check is implemented as a full 4 quadrant circuit with internal emulation of customer specific shunt resistor values. External shunt resistors are supported as well.

The signal bandwidth of the amplifier has been extended to 42,5 kHz. With conventional designs this would require sampling rates above 200 kHz. Due to the state of the art oversampling A/D converter design including adaptive filtering this bandwidth of the amplifier can be efficiently used sampling at 100 kHz. This feature allows the measurement of acoustic events e.g. due to airbag inflation during the crash. test.

The Minidau Advanced amplifier introduces overload detection. It is implemented between the amplifier part and the filter part removing high frequency disturbing signals. Overload conditions are sampled and stored together with the actual measurement data to allow in deep study of this phenomenon.

In contrast to former designs, the low-pass filter is a pure anti-aliasing filter with an adaptive cutoff frequency that fits to the currently selected sampling frequency. All necessary additional filtering, e.g. according to SAE filter classes, is done during post processing.

Sampling and Storage of measurement data has been implemented similar to the proven design of the conventional Minidau, using volatile sram memory during pretrigger and non volatile and flash memory for data storage. Batteries are not needed to retain the data. The Minidau Advanced can store data for a 50s cycle even at the full sampling rate of 100kHz which allows the user to start recording data before the vehicle or sled is actually started. This ensures that the measuring system functions correctly and prevents data loss, even in case of possible malfunctions of the trigger signal. This is the main error cause, apart from user errors. The trigger point is registered and recorded. Once a valid trigger point is stored in the Minidau Advanced data memory, the user can select only the actual measured data for transfer to a PC, it is not necessary to read out the complete data memory.